FACULTY
OF MATHEMATICS
AND PHYSICS

Charles University

DOCTORAL THESIS

Ivana Víšová

THE STUDY ON INTERACTIONS OF FUNCTIONAL SURFACES WITH BIOLOGICAL SYSTEMS

Supervisor: RNDr. Hana Vaisocherová-Lísalová, Ph.D., Institute of Physics of the Czech Academy of Sciences

Study program: Physics

Specialization: Biophysics, chemical and macromolecular physics

Prague 2021

I declare that I carried out this doctoral thesis independently, and only with the cited sources, literature and other professional sources. It has not been used to obtain another or the same degree.

I understand that my work relates to the rights and obligations under the Act No. 121/2000 Sb., the Copyright Act, as amended, in particular the fact that the Charles University has the right to conclude a license agreement on the use of this work as a school work pursuant to Section 60 subsection 1 of the Copyright Act.

In Prague March 2, 2021

Acknowledgments

I would like to thank my supervisor Dr. Hana Vaisocherová-Lísalová for all the scientific opportunities, challenges, and motivations, and to the whole team of the Laboratory of Functional Biointerfaces (especially Markéta Vrabcová, Michala Forinová, Alina Pilipenco, Judita Arnoštová and Dr. Nicholas Scott Lynn) for the support, encouragement, and always good mood in a lab! Special thanks also to Dr. Milan Houska, and Dr. Jakub Dostálek, who have provided me the valuable feedback for scientific writing (and for my thesis) and Dr. Alexandr Dejneka for his scientific and personal support.

I would like to express my gratitude to all who have helped me with my education and all colleagues and co-authors who have worked with me, have inspired me, and have always taught me something new. It is a long list of exceptional people I have been lucky enough to work with. Thank you all!

My deepest gratitude goes to my parents, and the best brother in the world for their love, support, and home-made food in the most critical moments, and my fur-princess Kersie for simply being here with me and being amazing!

Title: The study on interactions of functional surfaces with biological systems

Author: Ivana Víšová

Department: Institute of Physics of the Czech Academy of Sciences, Department of optical and biophysical systems.

Supervisor: RNDr. Hana Vaisocherová-Lísalová, Ph.D., Institute of Physics of the Czech Academy of Sciences, Department of optical and biophysical systems.

Abstract: This work is devoted to the study of processes influencing the performance of functional antifouling polymer brush coatings and their interactions with complex biological media. Specifically, both results of the fundamental and applied research on the i) functionalization processes influencing coating resistance, ii) tailoring of the physico-chemical properties of the antifouling coatings to minimize the nonspecific interactions with complex biological samples, and iii) behavior and performance of the polymer brush coatings in varying environments are presented. Acrylamide and methacrylamide-based polymer brushes with side hydroxyl, carboxybetaine, and sulfobetaine groups were studied, showing the great potential of their optimized copolymer structures as tunable antifouling functionalizable platforms for cell research or biosensor applications. Moreover, newly developed procedures for antifouling properties recovery after EDC/NHC activation and functionalization of poly(carboxybetaines) serves effectively to suppress nonspecific interactions while enhancing biorecognition capabilities. The acquired knowledge was successfully implemented in the applications, presenting newly developed antifouling biorecognition coatings and optimized functionalization processes as promising tools in cell research, or food-safety, and biomedical biosensing.

Keywords: antifouling functional coatings, zwitterionic polymer brushes, biosensors, functionalization, fouling

Contents

Introduction

In the last decades, a remarkable success and significant progress have been achieved in the fields of life sciences, such as biology, medicine, or biochemistry. With such a fast expansion of knowledge and breakthrough scientific achievements, the inherent physico-chemical limitations of techniques or study systems have inevitably become a key topic. When working with real-world complex samples, the nonspecific adsorption of biomass on the surfaces (fouling) of industrial tools, medical instruments, sensitive sensor surfaces, packages, or even compensatory and medical aids, interferes critically with their performance and affects their lifespan. The consequences are substantial — implant rejection, spread of nosocomial, foodborne, or other infectious diseases, impairment of biosensors and other analytical methods, ship hulls and underwater constructions deterioration are only a few examples (Dür; and Thomason; 2010; Chan; and Wong; 2010; Shirtliff; and Leid; 2009).

Considering the fouling-based limitations of technology performance, the limitations of transferring laboratory-developed technologies into real-world routine industrial practices, and the extra financial burden linked to damages caused by fouling, it is clearly necessary and scientifically and economically very essential to solve the fouling question once and for all. Consequently, a tremendous effort has been made to deal with the fouling phenomenon lately, raising the number of publications in a wide range of research fields in the last two decades remarkably (Figure 1).

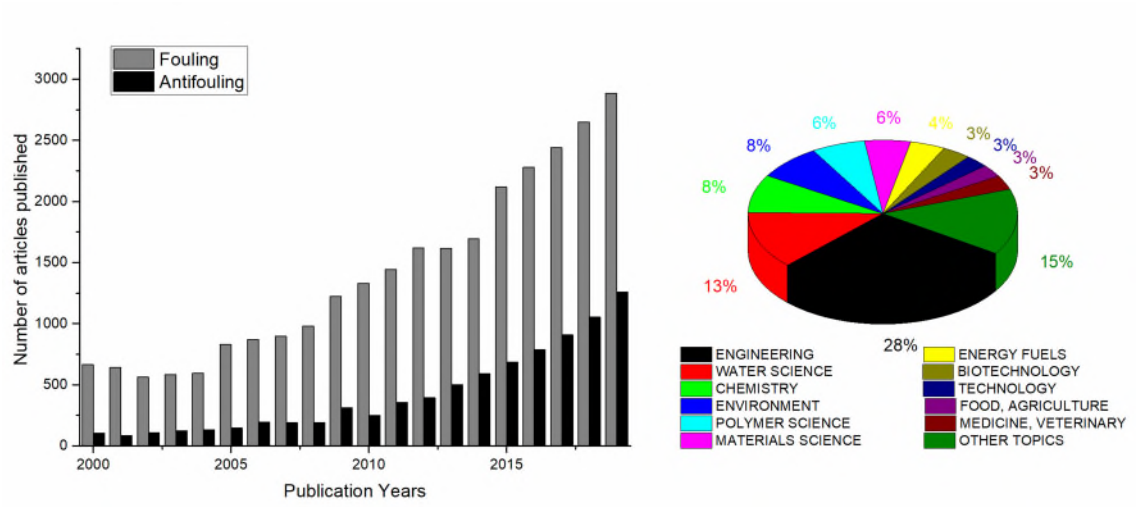

Figure 1: *Publication statistics: citation report for terms "fouling" and "antifouling" in years 2000–2019 from the Web of Science (Web of Science [v.5.35] – Web of Science Core Collection Basic Search; webofknowledge.com) on the 16th of December 2020. A: Number of publications per different years for both topics. B: Research areas dealing with fouling according to Web of Science.*

The critical topic in material research and life-sciences is the research of functional bio-interfaces. In-depth research of a wide range of functional coatings triggered advanced practical applications and stressed the importance of studying specific and nonspecific molecular interactions at the surfaces. To define precisely the interactions at the interface, dual-functional coatings effectively resisting fouling from complex media and simultaneously facilitating the functionalization (functionalizable antifouling coatings) are promising platforms.

This doctoral dissertation thesis aims to address the critical issues in functional antifouling materials and in coatings research. The physico-chemical properties of coatings bearing an antifouling character and the molecular processes influencing coating resistance, e.g. activation and deactivation, functionalization, or environmental changes, were extensively studied by a plethora of techniques. The acquired findings were then applied in engineering of new functionalizable antifouling materials with enhanced desired properties. Finally, the tailored coatings have been employed in a number of applications, studying specific interactions of complex biological samples with functional surfaces.

This work is divided into three parts. The first part (Part 1 — Theoretical Background) aims to summarize several key topics related to the study of biomolecular and biological interactions at the surfaces with the emphasis on a complex samples environment. It presents short reviews on the theory of the interactions between biomolecules and the surfaces, surface functionalization tactics and antifouling strategies. The second part (Part 2 — Experimental Methods) covers useful methods for surface-mediated biomolecular interaction research, which were used in this study. The third part (Part 3 — Results) summarizes results and findings obtained by the research during the course of the work. The Appendix to this work contains detailed outcomes of the research in the form of 8 publications in high-impact journals with the total of 186 citations (up to 02/18/2021; self-citations excluded; source: Web of Science™), one submitted manuscript and three manuscripts in preparation, to be submitted in March 2021. Moreover, three filed patent applications and one in preparation as well as two functional samples as a result of the applied research are appended.

PART I

Theoretical background

1. Biological systems and their complexity

A biological system is understood here as any formation consisting of a range of biomolecules or higher biological structures including interactions among them. For example, the biological system here can be an arrangement of cells in a cell growth medium, interactions between bacteria and their pathogens, or a set of biomolecules performing specific interactions in a real-world complex sample.

The term "complex sample " covers an inexhaustible number of different types of matrices, e.g., real-world water, soil, or other environmental samples, foods, drinks and other industrial products, or bodily fluids. Typically, such a sample contains orders of magnitude higher concentrations of a variety of biomolecules, other compounds and interactions among them, compared to investigated analytes or interactions. All matrices can be characterized by a range of physico-chemical properties, which may significantly differ among each other (e.g., tremendous diversity in physico-chemical properties in foods (Sikorski 2006) or among bodily fluids (Pereira et al. 2014; Yu et al. 2011)). Working with real-world complex samples means dealing with a wide range of pH, ion strength, viscosities, structures, and compositions. Such diversity is a great issue, hampering probing or controlling of specific interactions and the development of fast and versatile analytical or diagnostic methods.

Most of the time, the biological system is too complex to characterize single intended compound or interaction. On the other hand, the properties of each single component are dependent on the environment composition and complexity (Latham and Kay 2012; Yu et al. 2016). Therefore, significant insight can be obtained through detailed study of biological interactions in well-defined low-complex *in vitro* environments (e.g. buffer solutions), but the experiements performed in real-world complex samples or native environment are critical for comprehensive understanding of interactions taking place in real-world samples or *in vivo* experiements.

2. Interactions of biological systems with surfaces

In principle, surface-mediated interactions of any entity, inorganic or organic, can be distinguished according to target specificity into two groups — specific and nonspecific interactions. While the first group of interactions reaches a particular target or targets only (in some range of tolerance expressed as cross-reactivity), the second type is not selective. In all fields working with complex samples, especially in bio-interface engineering and research, it is essential to consider both types of interactions to find the best performing harmony between enhancement of the specific interactions and suppression of the nonspecific ones.

2.1. Nonspecific surface-driven interactions

By introducing any artificial surface into a complex sample, the nonspecific adsorption of biomaterial immediately starts accumulating on the surface (fouling). On a very general level, two types of fouling can be distinguished — inorganic fouling, caused mostly by deposits from corrosion, dirt, suspended particles, or crystallization, and organic fouling that appears due to organic mass nonspecific adsorption (Bhushan 2018; Bixler and Bhushan 2012). The organic fouling is triggered mostly by protein adhesion; however, at later stages of the organic fouling, the significant part of adhered biomass is formed by adhesion of microorganisms, macroorganisms (sometimes called “macrofouling”), and formation of colonies and is often addressed as biofouling. However, both terms, organic fouling, and biofouling are often used as synonyms. Further in this work, mostly organic fouling is discussed and is referred to as “fouling”.

It was proven that fouling is a dynamic and complex phenomenon (Casals et al. 2010). Highly motile smaller proteins adhered in the early stage of the fouling event are exchanged in time for less motile higher molecular weight proteins with higher affinity to

the surface (Figure 2). Such cascade of adsorption and replacement, so-called Vroman's effect, was reported for fibrinogen in human blood plasma in the '60s–'80s (Vroman and Adams 1969; Vroman et al. 1980). Even though some hypotheses to explain the effect in solutions of fibrinogen and other proteins have been raised lately (Jung et al. 2003; Noh and Vogler 2007), Vroman's effect has not been clearly explained on molecular nor confirmed on general level yet.

The fouling event can be divided into five steps (Norde 1986; Wahlgren and Arnebrant 1991) — transport towards the surface, adsorption, adsorption-induced conformational changes, desorption/exchange, and transport away from the surface. All the mentioned steps should be considered while attempting to control fouling, as all of them can in principle determine the rate of the fouling event.

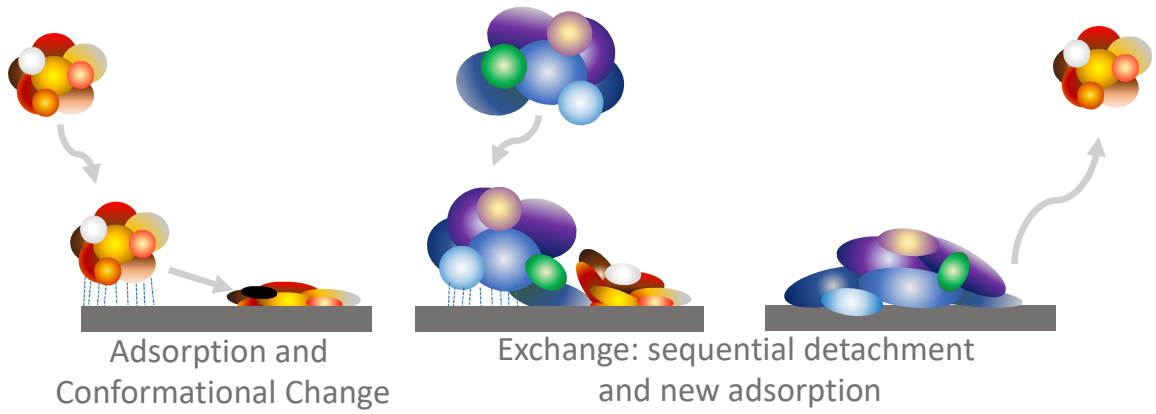

Figure 2: *Vroman's effect illustration. Upon contact with the surface, proteins get adsorbed and may change conformation. Subsequently, they are exchanged by bigger less motile molecules with higher affinity to the surface.*

2.1.1. Transport towards the surface

Transport of mass in liquids is generally described as convection and is composed of diffusion (non-directional transfer along the gradient of concentration) and advection

(transfer along with the bulk flow). There are different types of convection, depending on the driving forces of the particle movement. The most important are natural convection caused by temperature-related changes in the density of fluids affected by gravity, and forced convection driven by external forces, such as mixing or pumping (Mostafa 2018). However, regardless of the effectivity of forced convection, no-slip, or partly-slip boundaries are assumed on the surface/liquid interface in a good approximation (Lauga et al. 2007; Neto et al. 2005). As a consequence, a stagnant or nearly stagnant layer is formed on the surface through which the protein has to migrate by diffusion (Young et al. 1988). Indeed, especially for lower protein concentrations, diffusion appears to be a rate-limiting factor for adsorption (Norde 1986; Pignatello and Xing 1996; Zhdanov and Kasemo 2010).

The diffusion coefficient for a spherically shaped particle (approximate shape of a typical protein in an aqueous environment) is according to the Stokes-Einstein formula directly proportional to the temperature, and inversely proportional to the dynamic viscosity of the liquid, and the radius of a spherical particle (Peskir 2003). For the same liquid, larger particles will exhibit a lower diffusion coefficient, limiting their diffusion-driven motility and so postponing their access to the site of adsorption, compared to smaller and so more motile particles.

2.1.2. Adsorption and the interactions involved

After reaching the surface, the adsorption of small molecules (e.g., ions) and proteins onto the surface starts immediately. With increasing surface coverage, the adsorption rate is decreasing and can get below the rate of diffusion, becoming a new rate-limiting factor for the fouling (Norde 1986; Young et al. 1988).

Due to a wide range of interactions involved in the adsorption, mutually occurring among the proteins, the sorbent surface, other solvent molecules, and the low-molecular weight ions, the adsorption is a complex and still not fully described dynamic event.

Hydrophobic interactions

A major factor driving the adsorption of proteins onto surfaces is the entropy of a more-or-less ordered three-dimensional hydrogen-bonded water network nearby the surface. Specifically, in contact with non-polar surfaces with high interfacial energy, the water network arranges itself in a less dense highly ordered matrix to equilibrate chemical potential with bulk water (Gragson and Richmond 1997). Adsorption of molecules on the surface is then energetically preferable, as the replacement of ordered water molecules by adsorbed solute decreases interfacial energy, increasing the entropy of the system (Elwing et al. 1987). On the other hand, surfaces competing with the water-self association by offering sites feasible for hydrogen bond formation cause collapse of highly ordered water structure, decreasing interfacial energy and increasing entropy of the system. Adsorption becomes an energetically unfavorable process (Vogler 1998). The promptness of the surface to create hydrogen bonds with water molecules is referred to as hydrophobicity/hydrophilicity of the surface and can be described by measurement of water wettability of the surface using contact angle measurements (see also Chapter 4.5 Contact angle measurements or (Feng and Jiang 2006; Vogler 1998)).

Due to the propagation of the arrangement changes in the hydrogen-bonded water network, hydrophobic interaction may be effective till a distance of tens of nanometres, decaying exponentially from the surface (with surface-characteristic decay length). Typically, hydrophobic interaction in water is reported to be effective till ~ 1–50 nm from the surface (Ederth et al. 1998; Israelachvili and Pashley 1982). Though, regarding the pure intrinsic hydrophobic effect, later results lean more towards the lower limit of the range, assigning a longer-range part of the interaction to other effects (Ducker and Mastropietro 2016; Zeng et al. 2016).

Electrostatic interaction

Besides the entropically driven hydrophobic effect, intermolecular forces contribute to the fouling extensively (Hlady and Buijs 1996; Roth and Lenhoff 1993). The “long-range” force, acting for distances > 1nm, is Coulomb force, mediating electrostatic interaction

between fixed or induced charges. In any polar media, two main surface charging mechanisms are involved – i) adsorption of ions, ionic surfactants, or charged polymers, and ii) dissociation of chemically bound groups. Presenting charged surface to solvent, a thin layer of concentrated ions of the opposite sign will compensate the charge of the surface to fulfill the overall electroneutrality (Adamczyk 2003). Nevertheless, such uneven distribution of ions near the surface leads to local pH changes resulting in a different charge of pH-dependent ionizable groups in bulk solution and on the surface (Biesheuvel et al. 2005). Other changes in electrochemical properties of the interface after particle adsorption may happen due to other interactions, such as charge transfer or metallic screening. The overall charge of the surface evolves in time with new particles adsorbed, creating a different interface environment for new particles or molecules coming (Lang et al. 1985).

Depending on charges involved, Coulombic interaction can be attractive or repulsive. Overall surface charge and the charge of solutes are strongly influencing adsorption. In the basic theory, the energy decays as ~ $1 / \epsilon r$, where r is the distance between charges, and ϵ is the dielectric constant of the medium. So, in a polar medium (water) the distance is substantially decreased due to the high dielectric constant, but also due to other effects, such as dipole and ionic screening effects (Seyedi et al. 2019).

Van der Waals and solvation forces

Weak Van der Waals forces (Huber et al. 2019) and somewhat stronger hydrogen bonds operate in sub-nanometre to nanometre range, creating weakly bound molecular complexes (Blaney and Ewing 1976).

Van der Waals intermolecular forces term covers three major electrostatic interactions between electrically neutral molecules acting over nanometer-scale distances – Keesom interaction (electrostatic interaction between permanent multipoles, sometimes called as orientation force), induction or Debye force (interaction between permanent multipole and induced multipole), and dispersion or London force (attractive interaction between instantaneous multipoles created by quantum fluctuations in non-polar particles), all

decaying with distance proportionally to $\sim 1/r^6$. Usually (but not always), among Van der Waals forces in medium, dispersion force contribution is greater than the contribution of dipolar interactions (Israelachvili 2011b).

Based on previously described forces, another important effect arises in aqueous solutions. In highly polar solvents, such as water, a layer of oriented solvent molecules is created around dissolved ions (called solvated or hydrated ions). The so-called solvation pressure and solvation force arise due to different solvent densities around two interacting entities, such as surface/ion, two hydrated ions, or two surfaces. Solvation forces can be attractive, repulsive, or oscillatory and depend on properties of the solvent and physico-chemical properties of the surfaces (hydrophobicity, roughness, atomic structure, rigidity,…) (Israelachvili 2011a).

2.1.3. Adsorption-induced conformational changes

The substantial change in the environment of the protein near the surface typically causes a thermodynamically driven conformational rearrangement shift of the native structure to a new arrangement during adsorption (Ahmad et al. 2015). The final conformation depends on parameters, such as type of the surface, intramolecular forces stabilizing protein structure (Hlady and Buijs 1996), type and composition of the solvent, or amount of proteins adsorbed on the surface previously. It often leads to an alternation in biological activity and a more thorough attachment of the molecule.

In (Brandes et al. 2006) authors show, that a total collapse of the protein structure during adsorption is not common. Some residual structures are always retained, creating a conformationally heterogeneous population of adsorbed molecules (Zoungrana et al. 1997). Alfa-helical secondary motif seems to be the most sensitive structure regarding adsorption-induced rearrangement (Brandes et al. 2006; Zoungrana et al. 1997). The claim of the preservation of the part of the structure agrees with a work of Buijs et al.,

nevertheless, significant changes in β-sheet structure content were described in immunoglobulin G after adsorption (Buijs et al. 1996).

2.1.4. Desorption or Exchange

Due to the adsorption-induced conformational changes following adsorption, the process of adsorption appears to be essentially irreversible and the desorption hardly occurs upon a simple dilution (Hlady and Buijs 1996). The bonding participated in adsorption is rather a dynamic process of simultaneous creating and breaking bonds. The probability of simultaneous breaking of most bonds between molecule and surface is highly unlikely, making desorption upon simple dilution rather unfeasible (Wahlgren and Arnebrant 1991). However, weak forces are temperature, pH, or ionic-strength dependent — partial desorption (or stronger adsorption) can be achieved by changing these parameters.

Besides desorption, the adsorbent can be exchanged by other compounds of the solution by sequential detachment. While one segment of the adsorbed molecule is loosened for a while, a segment of another molecule can be adsorbed at the spot, leading to the eventual displacement of the previously adsorbed molecule and exchange for the new one. Such a process is more probable than the desorption by dilution, as the activation free energy depends only on one segment at a time, compared to the whole molecule at once (Norde 1986).

2.1.5. Transport away from the surface

Transport away from the surface is a process opposite to transport towards the surface, following the same rules. The first and most limiting step after desorption is the diffusion followed with the transport of the particle along with the flow of the convection. Once

desorbed, protein can either be transported completely away from the surface or can be only shifted to another spot of the surface and be adsorbed again.

2.2. Specific interactions and molecular recognition at the interfaces

Although the theory behind specific and nonspecific interactions is rather complex (Kiselev 1965; Leckband et al. 1994), for the purpose of this work the intuitive imagination of specific interaction as a "lock-key" system is sufficient. While nonspecific interactions happen always, spontaneously, and immediately after contact of any molecule with a surface, controlled interactions between molecules and unmodified surfaces are not so common. Usually, the interface has to be modified to be capable of controlled interactions. In practice, the modification means an immobilization of an element with desirable functionality in the way, that it will not lose its activity (functionalization).

The most common way to functionalize the surface is the immobilization of the bio-functional entities (e.g., biorecognition or bioactive elements, BEs). In this work, the most extensively studied functionality is a biorecognition, even though, it is important to stress out, that not only biorecognition functionality has been researched. The comprehensive review of all possible controlled functionalities, functionalization processes, and functional elements for surface functionalization is out of the scope of this work and can be found elsewhere (Gorb 2009; Hermanson 2013; Morales and Halpern 2018). Further, the selection of the most common or promising methods and BEs is presented.

2.2.1. Biofunctional elements

Nowadays, a wide set of different BEs with unique characteristics, such as physico-chemical properties, operating ranges, immobilization possibilities, affinities, or stability is available. They range from naturally occurring molecules (or complexes) benefiting from ages of evolution of physiological processes, to artificially designed structures developed to mimic natural interactions. While naturally occurring BEs usually exhibit great affinity to their target, they often lack stability in non-native conditions (e.g., after immobilization), wide ranges of pH, or temperature (Luan et al. 2018).

Antibodies

Among naturally occurring BEs, the most common in use for surface modifications are antibodies, performing so-called affinity-based biorecognition (Lin et al. 2010; Rusmini et al. 2007). These highly soluble serum glycoproteins (immunoglobulins) of the size of ~150 kDa consist of two regions, Fc (constant fragment) and Fab (antigen-binding fragment), created by 4 peptide chains fixed together by disulfide bridges — two heavy (50kDa each) and two light chains (25 kDa each) (Sharma et al. 2016) (Figure 3).

Production of antibodies is usually expensive and demanding, requiring work with either living animals (*in vivo* production of polyclonal antibodies by multiple B-lymphocytes in the blood of infected hosts), or hybridoma line (*in vitro* production of monoclonal antibodies by hybrid cell line based on a fusion of B-lymphocyte of infected host and myeloma cancer cells) (Pohanka 2009). Compared to monoclonal antibodies, polyclonal antibodies can be generated faster and cheaper. They are heterogeneous, binding a wide range of antigen epitopes. Their polyspecificity assures lower susceptibility of biorecognition activity to structural changes of antigen epitope or chemical modifications of antibody. Moreover, polyclonal antibodies are more stable regarding environmental conditions, such as pH or salt concentrations. However, they are more prone to batch-to-batch variability and cross-reactivity. Monoclonal antibodies, targeting only a single epitope, are produced in 10-fold higher concentration and much higher purity. Their

production, quality, and performance are highly reproducible and do not depend on the varying host response to antigen (Lipman et al. 2005).

Lately, recombinant antibodies, such as single-domain antigen-binding fragments known as nanobodies (Muyldermans 2013), have become popular as an alternative to monoclonal antibodies. These semi-natural and semi-engineered products are prepared in vitro typically by phage display using pre-prepared high-yield expression vectors containing genetic code of whole antibodies or the biorecognition part of antibodies (Bradbury et al. 2011). Recombinant antibodies are similar to monoclonal ones in their performance, bringing the highest level of reproducibility and consistency between production batches, allowing genetic modifications. The production is quick with very high throughput (Krebs et al. 2001). Phage-display antibodies and nanobodies are used in diagnostics applications (Hairul Bahara et al. 2013; Huang et al. 2010) and medical applications (Jefferis 2009).

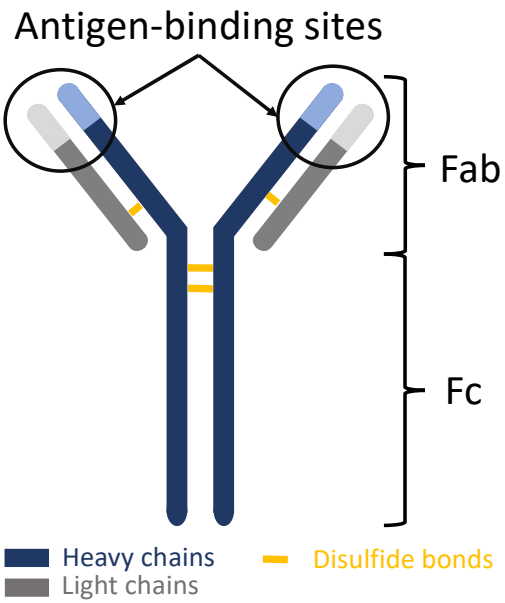

Figure 3: *Scheme of antibody IgG1. IgG consists of two heavy chains and two light chains fixed together by disulphide bridges. The structure consists of Fab (antigen-binding fragment) and Fc (constant fragment).*

Other protein-based BEs: receptors, enzymes, and short peptides

Natural molecular receptors are typically membrane proteins binding specific ligands, resulting in a cellular response in native conditions. Receptors can possess high affinity and specificity. Hardly detectable small molecules like toxins and mediators naturally target receptors, which can be used with an advantage for analytical applications (Subrahmanyam et al. 2002).

Enzymes are widely used in many scientific and industrial fields. They introduce biocatalytic functionality to the surface. However, immobilization of enzymes on a solid surface may produce alterations in their observed activity, specificity, or selectivity (Hoarau et al. 2017; Rodrigues et al. 2013). Moreover, poor stability and critical operational conditions influence enzyme activity. To address these issues, recombinant and modified enzymes have been developed lately (Bazin et al. 2017).

Short peptides can be easily designed to carry the required properties, such as charge, hydrophilicity, biorecognition abilities (Hoyos-Nogues et al. 2018), or can promote specific interactions with cells. For example, RGD-moiety containing peptides promote human cell adhesion (Takada et al. 2007; Víšová et al. 2020a) (APPENDIX VII), while other peptides are reported to have antimicrobial effects (Lim et al. 2013; Yasir et al. 2020).

Another group of non-antibody-based peptides/small proteins (~6.5kDa) reporting high affinity to target analyte consists of artificially engineered single domain proteins called affibodies. Affibodies may represent a superior alternative to antibodies, focusing on therapeutic, in vivo imaging, and biotechnological applications (Löfblom et al. 2010).

Nucleic acid-based BEs

Together with proteins/peptides and polysaccharides, nucleic acids belong to the group of the most important biopolymers creating life. They are composed of sugar-phosphate backbone, containing ribose in RNA and deoxyribose in DNA, and nitrogenous bases (pyrimidines and purines) (Figure 4). So-called base stacking, the negative charge of the

backbone, and hydrogen bonds between bases generate a stable structure and effective way of pairing complementary sequences into a secondary or higher-order structure (Figure 5). Typically, DNA tends to create a double helix structure joining two linear strands of complementary DNA, while RNA with a more flexible backbone and more hydrogen bond donors/acceptors in a structure may occupy more variable arrangements, creating for example loops, kissing loops, hairpins, bulges, or helical structures in a single strand or multi-strand manner (Figure 4). In general, nucleic acid-based detection may be more specific and sensitive than immunological-based detection, while the latter is faster and more robust (Iqbal et al. 2000).

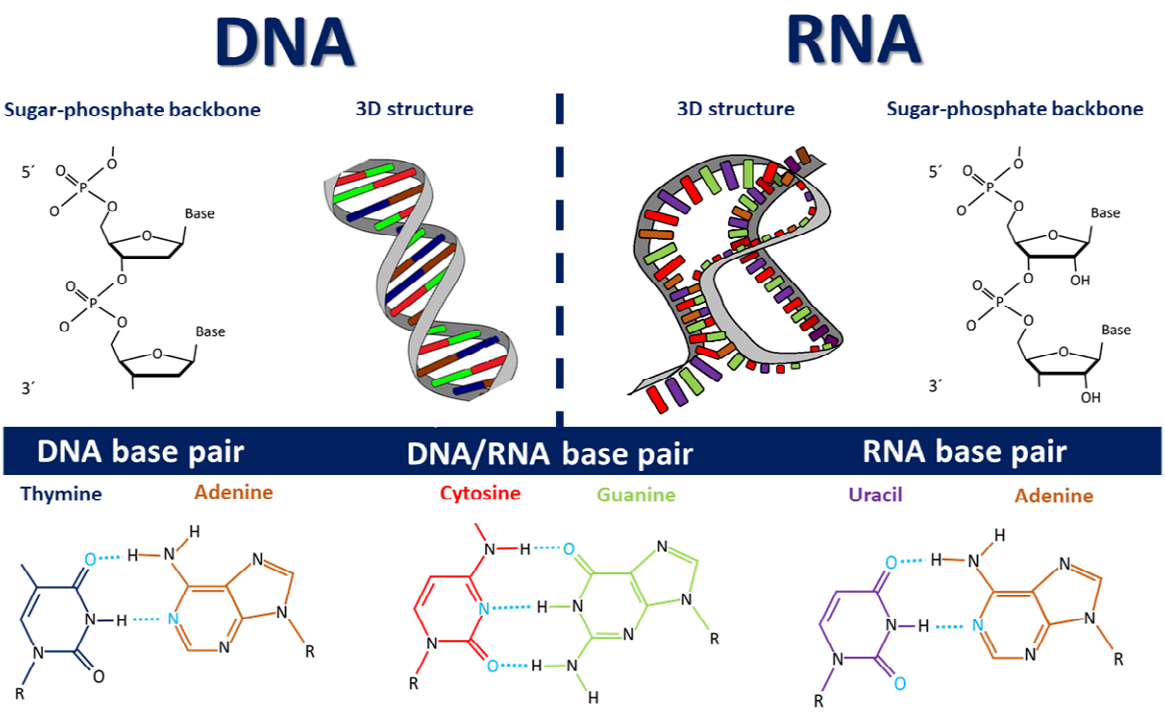

Figure 4: *DNA/RNA structure and Watson-Crick base pairing. The DNA structure contains a deoxyribose sugar and usually takes double helix form (upper left). RNA contains a ribose sugar, allowing for more flexible and less ordered 3D structures (upper right). Typically, DNA and RNA follow the so-called Watson-Crick base pairing (bottom), even though it is not the only possible way of pairing.*

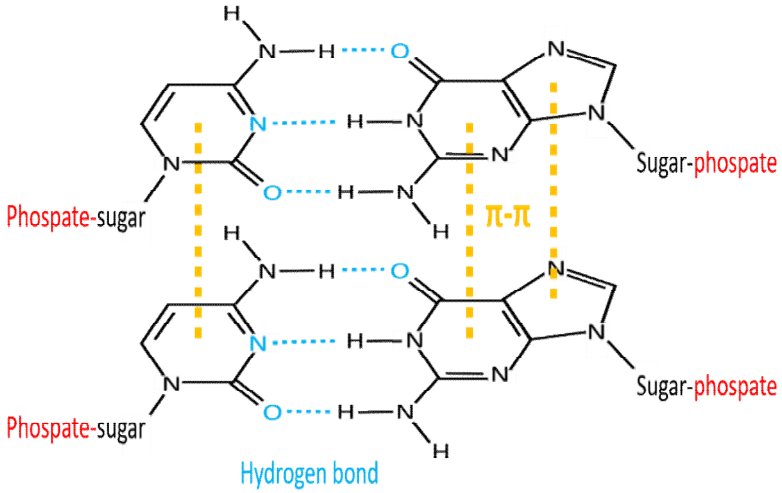

Figure 5: *Stabilization of DNA double helix by base stacking (π-π interaction, yellow dashed lines), hydrogen bonds (blue dashed lines), and negatively charged phosphates (red) stabilize the DNA double helix structure.*

The nucleic acid primary structure with the ability of highly specific complementary binding allows the use of nucleic acid-based BEs for biorecognition applications. In principle, any DNA or RNA sequence can be detected using a well-designed complementary short nucleic acid sequence as a probe immobilized on the surface (Kim et al. 2009; Nelson et al. 2001; Vaisocherova et al. 2015b) (APPENDIX I). Moreover, introducing a DNA probe on the surface can bring a possibility for subsequent surface functionalization by specific and highly selective attachment of other structures to the surface — e.g., nanoparticles (Kuzyk et al. 2012; Nie et al. 2018), biomolecules (Brambilla et al. 2021) or DNA origami (Stephanopoulos et al. 2010).

Effective use of the secondary, tertiary, or quaternary arrangements in the design of nanoengineered applications and advanced surface functionalizations approaches is mediated by nucleic acid polymer flexibility, thermodynamic stability, predictability, and programmability of interactions among structures and with the environment. DNA origami (Seeman and Sleiman 2017) are well-defined 1D–3D complex self-assembled structures with the possibility of additional and precisely located functionalization. Recently, a typical nanometre-scale size range of DNA structures was extended up to a

micrometer-scales (Yao et al. 2020). Representative applications cover assembling inorganic or organic nanostructures using DNA origami scaffolds (Paukstelis and Seeman 2016), creating nanocages (Douglas and Young 1998) used as nanoreactors, fine positioning of reaction reagents (Fu et al. 2012), or cells in the extracellular matrix (Wang et al. 2019), engineering of nanorobots capable of walking (Xing et al. 2017), or other nanomechanical tasks (Thubagere et al. 2017).

The structural flexibility of nucleic acids is used to bring a biorecognition functionality to a surface using nucleic acid aptamers (Iliuk et al. 2011). The single-stranded DNA or RNA strands selected in vitro from large libraries in procedure SELEX (Systematic Evolution of Ligands by Exponential Enrichment) are determined by their ability to create a tertiary structure with high affinity to almost any target molecule under study, mimicking selectivity and specificity of monoclonal antibodies (Mallikaratchy 2017). A wide range of targets have been used to prepare aptamers lately — from different ions (Liu et al. 2018; Liu et al. 2017), through small molecules and toxins (Kuang et al. 2010; Neves et al. 2015; Nguyen et al. 2013) to large biomolecules (Jiang et al. 2017). They offer key features like sensitivity, specificity, low immunogenicity, rapid response, and when aptamer is selected once, relatively cheap, fast, and very reproducible way of production. However, the susceptibility of aptamers to degradation by nucleases or low thermal stability still need to be addressed (Keefe et al. 2010; Kratschmer and Levy 2017). Moreover, due to the biorecognition activity dependency on the folding process and final tertiary structure, the resulting effectivity may be influenced by i) immobilization — the orientation, the surface net charge or length of the spacer between aptamer and surface play an important role in correct aptamer folding (Walter et al. 2008), and ii) the incubation conditions and running buffer/sample composition (Baldrich et al. 2004). When the conditions are optimal, and aptamer properly selected, the target-affinity can be similar or better compared to the affinity of antibodies (Crivianu-Gaita and Thompson 2016).

In 1982 a discovery of enzymatic activity of RNA structures (ribozyme) was announced (Kruger et al. 1982). From that time, ribozymes, DNAzymes, or aptazymes (ribozymes selected or engineered in the way, that their activity is modulated by the presence of target analyte) with a wide range of catalytic activities were identified or prepared.

Several different applications of DNAzymes/ribozymes can be found in literature, mostly serving as biorecognition elements for biosensing (Müller et al. 2006). For example, small peptide detection (2.4kDa) was performed using aptazyme immobilized on the quartz crystal microbalance (QCM) surface (Knudsen et al. 2006). Elsewhere, metal ions were detected using DNAzyme (Huang et al. 2017b; Zhang et al. 2011). In (Niazov et al. 2004) authors turn gold nanoparticles into catalytic labels by DNAzyme immobilization. In nanotechnology, DNAzymes are employed to obtain smart nanomaterials sensitive to chemical stimuli or to construct molecular motors with open-close or walking motions (Lu and Liu 2006; Ma and Liu 2020).

Artificial materials to mimic the function of natural BEs

To overcome insufficient stability, improve bioactivity or introduce greater variability of naturally occurring BEs, mimicking artificial constructs partly copying and partly modifying work of nature are developed. They range from semi-artificial, where at least part of the original structure is preserved, to fully artificial. Examples of semi-artificial structures are modified DNA or RNA strands resistant to nuclease activity (Beigelman et al. 1995; Keefe et al. 2010) or peptide nucleic acid (PNA). PNA is DNA-mimic polymer with negatively charged sugar-phosphate backbone changed for neutral *N*-(2-aminoethyl)glycine (Figure 6). In principle, glycine can be substituted with any other amino acid without hampering PNA properties, opening possibilities of additional engineering of final surface parameters (i.e. hydrophobicity or charge) (Nielsen 1997). Intramolecular distances are similar to the original DNA structure, so PNA can interact with other PNA or hybridize with DNA or RNA in a manner as DNA does. However, PNA is chemically stable and is resistant to hydrolytic or enzymatic cleavage, which makes it promising BE for medical, biotechnical, and biosensing applications (Cai et al. 2014; Endo et al. 2005; Moretta et al. 2020; Ray and Norden 2000).

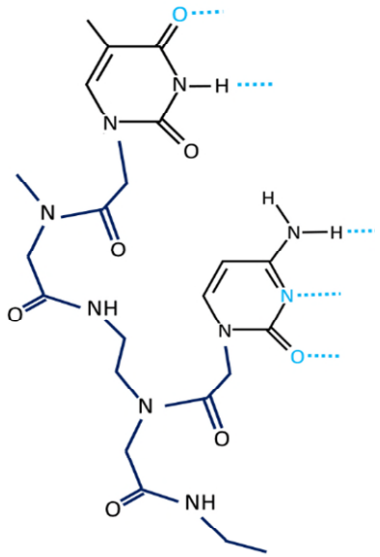

Figure 6: *PNA structure. Amino acid-based PNA backbone (dark blue) is decorated with purine or pyrimidine bases (black). Light blue dashed lines show possible hydrogen bonds with complementary bases of other PNA/DNA/RNA strand.*

Examples of purely synthetic alternatives to antibody-based molecular recognition are smart synthetic polymer materials prepared by templating the target analyte into the polymer structure (Figure 7) — so-called molecularly imprinted polymers (MIPs). Due to the intrinsically robust and stable nature of polymers, MIPs are a feasible alternative to antibodies for performing in extreme conditions, such as acid/basic environment, organic solvents, high temperatures or pressures, or after long term storage in a dry state at room temperature (Haupt and Mosbach 2000). Molecular imprinting methods are well established for small molecule biosensing (Cieplak and Kutner 2016; He et al. 2015; Ostovan et al. 2018). Last decade, MIPs used for cell recognition have been researched and reported (Pan et al. 2018).

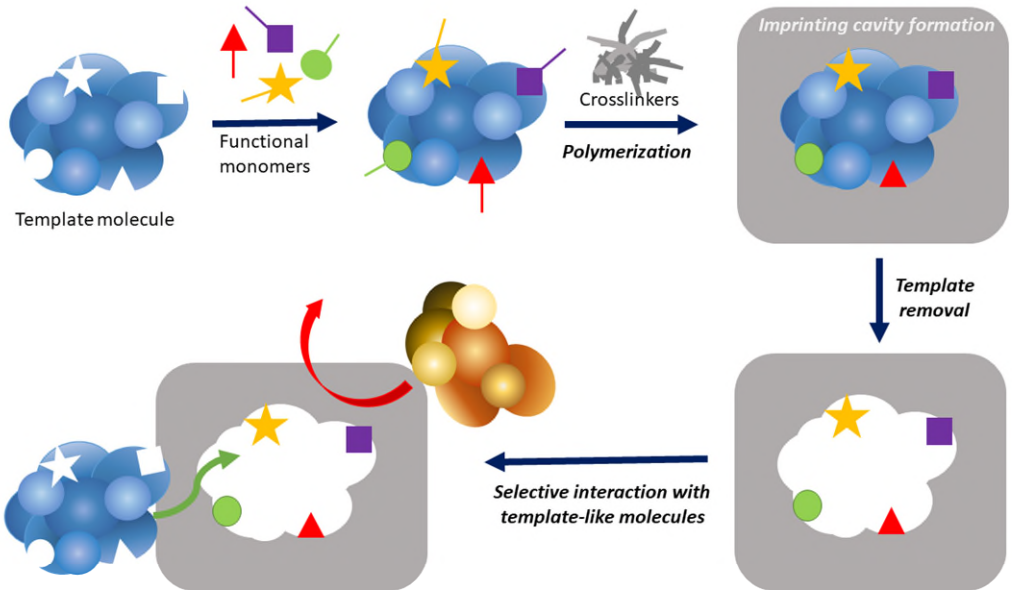

Figure 7: *Scheme of MIPs formation. The functional monomers are attached to the template molecule and subsequently, the crosslinked polymer with imprinting cavity is formed, followed by template molecule removal.*

Taking into account the inexhaustible amount of all possible functionalities that can be demanded to assign to an artificial surface for all different applications, it is clear, that there is no correct answer for the "What is the best BE?" question. There are multiple choices of different kinds of BEs for single target. For the best performance of the application, it is of great importance to select the optimal BE considering overall conditions, an environment of work, and demanding properties, such as selectivity, reusability, reproducibility, stability, reaction rate, or the possibility of long-term storage (Morales and Halpern 2018).

2.2.2. Surface Functionalization

Surface functionalization, i.e., introducing functionality to a surface (usually by the attachment of a BEs), is a complex process influencing both surface properties and bioactivity and the overall performance of the BE. The optimally functionalized surface performs its function strictly with the intended yield and activity. To achieve such a challenging outcome, the proper strategy of functionalization and a suitable type of the BE (see 2.2.1. Biofunctional elements) must be applied, so

- the BE is immobilized according to the application requirements (covalently, non-covalently, reversibly)

- the BE maintains its intended bioactivity after functionalization

- the BE is accessible to the environment if necessary for its performance.

The BE can be attached directly to the surface via adsorption. However, that may decrease bioactivity dramatically (see Chapter 2.2.2.1 Adsorption-driven functionalization). Typically, some intermediate layer (functionalizable coating) at the surface/BE interface is used as a platform for BE immobilization, preserving its bioactivity and improving overall surface performance. For most of the applications working with real-world complex samples, the “improvement of the performance” means ensuring resistance to nonspecific adsorption. Antifouling functional coatings will be discussed later in Chapter 3. Antifouling functional coatings.

The sorting of functionalization tactics is challenging, as often the processes employed during the immobilization can be included in more groups. Here, three main groups of tactics of functionalization are presented. It is non-covalent immobilization (adsorption), covalent bonding, or specific biochemical interactions. Examples are given, however, the classification of some of the examples may be questionable.

2.2.2.1. Adsorption-based functionalization

The easiest and most straightforward approach of BE immobilization on the surface is adsorption. Hydrophobic, electrostatic, weak Van der Waals intermolecular forces or hydrogen bonds can participate in adsorption (see also Chapter 2.1. Nonspecific surface-driven interactions) (Catimel et al. 1998; Jesionowski et al. 2014). However, adsorption as a direct way to immobilize BE on the surface may discredit its bioactivity by denaturation or random orientation (Sharma et al. 2016; Um et al. 2011). Moreover, adsorption is environmentally dependent and desorption can occur with the change in conditions such as pH, temperature, or ionic strength (see Chapter 2.1.4 Desorption or Exchange).

Physisorption

According to the changes in the electronic structure of BE upon adsorption, two types of the process can be distinguished. Physisorption is nonspecific interaction including weak Van der Waals forces and hydrophobic interaction, happening fast, while the electronic structure of the BE is only slightly modified. On the other hand, chemisorption is chemically specific, slower and the electronic structure of BE is changed significantly upon adsorption, creating new bonds with the surface (Leed et al. 2005; Long 2013). In (Huber et al. 2019) it was shown, that physisorption can evolve into chemisorption by simply changing environmental conditions. Physisorption as an immobilization technique usually leads to lower bioactivity of BEs. In (Kaur et al. 2016; Um et al. 2011) authors reported improved activity of antibodies electrochemically immobilized or covalently attached via EDC/NHS chemistry, compared to physisorbed ones.

Self-assembled monolayer (SAM)

The most common utilization of directional adsorption in surface functionalization is self-assembled monolayer (SAM). As a result of a complex and delicate combination of adsorption interactions between surface and adsorbate, and intermolecular and intramolecular interactions among adsorbates, highly ordered single-molecule thick assemblies are spontaneously formed on the surface under equilibrium conditions (Ulman

1996). Even though the fabrication of SAM layers is technologically attractive and cost-effective, SAMs are robust and stable and they do not tend to contain many defects, as these are thermodynamically unfavorable (Whitesides et al. 1991).

There are numerous mechanisms for SAM creation. For example, Langmuir-Blodgett films are formed when amphiphilic molecules (or nanoparticles) are spread on a liquid-air interface, creating a layer, which is transported on a solid surface via immersing (Davis and Higson 2005). Polymer and polymeric composite Langmuir-Blodgett films were applied in a wide range of fields, from biosensors, electroluminescence devices, polymeric light-emitting diode to microelectronic devices (Kausar 2017). Another example is electrostatic self-assembly (ESA) formed mostly due to the electrostatic interaction of oppositely charged ions. Multilayer polymeric thin films composed from polyanion and polycation layers were reported and applied in chemical sensing, non-linear optics, or as functional films in other applications (Decher 1997; Huie 2003; Vakurov et al. 2005; Wang et al. 2006b; Xu et al. 2005).

A special group of SAM consists of chemisorbed self-assembled monolayers, originated from an interaction between surface and specific functional group of adsorbent, resulting in the creation of chemical bond (Netzer and Sagiv 1983). The structure of such molecule can be written as R_1-(hydrophobic moiety)-R_2, where R_1 is a hydrophilic functional moiety, R_2 is a moiety chemically reactive to the substrate, and (hydrophobic part) is usually alkane chain $(CH_2)_n$, typically for $n > 11$. Hydrophobic interaction between the middle part and chemisorption of the reactive R_2 group onto the surface assures the creation of a densely packed and firmly bound layer of hydrophilic moieties facing into the biological sample (Figure 8). The commonly used R_2 groups for surface functionalization are silanes and thiols.

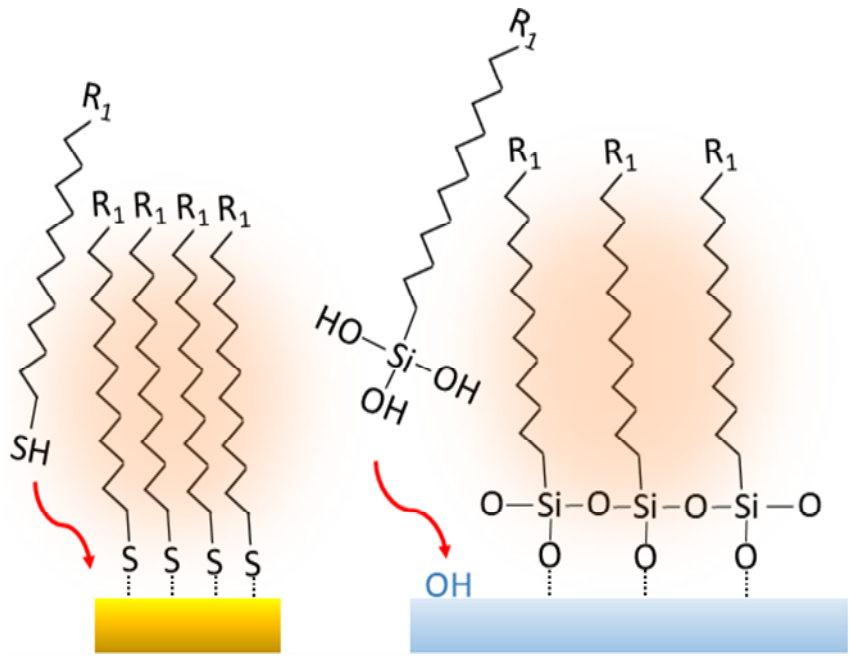

Figure 8: *SAM layer formation. The layer is formed by functional group adsorption (dashed black line) and hydrophobic interaction among alkan chains (orange). Left: Thiolated SAM layer on gold surface. Right: Silane SAM layer on hydroxylated surface.*

In situ formation of Si-O-Si bond between hydroxylated surface and organo-functional alkoxysilane molecules (Issa and Luyt 2019) allows the creation of SAM on surfaces, such as silicon oxide, aluminium oxide, quartz, glass, mica, zinc selenide, germanium oxide, gold (Ulman 1996) or even carbon nanotubes (Ma et al. 2006). The quality of SAM provided by the process of silanization is dependent on precise condition control – optimized concentration of water in the solution, temperature, or the structure of the surface can influence the result. The advantage of silanization is the possibility to functionalize transparent substrates, such as glass if needed for the application, thermal stability up to 250 °C, and the fact that they do not swell in the presence of solvents (Lessel et al. 2015). Silanes have been used in many applications to functionalize surfaces for cell adhesion studies (Faucheux et al. 2004), biosensors (Hideshima et al. 2013), engineering of higher

and more sophisticated structures (Ruckenstein and Li 2005) or to passivate the surface against nonspecific interactions (Cox et al. 2002).

Sulfur and selenium have a strong affinity to transition metal surfaces. The most frequently used metal surface for biomolecular interactions studies is gold, as can be used for electrochemical, SPR, or reflection-based measurements. A wide range of organosulfur compounds was reported to create a SAM layer on gold, the most popular and best understood are alkanethiols. A fully saturated surface exhibit a dense “standing up” position, creating an oriented few nanometres thick layer of functional molecules. The extended studies were performed to understand thiol-gold interaction and creation of SAM layer to be used in different chemical, biophysical, or sensing applications (such as surface passivation, creation of initiator layer for other chemical reactions, functionalizable biosensing platform, etc.) reviewed elsewhere (Al-Rawashdeh and Azzam 2011; Chaki and Vijayamohanan 2002; Luderer and Walschus 2005; Wink et al. 1997)

2.2.2.2. Covalent immobilization

Covalent attachment of BE is the most stable and long-term durable way of immobilization. Usually, the creation of a covalent bond between two naturally non-interacting biological moieties is thermodynamically unfavorable and requires some kind of activation – physico-chemical or chemical.

Depending on the technique used, covalent immobilization of BEs may lack control over orientation and accessibility of bioactive sites — especially when the immobilization chemistry depends on BE's endogenous functional groups which are not present only at a unique and site-specific location on BE surface. However, even in those cases, the immobilization is not completely random – before covalent attachment, BE must undergo physisorption. The orientation of the molecule during physisorption is dependent on pKa, an isoelectric point of BE, and pH of the environment. By optimizing the immobilization conditions, at least partial orientation after immobilization can be achieved (Pei et al. 2010; Yuan et al. 2012).

Carboxy group conversion

The direct conversion of a carboxylic acid into an amide in mild conditions is thermodynamically unfavorable, the equilibrium reaction of the carboxy group is esterification. To favor amide formation, activation of carboxylic acid carbon allowing subsequent attack by the amino group is necessary. A plethora of methods how to activate carboxy components can be found – acyl halides, acyl azides, acyl imidazoles, anhydrides, esters, etc (Montalbetti and Falque 2005). Every method has advantages and drawbacks, which can result in low yields, racemization, degradation, or difficult purification. For the field of surface functionalization, the most commonly used methods are the two listed below.

The most popular tactic to conjugate carboxy groups with primary amines is carbodiimide-based chemistry proceeding through the *O*-acylisourea intermediate. For carboxy activation in non-aqueous applications, (e.g., organic synthetic methods) dicyclohexylcarbodiimide (DCC) or diisopropylcarbodiimide (DIC) are feasible to use (Huang et al. 2017a). For bio-functionalization, the aqueous environment is usually required and so water-soluble molecule 1-ethyl-3-(3-dimethyl aminopropyl)carbodiimide (EDC) is the preferable choice. Figure 9 shows the reaction schemes. After the reaction of the carboxy group with the activation agent, an unstable *O*-acylisourea intermediate is formed. Further, four different pathways of reaction are possible. The entering reaction is reversible, so intermediate may decompose into original reactants. Also, a stable side product of the reaction *N*-acylurea can be formed. Finally, *O*-acylisourea can turn into amide either through an intermediate step (anhydride formation) or by nucleophilic attack from primary amine creating amid directly (Iwasawa et al. 2007).

O-acylisourea is prone to fast hydrolysis in aqueous solutions. The resulting low reaction yield can be improved using additives like *N*-hydroxysuccinimide (NHS) or sulfo-NHS, converting unstable *O*-acylisourea into a more stable NHS-ester, which efficiently forms

an amide with a primary amine in a slightly alkaline solution at room temperature (Yan et al. 2015).

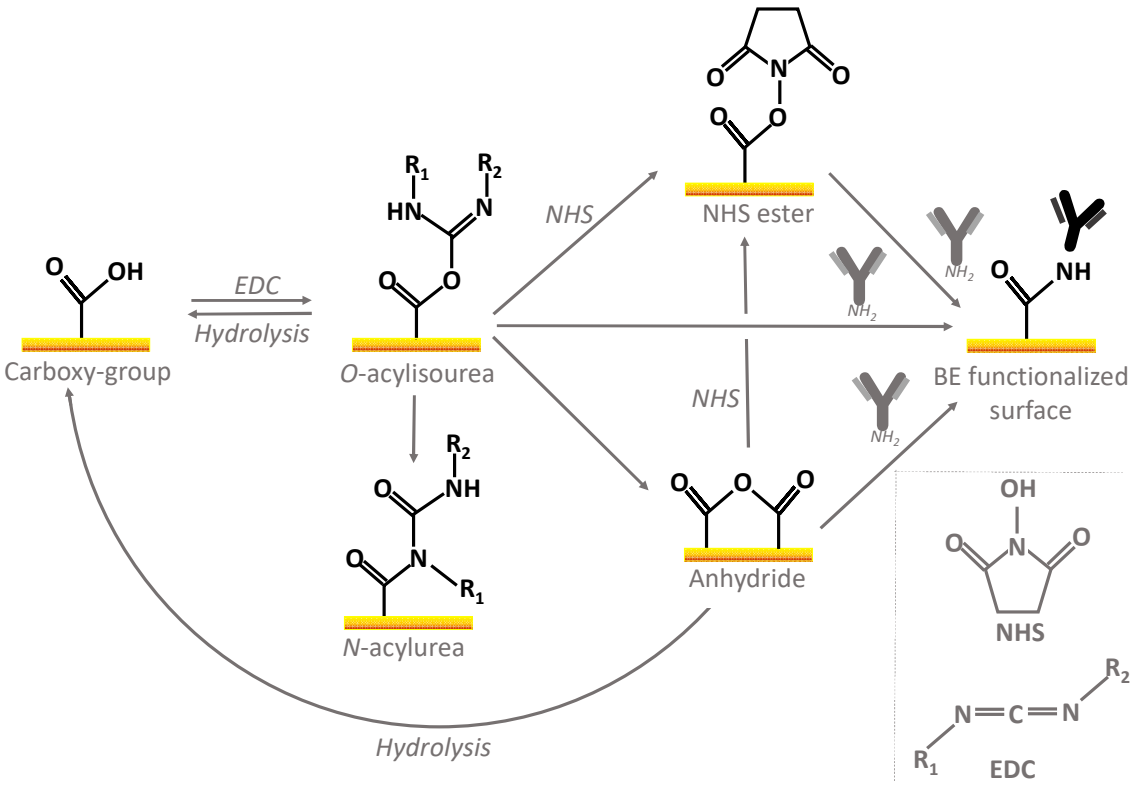

Figure 9: *Scheme of the EDC/NHS based functionalization. Surface carboxy groups are EDC activated to form O-acylisourea. O-acylisourea can be subsequently hydrolysed back to carboxy groups, rearranged into a stable side product of N-acylurea, reacted with NHS to form more stable NHS-ester or turned into amide directly or through an intermediate step of anhydride formation.*

Generally, it is assumed that unreacted NHS esters may be effectively hydrolyzed and all the corresponding carboxy groups recovered (Lim et al. 2014). Even though amine-reactive NHS ester in solution was reported to hydrolyze fast (Cline and Hanna 1988), Schönherr et al. showed a significant decrease in rate constants of hydrolysis of active

esters bound to surface caused by in-plane confinement effects (Schönherr et al. 2003). Later, Lísalová at al. observed only partial hydrolysis of NHS-esters in zwitterionic polymer brush coatings even after tens of minutes of hydrolysis (Lísalová et al. 2017) (APPENDIX IV). The residual NHS esters may potentially react with smaller non-target nucleophiles presented in the analyzed medium, therefore it is of great importance to include a proper deactivation step into a functionalization procedure. Besides hydrolysis, the most commonly used EDC/NHS deactivation is the covalent attachment of small molecules containing primary amines, such as ethanolamine. Lately, for zwitterionic structures, more advanced deactivation procedures were suggested (Lísalová et al. 2017) (APPENDIX IV, APPENDIX XIII, APPENDIX XIV, APPENDIX IX, APPENDIX XVI). The further study on deactivation processes in zwitterionic structures is a part of this thesis — more information can be found in Chapter 5.2.

Hydroxyl group conversion

In general, the hydroxyl group is not very reactive, therefore it needs to be activated before the amid formation (Morpurgo et al. 1999; Rodriguez-Emmenegger et al. 2011b). Frequently used reagent *N*,*N´*-disuccinimidyl carbonate (DSC) is not water-soluble, and in aqueous solutions hydrolyze fast into two molecules of NHS and carbon dioxide. In the non-aqueous environment, DSC reacts with the hydroxyl group creating succinimidyl carbonate and subsequently, after reaction with a primary amine, highly stable carbamate (Figure 10). To increase the reaction yield and decrease side products, additive 4-(dimethylamino)pyridine (DMAP) or hydroxybenzotriazole (HOBt) can be used. DSC/DMAP immobilization tactic was used for example to attach anti-bacterial antibody onto hydroxy-functional poly(2-hydroxyethyl methacrylate) (pHEMA) polymer brush. However, once the surface was activated, it completely lost its resistance to fouling (Vaisocherova et al. 2014). Elsewhere, poly(oligo(ethylene glycol) methacrylate) (pOEGMA) brushes were successfully streptavidin-functionalized using DSC chemistry (Trmcic-Cvitas et al. 2009).

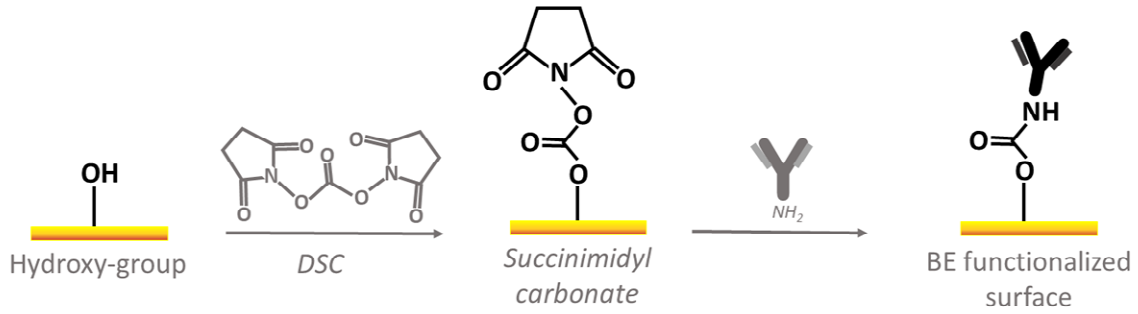

Figure 10: *Scheme of DSC based surface functionalization. The surface-attached hydroxyl group is activated by DSC creating succinimidyl carbonate and subsequently, after reaction with a primary amine-containing molecule the carbamate covalent bond between the molecule and surface is creating.*

Epoxide-amine reaction

Due to the electrophilic character of the heterocyclic moiety and ring strain, epoxides (also called oxiranes) are prone to nucleophilic ring-opening reactions. Nucleophilic attack on the epoxide group has been demonstrated using nitrogen nucleophiles (Fan et al. 2006b), carbon nucleophiles (Faiz and Zahoor 2016), or sulfur (Polshettiwar and Kaushik 2004) nucleophiles. Depending on the nucleophile used and the structure of the molecule bearing epoxide moiety, the product of the epoxide ring-opening reaction can be flexibly varied (Figure 11).

Mostly, the ring-opening reaction is used as a polymerization tactic, even though BE functionalization can be found in literature too. In a review, Wheatley and Schmidt discuss the enhancement of the immobilization of BEs (proteins, oligonucleotides, and peptides) to epoxide-activated silica or polymers using high concentrations of certain salts, such as ammonium sulfate and potassium phosphate (Wheatley and Schmidt Jr 1999). In (Thomas et al. 2014) authors utilize surface epoxide groups on the graphene oxide to functionalize it with thiol groups, further used for functionalization. Elsewhere, authors used epoxide-opening ring reaction to create antibacterial polypeptoid containing sulfonium and oligo(ethylene glycol) (OEG) moieties (Zhang et al. 2020). In (Li et al. 2008) authors used

epoxide-amine coupling reaction to immobilize DNA onto epoxide group-containing coating of an electrochemical biosensor.

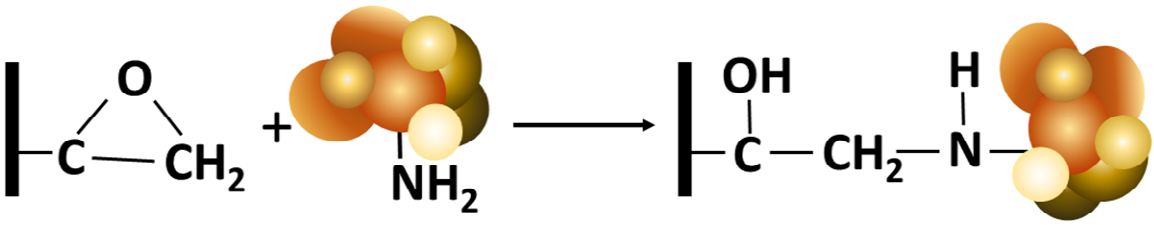

Figure 11: *Epoxide-amine ring-opening reaction in surface functionalization. Nucleophilic attack of a primary amine of a molecule on the surface-immobilized epoxide group creates a covalent bond between the surface and the molecule.*

Photoactivation

Besides chemical-based activation, photoactivation has been studied intensively. The light-induced reaction between photoreactive probes (such as benzophenone) and C-H bonds of BE can create a covalent bond (Browne 2008). Unlike chemical activation, photoactivation allows using of the photolithographic approaches, producing BE micropatterning (Hahn et al. 2006). Such a method can be used for the preparation of polymer-modified surfaces using spin-coating of polymerizable monomers on the substrate, followed by polymerization using UV light. For example, in (Wang et al. 2010) such coating was used in a biosensor for IgG detection based on optical waveguide spectroscopy. Nahar et al. used UV irradiation of photoreactive aromatic azide 1-fluoro-2-nitro-4-azidobenzene to activate polystyrene surface for subsequent enzyme immobilization (Nahar et al. 2001). Photoactivation can be used to induce polymerization during MIPs preparation (see also Chapter 2.2.1) (Piletsky et al. 2000), or to induce a click-chemistry-based reaction, e.g. thiol-en reaction (Uygun et al. 2010).

Click-chemistry

To solve the non-oriented immobilization problem and possible loss of the bioactivity of BE when endogenous groups are used in the covalent attachment, bioorthogonal chemistry was introduced to the field of functionalization. Bioorthogonal chemistry is a subclass of the so-called click chemistry. It covers a group of highly selective reactions that with high yield, under ambient conditions, without side-products, and without interfering with any biological or chemical process create covalent bonds (Jewett and Bertozzi 2010). Specifically, the presence of the biorthogonal group is not influencing or cross-reacting with BEs endogenous functional groups and it is not altering its bioactivity, however, it reacts with functional groups of the surface, enabling the specific immobilization of target BEs in a spatially confined fashion under mild conditions.

The most common orthogonal click-chemistry reaction is copper-catalyzed azide-alkyne cycloaddition (CuAAC) or strain-promoted 1,3-dipolar cycloaddition (SPAAC) of azides and alkynes (Figure 12 A and B) (Dommerholt et al. 2016; Parrillo et al. 2017; Rostovtsev et al. 2002). The azide-based click-chemistry was used for example in (Alemán et al. 2009) for DNA immobilization for single-molecule fluorescence studies, or in (Huang et al. 2014) to immobilize sulfobetaine groups on cellulose membranes.

Another example of click-chemistry is a thiol-en reaction, which after photochemical or thermal initiation creates a covalent thioether bond between thiol and alkene (Figure 12 C) (Campos et al. 2008; Connal et al. 2009). In (Mahmoud et al. 2011) authors presented copper(I)-catalyzed azide-alkyne and thiol-en click-reaction for self-assembled coiled-coil peptide fibers functionalization. Thiol-maleimide interaction (Figure 12 D) (Northrop et al. 2015) was used in bioconjugation (Martínez-Jothar et al. 2018; Miyadera and Kosower 1972) and polymer and material synthesis (Pounder et al. 2008; Qin et al. 2017; Stenzel 2013).

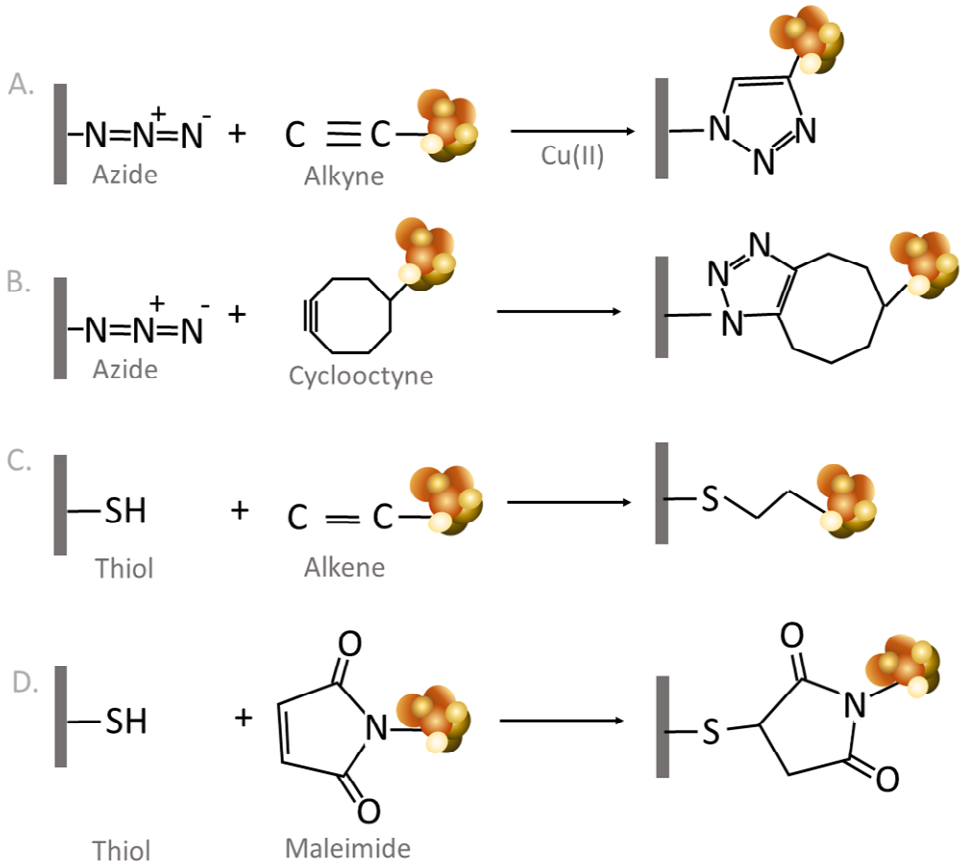

Figure 12: *Examples of click-chemistry reactions. A: Copper-catalyzed azide-alkyne cycloaddition (CuAAC). B: Strain-promoted cycloaddition (SPAAC). C: Thiol-en reaction. D: Thiol-maleimide reaction.*

2.2.2.3. High-affinity molecular systems

Due to the frequent use, a specific high-affinity molecular systems earn its category among previously described interactions. The affinity is given by a combination of non-covalent forces and steric complementarity. Such a system can be used for bio-detection directly (as BE and target pair), or another BE can be modified using one of the two affinity partners to be attached on the surface using high-affinity pair interaction. A list of examples is given below.

Streptavidin/avidin/NeutrAvidin – biotin interaction

Streptavidin, avidin, or NeutrAvidin are tetrameric proteins isolated from actinobacterium Streptomyces avidinii, eggs of birds, or engineered from avidin, respectively. The high affinity of all of them to small molecule biotin (dissociation constant K_d~10^{-15} M) is given by the formation of multiple hydrogen bonds, van der Waals forces, and steric effects given by changes in streptavidin structure after binding of the biotin (Weber et al. 1989). One protein can bind up to 4 biotins.

Even though avidin and streptavidin show similarities in structure and affinity to biotin, they report very little amino acid homology. Avidin is highly glycosylated and has a basic isoelectric point (10–10.5), therefore it is easily soluble in aqueous solutions. On the other hand, streptavidin has no carbohydrates and an acidic pI (5) resulting in lower solubility in water. Moreover, streptavidin is more costly to produce (Almonte et al. 2014; Chaiet and Wolf 1964). Streptavidin suffers less from nonspecific binding (especially due to the absence of lectin-carbohydrate reactions and lower pI) compared to avidin. However, streptavidin contains bacterial recognition RYD motif, which can cause nonspecific background in some applications. To overcome most of the disadvantages, artificially engineered deglycosylated avidin called NeutrAvidin was introduced. It reduces lectin binding, has nearly neutral pI (6.3), and does not have an RYD motif, which all significantly decrease nonspecific interactions in typical applications.

Avidin/streptavidin/NeutrAvidin-biotin interaction is considered to be the strongest non-covalent interaction between protein and ligand, fast and stable in extreme pH, temperature, organic solvents, or presence of denaturing agents. Many applications use biotinylation of targets or BEs as a gentle method to tag proteins and/or to immobilize them on avidin/streptavidin/NeutrAvidin surface (Figure 13). For example, in (Caswell et al. 2003) authors used a biotin-streptavidin-biotin system for the end-to-end connection of biotin-functionalized nanorods creating µm-range sized constructs. Streptavidin-coated metal nanoparticles can be used for signal amplification in SPR biosensors – for example, Vaisocherová et al. showed up to two orders of magnitude increase in SPR signal after interaction of streptavidin-coated gold nanoparticles with biotin-labeled anti-

bacterial antibodies used in the sandwich assay for the detection of *Escherichia coli (E. coli)* O157:E7 in crude food samples (Vaisocherová-Lísalová et al. 2016b) (APPENDIX II). Biotinylated DNA probe was immobilized on avidin layer prepared on QCM surface in nucleic acid biosensor development (Caruso et al. 1997).

However, one has to keep in mind, that there may be more biotin-binding molecules in complex samples and that biotin is a naturally occurring molecule in bodily fluids or foods. Non-zero background, cross-reactivity, and specificity issues must be considered in experiments using avidin/streptavidin/NeutrAvidin-biotin interaction.

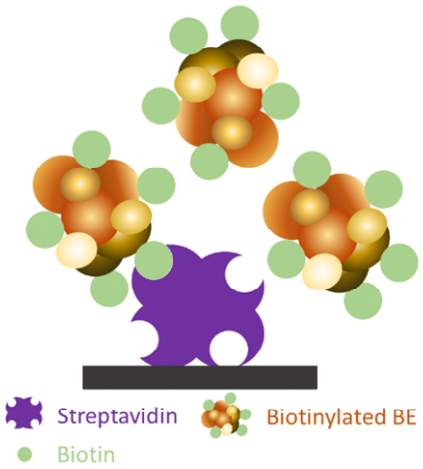

Figure 13: *Streptavidin-biotin based BE immobilization.*

Immunoglobulin-binding proteins

Protein A, G, and L are cell wall surface proteins from the *Staphylococcus aureus (S. aureus), Streptococcal bacteria,* and *Peptococcus magnus*, respectively. While protein G and A show a high affinity for the binding of the heavy chain of the Fc region of most immunoglobulins, protein L binds immunoglobulins specifically through the variable domain of Ig light chains, without interfering with the antigen-binding site (Björck 1988; Nilson et al. 1993). Therefore, protein L binds representatives of all classes of antibodies, single-chain variable fragments, and Fab fragments. Comparing protein A and protein G avidity for IgG, protein G reports greater avidity than protein A although over a narrower spectrum of Ig classes (Kim et al. 2010).

Often, the protein A and G are used to create easy-to-use chromatography media for routine purification of antibodies (Liu et al. 2010). Also, both proteins are used for oriented immobilization of antibodies (Bae et al. 2005; Horáček and Skládal 2000; Lu et al. 2008). Oriented immobilization of haptoglobin antibodies on gold nanoparticles deposited on QCM crystal was performed using protein A and used for biosensing (Wang et al. 2004). In (Yamazoe 2019) authors show improvement in biotin binding capacity of anti-biotin antibodies immobilized using protein G compared to covalently attached antibodies randomly immobilized using EDC/NHS chemistry. Elsewhere, protein G was conjugated with a short single-strand DNA sequence and immobilized on the surface using a complementary DNA probe. After, the anti-human prostate-specific antigen antibody was immobilized using protein G interaction, and detection of prostate-specific antigen was performed (Jung et al. 2007).

It is worth mentioning, that different recombinant forms of protein A, G, and L can be found in the literature. In (Seo et al. 2013) authors introduced recombinant protein A, G, and L containing antibody binding motifs while C-terminal possesses motifs for further click chemistry application. Protein AG (Eliasson et al. 1988) or LG (Kihlberg et al. 1996) are recombinant fusion proteins combining IgG binding domains of protein A and G or proteins L and G.

Lectin-glycan interaction

Lectins are carbohydrate-binding proteins, highly specific for carbohydrate groups (Duverger et al. 2003). They are used in a wide range of applications, e.g., cell studies, bacterial detection and biosensors, blood typing, or therapeutics research. Comparing to antibodies, lectins are cheaper and bind generally specific groups of glycans, while antibodies show higher specificity to certain glycans (Cummings and Etzler 2009).

For example, in (Garcia-Gradilla et al. 2013) authors engineered magnetically guided ultrasounds-powered nanowire motors functionalized with lectin and anti-protein A antibody to capture and transport bacteria *E. coli* and *S. aureus*. Perhaps the most widely used plant lectin is α-mannose / α-glucose-binding lectin concanavalin A (ConA) extracted

from *Canavalia ensiformis* containing 4 binding sites for glucose per one molecule. ConA was extensively studied as a receptor in glucose sensors (Pickup et al. 2005) or as a receptor used for bacterial separation (Campuzano et al. 2012). ConA conjugated to pesticide 2,4-dichlorophenoxyacetic acid was attached to surface using SPR chip modified with covalently bound *α*-d-glucose, creating regenerable indirect detection assay for pesticide detection (Švitel et al. 2000).

Coiled-coil protein motif

The coiled-coil is a motif of tertiary protein structure created by amphipathic interaction between two zipping domains. Both domains have a specific repetition-based primary structure allowing interaction of both domains and creation of tertiary structure in a manner, that hydrophobic amino acid residues (leucine or leucine-like residues) can be buried at the interface of both domains, while other hydrophilic residues face the environment (Figure 14). The resulting motif is made of two α-helices wrapping around each other forming a stable supercoil (Yu 2002). Coiled-coil motifs were extensively studied and de novo engineered structures were suggested for biosensor applications (Chao et al. 1998) or self-assembled protein architectures, such as nanocages and nanocarriers used as cargo delivery (Lim et al. 2017). For example in (Kruis et al. 2016), leucine zipper (subgroup of coiled-coil motifs) interaction was used for site-specific protein immobilization in biosensor application. Another functionality brought coiled-coil structures to mesoporous silica nanoparticles, where it works as thermoresponsive valves for cargo releasing (Martelli et al. 2013). Coiled-coil tethering was used for growth factors immobilization on chondroitin sulfate coating while preserving growth factors bioactivity (Lequoy et al. 2016).

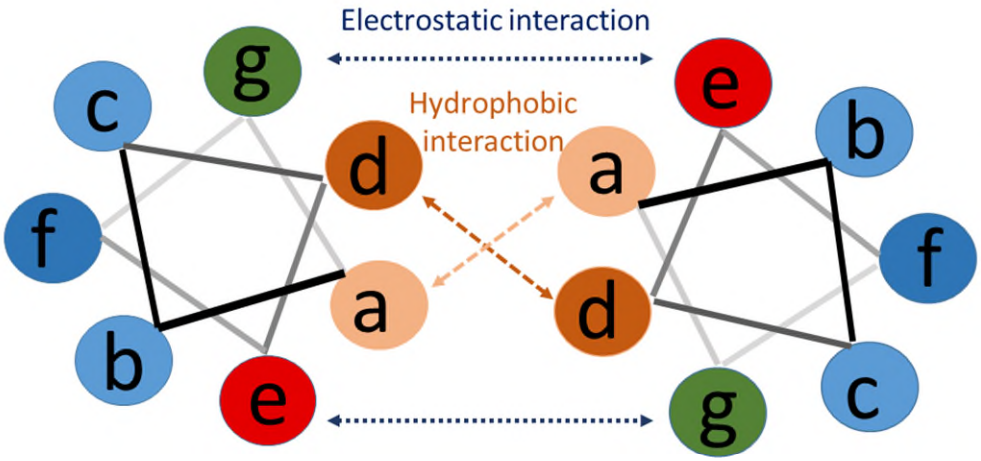

Figure 14: *Scheme of the typical coiled-coil arrangement. Amino acids are arranged in repeating blocks of 7 residues. Residuum "a" and "d" are hydrophobic, "e", "g" usually oppositely charged and "b", "c", "f" are hydrophilic.*

Mussel adhesive proteins

The inspiration by nature brought mussel-inspired adhesive peptides into a focus of surface engineering and research of adhesives, as a universal anchor for surface modification. A mussel produces 20 types of adhesive mussel foot proteins, performing extraordinary long-term adhesive capabilities even in a wet and saline environment, adhering to virtually all types of inorganic and organic surfaces (Lee et al. 2006). Further research of the proteins pointed out the amino acid 3,4-dihydroxy-L-phenylalanine (DOPA) containing catechol group as a key component in the adhesion process. Lately, proteins and polymers incorporating DOPA or other catechol group moiety have been engineered.

Catechol group in a helical *N*-propargylamide copolymer provided structure with metal ion-adsorption abilities (Li et al. 2010). Elsewhere, a catechol group was used in the preparation of hydrogel structure to introduce extraordinary stretchability, high toughness, and stimuli-free self-healing ability. Importantly, the hydrogel film could be repeatedly adhered on / stripped from a variety of surfaces, introducing a great platform for further functionalization of various surfaces (Han et al. 2017). Catechols are used as

anchoring layers for antifouling and antibacterial polymer brushes (Kirk et al. 2013; Li et al. 2011; Sundaram et al. 2014; Yang et al. 2011b; Yu et al. 2014) or immobilization of BEs. ConA immobilized on gold, indium, and iridium (Morris et al. 2009), bovine serum albumin (BSA) on diamond-like carbon, or polyethylene membranes (Tao et al. 2009; Zhu et al. 2011), bone morphogenetic protein 2 on TiO_2 nanotubes (Lai et al. 2011), or heparin on poly(vinylidene fluoride) (Zhu et al. 2009) were reported.

The great advantage of catechol-based interaction is a wide range of organic and inorganic surfaces where the adhesion is effective. On the other hand, nonspecific interactions with complex samples must be actively suppressed, otherwise, they will strongly interfere with the experiments.

Disulfide bridge

Disulfide bridges are formed after oxidation of two thiol groups. It is typical interaction between two cysteines, helping to create and hold the secondary, tertiary, or quaternary structure of the proteins. The disulfide bridge is stronger than the hydrogen bond, but weaker than the covalent bond and is feasibly cleavable in mild conditions using a reducing agent. In (Kam et al. 2005) authors created thiol-functionalized single-walled carbon nanotubes for repeatable functionalization. Disulfide bridges are used in the preparation of degradable polymers (Tsarevsky and Matyjaszewski 2005), for preparation of thiol-functionalized polymers for attachment of biomolecules (Bontempo et al. 2004) or in reversible photopatterning strategy based on a photoinduced disulfide exchange reaction allowing reversible photofunctionalization, patterning, or removal of surface functional groups (Du et al. 2015)

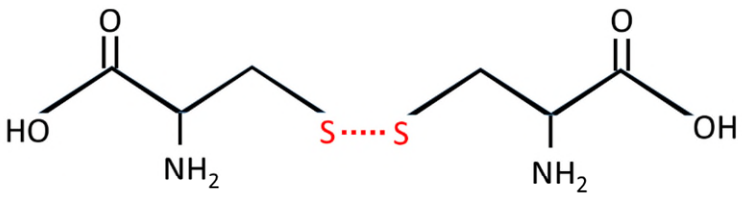

Figure 15: *Disulfide bridge between two cysteines.*

Specific metal-protein interactions

Metal affinity non-covalent interactions between complexes of nitrilotriacetate with Ni^{2+} or Cu^{2+} and oligohistidine sequence is typically used in biochemical and bioanalytical applications. Polyhistidine tags are used for surface-based protein purification in metal-affinity chromatography (Arnold 1991; Block et al. 2009; Jain et al. 2007; Xu et al. 2011), protein interaction studies (Li et al. 2016), or in biosensors (Auer et al. 2017; Ferapontova et al. 2001). For example, reversible oriented immobilization of histidine-tagged anti-lysozyme fragment onto a gold surface using self-assembled synthetic chelator thioalkane was used to demonstrate the usefulness of such immobilization method for bioanalytical applications (Kröger et al. 1999).

3. Antifouling functional coatings

Working with biological and real-world complex samples inevitably leads to a need for an extra surface functionality – resistance to nonspecific fouling. Reducing fouling-based interferences provides a control over the unique functionalities and the interactions occurring at the functionalized surface. A common approach to reduce the fouling used to be using of the dextran surface chemistry, surfactants (e.g., Tween), or additives (e.g., BSA or casein) to saturate possible binding spots on the surface before complex sample introduction. However, such blocked surfaces have only limited antifouling properties (Masson 2017). Moreover, blocking the surface may lead to a substantial reduction in the biorecognition activity of immobilized BEs (Vaisocherová-Lísalová et al. 2016b; Vaisocherova et al. 2014; Vaisocherova et al. 2008) (APPENDIX II). To achieve high-performing functionalize antifouling coatings, other approaches need to be adopted.

As the best-proven designer, nature has effective tactics to teach us how to avoid fouling. Hydrophobic surfaces of plants, butterflies' wings or feathers of birds, active cleaning mechanisms to remove any undesirable impurities – mechanically or using a secretion, low drag shapes and microtextures, sloughing layers, or even more sophisticated methods, such as highly hydrophilic zwitterionic moieties employment (Bixler and Bhushan 2012; Jiang and Cao 2010). Studying nature's tactics, practically three approaches to diminish fouling can be distinguished. It is either super-hydrophobic or super-hydrophilic surface treatment or active removal of fouling using chemical additives or stimuli-responsive smart materials.

3.1. Super-hydrophobic surface treatment

Employing unique chemical properties and specifically designed nanostructures, super-hydrophobic surfaces were created to repel water molecules. The contact angle is usually greater than 150°, introducing an air barrier between water and surface (Simpson et al. 2015). Even though such coatings have been proven to protect the surface from fouling, they are not feasible for further functionalization nor biomolecular interaction studies.

In biological and biomolecular research, super-hydrophobic coatings are usually used to either diminish fouling completely, create micropatterning, or control the flow of water-based fluids. For example, hydrophobic Slippery Liquid-Infused Porous Surfaces is claimed to reduce bacterial biofilm approximately 35 times better and over a longer timeframe compared to state-of-the-art PEGylated surface (Epstein et al. 2012). Wang et al. created micropatterning of living cells using hydrophilic/super-hydrophobic patterned surface (Wang et al. 2006c). In (Chen et al. 2019a) authors used super-hydrophobic-based concentration of molecules for SERS-based detection. Other non-biological applications of hydrophobic treatment are self-cleaning surfaces, fluidic drag reduction and controlled fluid transportation, humidity-proof coatings for electronic devices, super-hydrophobic textiles, or micro condensation (Ma and Hill 2006; Zhang et al. 2008).

3.2. Hydrophilic antifouling coatings

3.2.1. Key parameters for antifouling properties

Hydrophilicity

Hydrophilicity is one of the key properties of antifouling coatings. When two hydrophilic surfaces are separated by a very thin water layer, the hydration (solvation) repulsive force prevents them from approaching. So, the hydration level formed by the water near

hydrophilic surfaces presents an extra energy barrier for molecules to be adsorbed, preventing the fouling (Chen et al. 2010; Kanduč et al. 2016; Zheng et al. 2005).

Hydrophilic non-charged structures get hydrated using weak and temperature-dependent hydrogen bonds between water and surface-attached hydrogen bonds donors/acceptors (Corkhill et al. 1987), while charged structures employ stronger electrostatic-based ionic solvation. Generally, both electrostatically induced hydration and hydration via hydrogen bonds are influenced by environmental properties, such as salt ion presence. In theoretical work (Urbic 2014) author shows that the presence of ions in the proximity of hydrogen donors/acceptors will change the strength of hydrogen bonds which can lead to the rearrangement of water molecules in the structure. In (Leng et al. 2014) the SFG results indicate that the surface hydration of zwitterionic materials is mediated by environmental parameters including ionic strength, ion size, charge, and pH.

A typical strategy to increase the hydrophilicity of the surface is introducing some hydrophilic moiety into the coating — hydrophilic peptides, zwitterionic groups, oligo- or poly(ethylene glycol) group (OEG or PEG, respectively), or saccharide based hydrophilic moieties, such as hyaluronic acid or dextran sulfate polymers.

Thickness

The other crucial parameter for antifouling properties is the coating thickness, creating steric hindrance between sample matrix and hydrophobic substrate (Chen et al. 2014; Chou et al. 2016b; Yang et al. 2008; Zhao et al. 2011). Depending on the coating flexibility and level of hydration, the thickness may be a dynamic variable responding to the environment (ionic strength, pH, temperature) (Víšová et al. 2020c) (APPENDIX VI). Transition changes between hydrated and dehydrated states are called swelling or collapse. The dry thickness, corresponding to the collapsed dehydrated material of the coating, is the most commonly used parameter to characterize coatings. However, the swelling after hydration may change the thickness up to 3 orders of magnitude, as was reported for example in hydrogel structures (Hoffman 2012). Subsequently, the sensitivity and reliability of surface-sensitive characterization methods (e.g., surface plasmon

resonance (SPR), surface-enhanced vibration spectroscopies, or ellipsometry) may be impaired.

Charge

The electrostatic force is an important part of the nonspecific interactions, therefore charge control is crucial in antifouling coatings. The coating can be designed according to the application needs — it can be positively charged, negatively charged, neutral or zwitterionic. The best performing antifouling coatings are typically either neutral or zwitterionic. In some applications, the original charge of the surface may be used to streamline the immobilization, while after BE attachment subsequent reactions turn coating into a charge-neutral surface. Such strategy is used for example in negatively charged alkanethiolated SAMs with carboxy functional groups. After EDC/NHS activation and BEs attachment, the deactivation step turns remaining active esters into non-reactive neutral hydroxyl groups using covalent attachment of small molecule ethanolamine (Chadtová Song et al. 2019; Špringer et al. 2020; Vaughan et al. 1999).

Zwitterionic materials, inspired by the surface of mammalian cell membrane rich in zwitterionic phosphatidylcholine, introduce very promising antifouling properties. An ionic molecule with a neutral net charge is created by the same amount of negative and positive charges situated close to each other. Such coatings naturally decreased electrostatic nonspecific interactions and possess a high level of strong hydration, supported by hydrogen bonds and ionic solvation. However, their isoelectric point should be considered during the design of the application, as pH can change the coating charge and subsequently its properties (Guo et al. 2015). Some of the more common zwitterionic functional groups used in antifouling coatings are amino acid cysteine, phosphorylcholine, or betaines (e.g. sulfobetaine, carboxybetaine, phosphobetaine, sulfopyridinium betaine, or sulfobetaine siloxane) (Schlenoff 2014). Using zwitterionic functional blocks, different structures can be built — from SAM layers to polymer brush coatings or hydrogels. A short review of such coatings will be given further in appropriate sections.

Resistance

The combination of the previously mentioned parameters generates the surface resistance. In (Vaisocherova et al. 2015a) Vaisocherová et al. defined three categories of functionalizable resistant coatings according to nonspecifically adsorbed mass after exposure to the complex samples. Coatings with the fouling level < 100 ng/cm^2 in single-protein or complex solutions are in general referred to as antifouling coatings. However, there is a great difference in the performance of such coatings when exposed to undiluted blood plasma. Coatings with undiluted blood plasma-fouling levels < 10 ng/cm^2, < 5 ng/cm^2, and below the detection limit of the technique used are classified as low-fouling, ultra-low fouling, and non-fouling coatings, respectively. Using such categories may look helpful at first glance, however, the technique used for fouling level assessment, experimental conditions, and the reading of the fouling level from the data collected influence the result significantly, making most of the results in literature very hard to compare [APPENDIX VI, X, (Víšová et al. 2020c)].

3.2.2. Architectures of hydrophilic antifouling coatings

Considering parameters important for antifouling properties (chapter 3.2.1. Key parameters for antifouling properties), different strategies of coatings preparation have been reported. Typically, antifouling SAM layer, polymer brush coating, or hydrogels are applied to reduce fouling and introduce sites for further functionalization.

3.2.2.1. Antifouling SAM layers

The alkanethiolated oligo(ethylene glycol)-terminated carboxy-functional SAMs (AT-OEG SAM) on the gold substrate have been recognized as the standard and the most widely used antifouling coatings in the field of bioanalytics (Figure 16). Even though AT-OEG SAMs were reported to present nearly non-fouling resistance against single-molecule solutions (Harder et al. 1998; He et al. 2008; Herrwerth et al. 2003; Li et al. 2005; Prime

and Whitesides 1993; Zheng et al. 2004; Zolk et al. 2000), they fail in complex samples such as blood plasma or blood serum, showing fouling level of ~100–300 ng/cm^2 (Benesch et al. 2001; Bolduc et al. 2009; Rodriguez-Emmenegger et al. 2011b; Vaisocherova et al. 2014). Other non-AT based OEG/PEG SAM layers are mentioned in Chapter 3.2.2.2.

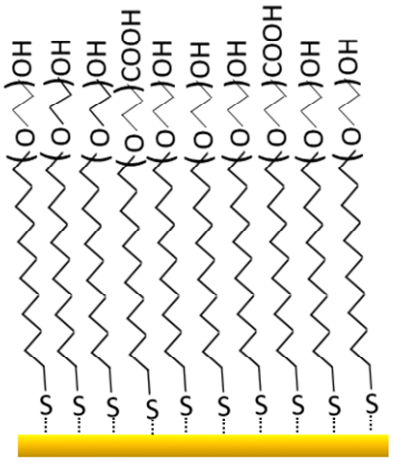

Figure 16: *Scheme of the AT-OEG SAM on gold.*

The screening of the resistance of the SAM created by short peptides of different composition and length using 3-mercaptopropionic acid linker (3-MPA) to attach the peptides onto a gold SPR chip was performed by Bolduc et al. While the best performing homopeptide coating consists of non-ionic 3-MPA-(serin)$_5$-OH SAM, showing fouling level of 132 ng/cm^2 after exposure to undiluted bovine serum (Bolduc et al. 2009), using binary patterned block peptides 3-MPA-(A)$_3$(B)$_2$-OH (for A: S, H, L, D, and B: D, S, H) decreased the fouling level to 23–79 ng/cm^2 (Bolduc et al. 2010).

Zwitterionic SAMs were introduced in few different forms. Holmlin et al. prepared the SAM layer as a 1:1 mix of alkanethiols terminated with positively charged tri(methyl)ammonium and negatively charged sulfonate group. They demonstrated an influence of the surface net charge on the fouling from a solution of negatively and positively charged proteins fibrinogen and lysozyme, respectively (Holmlin et al. 2001). Mixed SAM of zwitterionic peptide EKEKEKE-PPPPC and adenosine-triphosphate (ATP)-

binding thiolated aptamer was attached to the gold electrode decorated with electrodeposited gold nanoparticles. The surface was further passivated by 6-mercaptohexanol and used for the detection of the ATP in biological media. Even though the limit of detection (LOD) of ATP aptasensor was estimated as 0.1 pM in PBS, characterization in 1 % blood plasma and 5% whole blood showed detectable fouling already (Wang et al. 2018). SAMs composed of alkanethiols with zwitterionic end groups, such as sulfobetaine (Holmlin et al. 2001; Shen and Lin 2013), phosphorylcholine/oligophosphorylcholine (Chen et al. 2006; Tegoulia et al. 2001), or carboxybetaine (Bertok et al. 2015) were presented to improve fouling typically from single protein solutions only. In (Yang et al. 2014) authors showed crosslinked carboxybetaine SAM coated nanoparticles resisting the fouling from undiluted blood serum.

SAM layers prepared using a variety of other hydrophilic groups demonstrated the high resistance to single protein solutions (Bandyopadhyay et al. 2011; Deng et al. 1996; Luk et al. 2000; Wyszogrodzka and Haag 2009), but only partial resistance to complex solutions (Aubé et al. 2017). Generally, SAM coatings are usually highly reproducible and well-described structures creating a great tool to study molecular interactions in a non-natural and well-defined environment, such as buffer solution or very highly diluted (1–5 %) biological samples. However, if exposed to real-world complex samples, such as bodily fluids, the fouling level increases up to 50–400ng/cm^2.

3.2.2.2. OEG and PEG-based coatings

Poly(ethylene glycol) is a widely used flexible, uncharged, and hydrophilic polymer formed by repeating units of ether oxygen with the chemical structure of $H{-}(O{-}CH_2{-}CH_2)_n{-}OH$. Even though PEG naturally bears only hydroxyl group, OEG or PEG can be in principle functionalized by further modifications (Cui et al. 2016; Cheng et al. 2007; Wang et al. 2001).

PEG has been considered biologically inert, biocompatible, and safe to use in *in vivo* studies and therapies by the regulatory authorities. The PEG-modification of biomolecules

and nanoparticles in therapeutics and especially in drug delivery is a widely adopted approach to extend circulation time, and improve drug efficacy (Huckaby and Lai 2018; Kingshott and Griesser 1999; Otsuka et al. 2003). However, only recently the evidence of the immune answer to PEG has appeared (Yang and Lai 2015). Anti-PEG antibodies were reported not only in humans using PEG-containing therapy, but even in a wide healthy population, possibly evoked by long-last exposure to free PEGs in cosmetics, pharmaceuticals, processed food, etc. (Armstrong 2009; Garay et al. 2012; Hong et al. 2020). Moreover, the percentage of the population never cured by PEG-containing therapies yet having a measurable level of the anti-PEG antibodies in the blood increased from 0.2 % in 1984 (Richter and Åkerblom 1984) to 25 % in 2009 (Armstrong 2009) (depending on detection limits of methods used for the detection). Most recent studies show up to 72 % of the healthy population with pre-existing anti-PEG antibodies (Yang et al. 2016). Such immunization of the population may lead to accelerated blood clearance pushing down drug circulation time, significantly decreasing the efficiency of PEG-based drugs. In the future, alternative high hydratable, fouling resistance, biocompatible but non-immunogenic, and non-antigenic coating will be of great importance for drug delivery and biomedical applications.

Except for biomedical applications, PEGs are widely used in analytical methods and surface engineering as surface passivation agents, introducing antifouling properties onto the surface (Lowe et al. 2015). For example, the procedures for passivation glass against nonspecific interactions from single protein solutions or cell suspensions by grafting PEGs using silane-based chemistry are widely used in microscopic techniques or cell studies (Gidi et al. 2018; Chandradoss et al. 2014; Jo and Park 2000; Sauter et al. 2013).

Electrostatic or hydrophobic physisorption has been attempted as another way of PEG coating immobilization on different substrates; however, only poor stability and poor resistance to fouling were observed (Amiji and Park 1992; Orgeret-Ravanat et al. 1988). Thiolated PEGs were grafted onto gold surfaces (Du and Brash 2003; Unsworth et al. 2005b) while catechol containing PEGs were grafted onto different metal oxides (Dalsin et al. 2003). In (Dalsin et al. 2005) authors show a strong correlation between the thickness and the surface density of the adsorbed PEG-DOPA chains on TiO_2 substrate and

the fouling level from serum. In the most optimal case, the fouling level was reported to be below 1ng/cm^2, the detection limit of the technique used.

One of the limiting factors for the creation of the ultra-resistant PEG-based coating is the low grafting density of the chains. A dense PEG coating was prepared by melting PEG at 75 °C on epoxide-functionalized silanes attached to the silica surface. Upon incubation with 10 % calf serum, the fouling level was 15 ng/cm^2 (Piehler et al. 2000). The maximal grafting density on any kind of surface was reported using dopamine-melanin anchoring layer and subsequent grafting of PEG from the melt. The optimized grafting conditions led to the ultra-resistance of the coating (2 ng/cm^2 and 14 ng/cm^2 from human blood plasma and human blood serum, respectively). However, after only one day of storage in PBS, the resistance of the coating was impaired (90 ng/cm^2 and 23 ng/cm^2 from human blood plasma and human blood serum, respectively) (Pop-Georgievski et al. 2011).

PEGs were reported to be prone to degradation by oxidation (Han et al. 1997; Kawai 2002), hydrolysis (Haines and Alexander 1975), photooxidation (Morlat and Gardette 2001), or thermal-oxidative degradation (Han et al. 1997; Yang et al. 1996) in the most of the biochemical solutions (Zhang and Chiao 2015). Therefore, despite the promising antifouling properties, PEG-based coatings suffer from only short-term stability in biological media, hampering their performance as antifouling surface coatings.

3.2.2.3. Polymer brush coatings: theory

Polymer brushes are 3D-structures formed by polymer chains one end-tethered to the interface. The attachment can be mediated either by an end-functionalized polymer chain reacting with the substrate via physisorption, chemisorption, or covalent bond (“grafting to” method) or can be surface-initiated when the polymer grows from the initiator immobilized on the surface (“grafting from” method) (Minko 2008). “Grafting to” method allows grafting density and chain-molecular mass control. However, due to steric hindrance caused by previously attached chains, “grafting to” methods usually result in less dense polymer brushes compared to more demanding “grafting from” methods (Brittain and Minko 2007)(Figure 17). Typically, the fouling decreases with increasing

grafting density and/or increasing length of the attached polymer (Norde and Gags 2004; Szleifer 1997; Unsworth et al. 2005a; Yoshikawa et al. 2012).

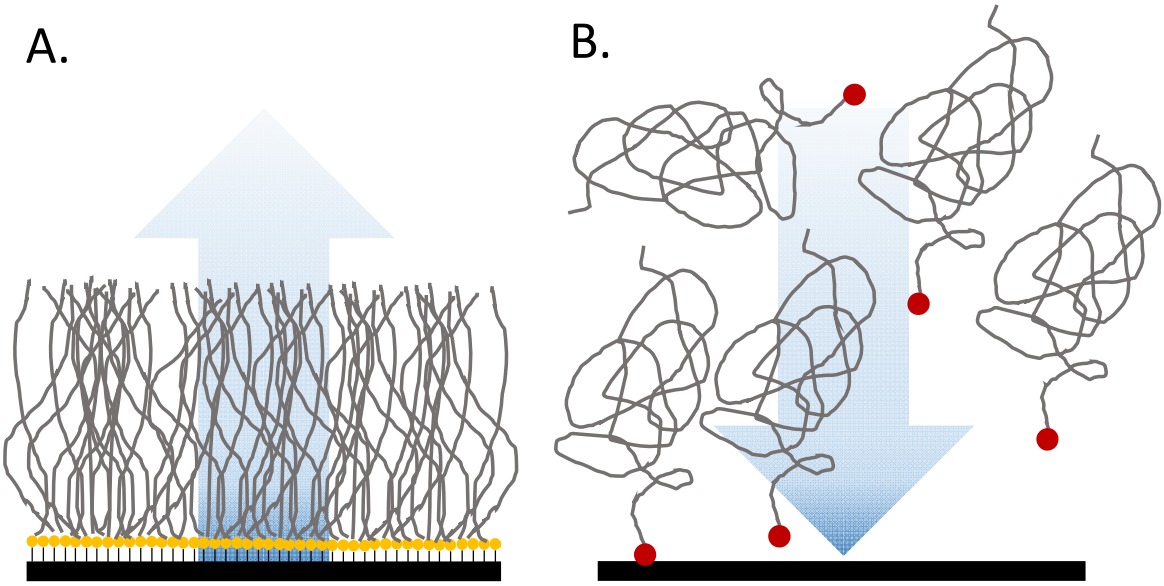

Figure 17: *Scheme of the approaches for polymer brush preparation. A. "Grafting from" method: polymer brush grows from the initiator layer fixed on the surface. B. "Grafting to" method: pre-prepared polymer chain with attaching moiety (red) is immobilized on the surface. The functional attaching groups are typically thiols, NHS-esters, or catechol-based moieties.*

The theories describing thermodynamic and physical properties of polymer brushes, such as the brush conformation dependency on the length, or the density of the polymer chains, or the phase transition of the structure with changing of the external parameters have been reported during the time. The first and successful approach describing polymer chain conformation in a real polymer brush where non-neighboring monomers can interact with each other is the Flory theory (Bhattacharjee et al. 2013).

The Flory theory predicts chain expansion in a solvent where the monomer-monomer interactions are not attractive (so-called good solvent) and every monomer unit occupies

the volume that cannot be occupied by any other monomer unit (excluded volume) at the fixed temperature. The free energy of the system is composed of two contributions — the osmotic pressure which tends to swell the chain, and the conformational entropy giving elastic retracting force arising from the coil expansion to a less probable arrangement of bonds (Flory 1949). By minimizing the free energy, the theory shows that the equilibrium average dimension R of a polymer with N monomer units becomes asymptotically proportional to N, $R \cong N^{3/5}$. Lately, more advanced Flory-type self-consistent field theories for the description of the thermodynamic and structural properties of the flexible single polymer chains in a solvent under the different external stimuli (e.g., temperature, pH, solvent composition, pressure, or external electric field) have appeared (Budkov and Kiselev 2017; Currie et al. 2003).

The chains end-grafted onto the surface in a low density adopt different conformations according to a solvent-chain and surface-chain interactions. In a good solvent non-absorbed polymer tethered to a surface will be in a coil conformation (sometimes called mushroom-like conformation), follows original Flory's dependence. Under so-called bad solvent conditions, where the monomer-monomer interactions are attractive, the polymer chain will adapt collapsed globule conformation, showing $R \cong N^{1/3}$. For the surface-polymer system, where the polymer is effectively attracted to a surface, the chain may adopt the so-called flat pancake conformation under the good solvent conditions with predicted $R \cong N^{3/4}$ (Currie et al. 2003) (Figure 18 A–C).

When the number of chains per unit area (grafting density) crosses above the critical value and the distance between chains is smaller than R, the intermolecular osmotic interactions result in stretching of the grafted polymers away from the surface, creating polymer brush structure (de Gennes 1980; Milner et al. 1988) (Figure 18 D).

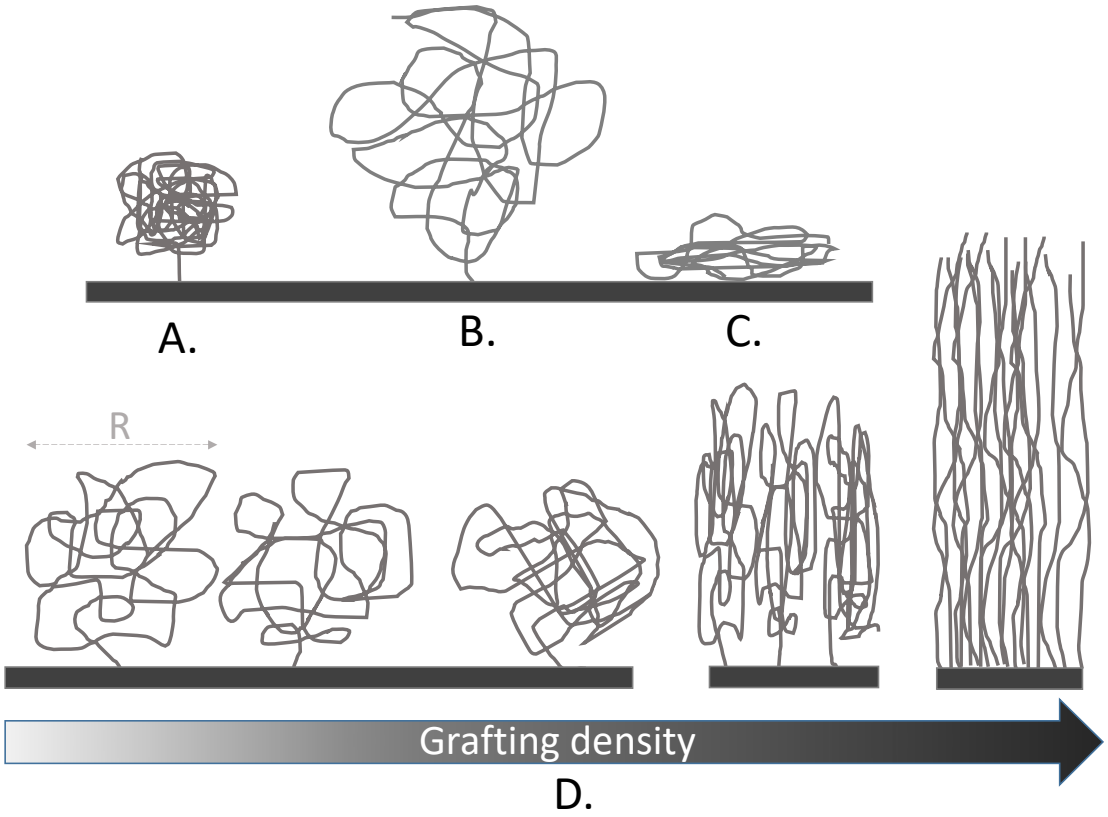

Figure 18: *Theoretical conformations of polymer chain attached to the surface. A: Polymer chain in collapsed globule conformation in a bad solvent. B: Polymer chain in coil conformation (mushroom-like conformation) in a good solvent. C. Polymer chain attracted to a surface in a flat pancake conformation in a good solvent. D. Increasing grafting density of the polymer chains creates brush-like structure.*

The polymer brush conformation and so its properties are highly dependent on the solvent-chain and chain-surface interactions (allowing dynamic regulations using external stimuli) and polymer chain density and length (allowing optimization of the dynamic response range for different applications). Due to that, the polymer brushes may create smart materials with tunable properties, such as wettability (Azzaroni et al. 2007), self-cleaning properties (Howarter and Youngblood 2007; Chen et al. 2019b; Kroning et al. 2015), controlled cell adhesion (Mizutani et al. 2008; Okano et al. 1995), controlled drug delivery (Bajpai et al. 2008) or antifouling background for bioanalytical applications (Halperin and Kröger 2009; Ma et al. 2019).

3.2.2.4. Antifouling functionalizable polymer brush coatings

Generally, the best performing antifouling functionalizable coatings are neutral polymer brushes — either non-ionic or zwitterionic. The 3D structure of the non-charged hydrophilic brushes possesses a great fouling resistance and usually high loading capacity for subsequent BE immobilization (Figure 19). Typically, antifouling polymer brush structures contain acrylamide, methacrylamide, acrylate, or methacrylate backbone with various pendent groups or short chains, e.g., PEG / OEG, hydroxy-, or zwitterionic moieties.

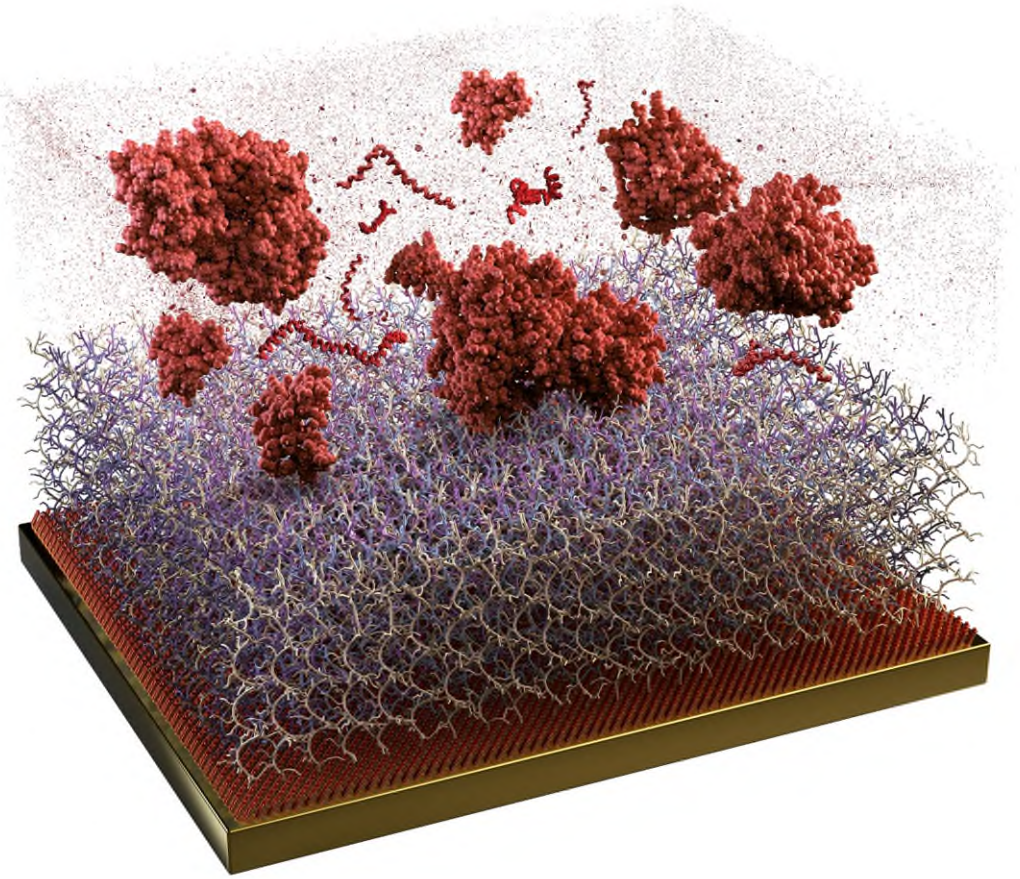

Figure 19: *Antifouling polymer brush coating preventing fouling from a complex sample. Every side chain of the structure may possess the ability for further functionalization. Design of the figure: Daniel Špaček, neuroncollective.com.*

Polymer brush coatings with OEG side chains were reported as thermoresponsive (Hu et al. 2010; Vancoillie et al. 2014) and antifouling coatings (Ma et al. 2004). Mono-hydroxy and mono-methoxy terminated poly[oligo(ethylene glycol)methacrylate] (pHOEGMA) and poly[oligo(ethylene glycol) methyl ether methacrylate] (pMeOEGMA) were prepared via controlled atom transfer radical polymerization (ATRP) (Brown et al. 2005). The authors presented simple thickness adjustability by polymerization time control. Later, the optimal thickness of pMeOEGMA or pHOEGMA brush to decrease the fouling was reported to be ~ 30 nm, showing fouling level from undiluted complex samples, such as blood plasma, 25–50 ng/cm^2 (Riedel et al. 2013; Rodriguez-Emmenegger et al. 2012a; Rodriguez-Emmenegger et al. 2012b; Rodriguez-Emmenegger et al. 2011c). Functionalization of OEG-based brushes was performed using DSC chemistry and the enhanced binding specificity/capacity of pHOEGMA brushes compared to SAM layer was reported (Lee et al. 2007). Elsewhere, the pHOEGMA-based copolymer was functionalized with a natural antibacterial peptide to prepare antibacterial coating (Glinel et al. 2008). The dependence of the durability of the cell fouling resistance on the number of ethylene glycol units in the side chains of 100 nm thick pMeOEGMA on Ti substrate was shown in (Fan et al. 2006a). The longest studied side chain containing 23 ethylene glycol monomers resists cell attachment for 11 weeks.

The hydroxy-functional polymer brush coatings with high fouling resistance, particularly the poly(2-hydroxyethyl methacrylate) (pHEMA) (Beers et al. 1999; Horak 1992; Montheard et al. 1992; Robinson et al. 2001), poly(3-hydroxypropyl methacrylate) (pHPMA), or poly(N-(2-hydroxypropyl) methacrylamide) (pHPMAA) (Raus and Kostka 2019) were reported to be prepared by various “grafting to” and “grafting from” techniques and have been used in biomedical applications widely as the hydroxyethyl or hydroxypropyl groups in the structure confer high hydrophilicity and good biocompatibility of the material.

In (Yoshikawa et al. 2012) authors showed the dependence of antifouling properties on grafting density of pHEMA brush. With optimized grafting density, pHEMA brush showed non-fouling properties in undiluted fetal bovine serum or after 24 hours of adhesion test of human umbilical vein endothelial cell. Zhao et al. define the optimal thickness of

pHEMA for antifouling properties in a range between 20–45 nm. From undiluted human blood serum and plasma, they reported fouling of 3 and 3.5 ng/cm^2, respectively (Zhao et al. 2011). In another study, 3T3 fibroblast adhesion on RGD-functionalized pHEMA brushes with RGD buried in different depths in the polymer brush structure was studied, showing that RGD deeper than 42 nm from the brush interface does not promote cell adhesion anymore. Bare pHEMA resists cell adhesion even after 48h (Desseaux and Klok 2015). In biosensors, pHEMA brush was used for fast and sensitive detection of aflatoxin M1 (Karczmarczyk et al. 2016) or Cronobacter (Rodriguez-Emmenegger et al. 2011a) in milk, showing non-fouling properties (unlike OEG-based polymer brush coatings). On the other hand, another hydroxy-functional methacrylate pHPMA was reported to exhibit only limited resistance compared to other hydroxyl-based polymer brush coatings. The pHPMA brush with the thickness of 25–40 nm show fouling level from undiluted blood serum and plasma in a range of 25–53 ng/cm^2 (Rodriguez-Emmenegger et al. 2011b; Zhao et al. 2010), which may be too high for biosensor applications.

Non-fouling properties were reported using pHPMAA brush coatings. The level of undiluted blood plasma fouling was reported to be below 0.03 ng/cm^2, the detection limit of the method used (Rodriguez-Emmenegger et al. 2011b). Unlike OEG-based coatings, pHPMAA brushes were shown to keep their resistance even after two years of storage in PBS. Moreover, unlike other functionalizable antifouling structures, pHPMAA exhibits non-fouling properties across all different complex samples, such as bodily fluids from single donors, pooled bodily fluids, or food samples (Pereira et al. 2014; Rodriguez-Emmenegger et al. 2012b; Vaisocherová-Lísalová et al. 2016a) (APPENDIX III). Despite its outstanding non-fouling properties, pHPMAA is not widely functionalized in biosensor applications. In (Vaisocherova et al. 2014) authors show the impairment of hydroxy-functional polymer brush fouling-resistance after DSC-based functionalization. Therefore, to avoid hydroxy- group activation, pHPMAA was copolymerized with carboxy-functional monomers. Such coatings perform excellent resistance to fouling and high BE loading capacity without significant resistance impairment after EDC-based activation (Kotlarek et al. 2019; Riedel et al. 2017; Riedel et al. 2016; Vaisocherová-Lísalová et al. 2016a) (APPENDIX III).

Nowadays the most promising functionalizable and ultralow fouling polymer brushes are prepared using zwitterionic compounds (Jiang and Cao 2010; Mi and Jiang 2014; Schlenoff 2014). Due to high hydrophilicity and wettability, poly(carboxybetaine acrylamide) (pCBAA) and poly(carboxybetaine methacrylamide) (pCBMAA) perform ultralow- to non-fouling resistance from different kinds of complex samples, only slightly lower compared to pHPMAA brushes (Lísalová et al. 2017; Pereira et al. 2014; Rodriguez-Emmenegger et al. 2012b; Vaisocherova et al. 2015a; Vaisocherova et al. 2014) (APPENDIX IV). They exhibit a high BEs loading capacity using amino coupling-based functionalization and biocompatibility (Víšová et al. 2020b) (APPENDIX V). Specifically, pCBAA show higher resistance to fouling from complex samples compared to pCBMAA, while pCBMAA was shown to copolymerize easily with other methacrylates, such as pHPMAA (Vaisocherová-Lísalová et al. 2016a) (APPENDIX III).

Typically, pCBAA polymer brush coatings are used as biosensing platforms. Yang et al. present the optimal thickness of antifouling pCBAA coatings to be ∼20 nm and perform the detection of ALCAM in blood serum using anti-ALCAM antibody functionalized pCBAA polymer brush (Yang et al. 2009). In (Vaisocherová-Lísalová et al. 2016b) (APPENDIX II) the detection of foodborne bacteria was conducted from food samples using the pCBAA-based platform with a detection limit of 57 CFU/mL in hamburger samples. pCBAA functionalized with amino-modified probes was used for detection of microRNA from 90% erythrocyte lysate at a subpicomolar level without the need for RNA extraction. The fouling level was reported lower than 2 ng/cm^2 (Vaisocherova et al. 2015b) (APPENDIX I). Carboxybetaines were used for two-layer polymer brush architecture with the bottom denser antifouling layer and the loose second layer for BE immobilization. For optimized coating, fouling from undiluted blood plasma was reported < 2 ng/cm^2 (Brault et al. 2012).

Another commonly used zwitterionic compound is sulfobetaine. However, the lack of functionalization capabilities hampers the versatile use of SB-based coatings. Due to their biocompatibility (Kim et al. 2012a) and low-fouling properties, they are used as antifouling coatings to diminish cell adhesion and control cell patterning (Chou et al. 2016a; Kim et al. 2012b; Leigh et al. 2017; Quintana et al. 2014; Sun et al. 2018; Ye et al. 2016), or as a moiety for copolymerization with other functionalizable compounds (Berlinova et al.

2000; Wang et al. 2006a) (APPENDIX XII). Recently, Lange et al. introduced an orthogonal chemistry approach for the preparation of functionalized p(SB)-based brushes. Copolymerization of a new sulfobetaine-based monomer equipped with a clickable azide moiety with well-established standard sulfobetaine monomer resulted in an antifouling polymer brush structure with a tunable number of clickable groups ready for functionalization (Lange et al. 2016).

p(SB)-based coatings show a lower degree of resistance compared to p(CB) coatings (Leigh et al. 2017; Rodriguez-Emmenegger et al. 2009), however due to very low pI of sulfo-group, the zwitterionic character of the sulfobetaine remains unchanged in a wide range of pH. Chang et al. found the fouling resistance to a single protein solution of poly(sulfobetaine methacrylate) remains low in a pH range of 7.4–11.0 and ionic strength range of 0.1–1.0 M (Chang et al. 2008).

3.2.2.5. Antifouling functionalizable hydrogels

Hydrogels are composed of a 3D polymer network with a high swelling capacity resulting in a high water content, softness, flexibility, and biocompatibility. The swelling after exposure to water may reach up to 3 orders of magnitude (Hoffman 2012). Due to their remarkable hydratability, hydrogels are extensively used in tissue engineering (Camci-Unal et al. 2014), drug delivery (Hamidi et al. 2008), and other biomedical and bioengineering applications (Hoffman 2012; Peppas et al. 2006).

Typically, hydrogel coatings are prepared by physical or chemical crosslinking of hydrophilic polymer chains. The polymers used for hydrogel construction may be natural (e.g., hyaluronic acid, fibrin, agarose, or chitosan), synthetic (e.g., pHEMA, PEG, pCBAA), or biohybrid. Combining both groups the tailored properties can be achieved, such as desired biodegradability (Hennink and van Nostrum 2012; Hoare and Kohane 2008), or responsivity (Bajpai et al. 2008; Qiu and Park 2001; Tokarev and Minko 2009; Ulijn et al. 2007).

Mostly, the functionality of hydrogels is given by their stimuli-responsivity and fouling resistance, so further functionalization is not usually employed (Bajpai et al. 2008; Richter

et al. 2008). For example, Cao et al. prepared a smart hydrogel coating with two switchable regimes. Under acidic conditions, the positively charged carboxybetaine derivative-based hydrogel coating had antibacterial properties, while in a basic environment it turned into ultra-low fouling zwitterionic regime, releasing killed bacteria and other adhered material (Cao et al. 2013). pHEMA hydrogels have been widely used as a highly wettable and biocompatible (Klomp et al. 1983) material for implant coating (Chirila et al. 1993), drug delivery (Hsiue et al. 2001), or in ophthalmology for hydrogel contact lenses (Chirila et al. 1998). Antifouling pCBAA hydrogel thin film prepared using carboxybetaine diacrylamide crosslinker exhibited fouling from undiluted blood plasma < 5 ng/cm^2, showing high BE loading capacity without compromising its resistance (Chou et al. 2016b). In other work, Yang et al. used p(CB)-based hydrogel to protect implantable electrochemical glucose biosensor in undiluted blood plasma (Yang et al. 2011a).

PART II

EXPERIMENTAL METHODS

4. Methods for probing the biomolecular interactions at interfaces

The technical part of the study of biomolecular interactions at interfaces is specific – the presence of the surface and native (aqueous) environment at the spot of the measurement may be challenging. A list of a few examples of experimental methods used for the research in this work is presented.

4.1. Surface plasmon resonance (SPR)

SPR biosensors represent a surface-sensitive optical method based on the interrogation of changes in the propagation constant of an electromagnetic surface wave mode travelling along the interface between a metal and a dielectric. This interface supports surface plasmon polaritons (SPPs) that originate from collective oscillations of charge density and associated electromagnetic field. The most common approach to optically excite the SPPs is using a prism coupler relying on the attenuated total reflection method (Figure 20). The SPPs are then coupled with an evanescent field formed upon the total internal reflection of the excitation light beam at prism base carrying a thin metallic film. The coupling is only possible when the propagation constant of the SPP at the interface (β^{SP}) matches the parallel component of the propagation constant of the excitation beam forming the evanescence field (β^{EW}). For λ being a free-space wavelength, the resonant coupling occurs when the following equation holds:

$$\beta^{EW} = \frac{2\pi}{\lambda} n_p \sin\theta = Re\{\beta^{SP}\} = Re\left\{\frac{2\pi}{\lambda}\sqrt{\frac{\varepsilon_d \varepsilon_m}{\varepsilon_d + \varepsilon_m}} + \Delta\beta\right\}, \quad (1)$$

where the real part of β^{SP} is a function of the permittivity of the dielectric environment ε_d, metal permittivity ε_m, and $\Delta\beta$ relates to the small changes in the SPP propagation constant due to the prism presence and finite thickness of the metal layer. The parallel component of the propagation constant of the incident beam depends on the angle of incidence θ and refractive index of the prism n_p (Homola 2006). Importantly, this phase-matching condition is altered when the permittivity of the dielectric environment ε_d changes and thus it leads to variations in the coupling between the incident optical beam and the SPPs at the metal surface.

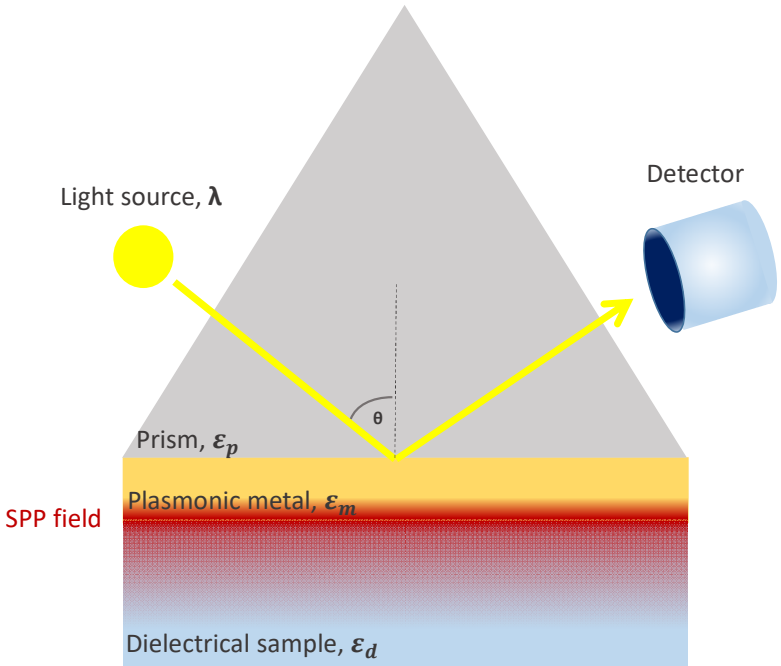

Figure 20: *Prism-based SPR experiment layout.*

The three most common modulated parameters in SPR-based biosensing are the angle of incidence, wavelength, or intensity of incident light. Angular SPR sensors use monochromatic light to excite an SPP. Subsequently, they interrogate the angular dependency of the intensity of the light reflected from the surface. The wavelength-modulating SPR sensors use polychromatic light at a fixed angle of incidence, studying the spectral changes after light reflection. The coupling of SPP and incident light is observed as a dip in the reflectance spectrum for a particular angle or wavelength, respectively. The

intensity-based SPR sensors measure the change in reflected light intensity at a fixed angle for a fixed wavelength. Time dependency of the dip position or intensity change gives SPR sensorgram and allows for real-time kinetic measurements (Figure 21).

Real-time kinetic measurements of biomolecular interactions (Karlsson et al. 1991; Peterlinz and Georgiadis 1996; Schuck 1997) or detection of minute amounts of target chemical or biological species (Homola 2003; Homola et al. 1999; Nguyen et al. 2015;

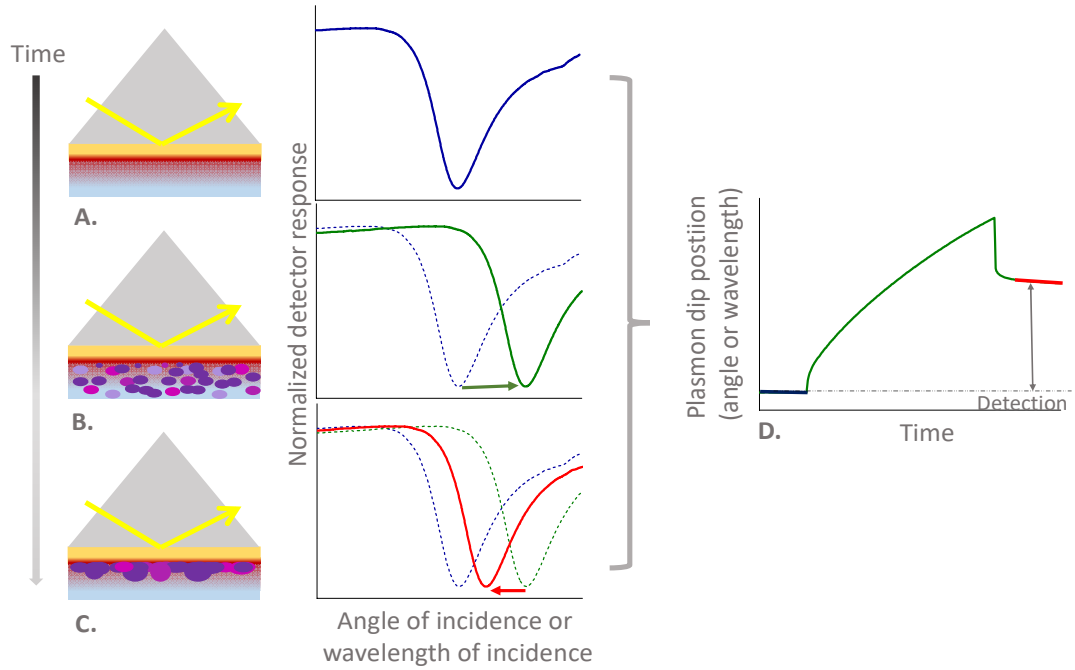

Figure 21: *Typical angle-interrogation or wavelength-interrogation SPR for the monitoring of biomolecular binding events. A: SPR surface is brought in contact with a buffer solution and a stable baseline is established in a real-time sensorgram D (blue). B: Analyzed complex sample is contacted with the SPR surface. Permittivity change related to the presence of the biomolecules in the sample and their binding to the surface is causing a gradual shift of SPR dip, corresponding to a kinetic in a real-time sensorgram (green). C: SPR biosensor surface is washed with a buffer solution. Bulk sample and only weakly-bound mass are washed off. The remained mass (specifically or nonspecifically bound) is ascribed to a shifted SPR in the equilibrium (red) with respect to the blue or green ones. D. SPR sensorgram showing time dependency of the SPR dip position. The difference between the blue and the red baseline corresponds to a mass adsorbed/detected on the SPR-surface (grey arrow in D).*

Scarano et al. 2010) are the most common applications in SPR biosensors. The SPR biosensors are commercially available, typically with refractive index detection resolution ~ 5 x 10^{-7} RIU for angular and ~ 10^{-6} RIU for spectral interrogation SPR (Ho et al. 2017).

SPR sensor sensitivity to the permittivity changes close to the plasmonic surface brings three main considerations. i) Permittivity change is not molecular-specific, therefore SPR needs a BE attached to its surface. Effectivity of the BE, nonspecific interactions, and cross-reactivities are limiting factors for the applications. In addition, robust surface chemistry for the coupling of BE to the SPR biosensor surface (typically gold) is a key for the successful implementation of SPR biosensor for the aimed applications. ii) The SPP field decays exponentially from the surface into the dielectric environment and is characterized by the penetration depth (distance from the surface, where the field decrease by factor 1/e). The penetration depth ranges between ~100–600 nm depending on the wavelength used. The longer wavelength, the higher the penetration depth. As a consequence, only coatings with limited thickness may be used for a standard SPR sensor surface functionalization. Moreover, using an angular SPR system with monochromatic light, different results are obtained for different wavelengths used. The sensitivity of the SPR dip position-change caused by changes at the surface interface is lower for longer wavelengths compared to shorter ones. iii) Environmentally-dependent swelling of the coating may significantly interfere with SPR kinetic or sensing measurements. The theory for the deconvolution of the swelling contribution to SPR dip shift is still missing.

The SPR experiments in this work were measured using a wavelength-modulation based four-channel spectroscopic SPR sensor (Homola et al. 2002) and high-resolution SPR imaging (SPRi) system with polarization contrast and internal referencing (Piliarik et al. 2010) developed at the Institute of Photonics and Electronics of the Czech Academy of Sciences (Prague, Czech Republic), and four-channel angular MP-SPR system NAVI 200 with LED sources of 670 nm and 785 nm (BioNavis Ltd, Finland).

4.2. Spectroscopic ellipsometry

Ellipsometry is a powerful optical technique for the characterization of thin layers and multilayers. It measures the complex reflectance ratio of a system, parametrized by the amplitude component Ψ and the phase difference Δ. Specifically, the complex reflectance ratio ρ measured by ellipsometry is given as a ratio of the reflected polarization state component oscillating parallel to the plane of incidence ($\left|E_p^{ref}\right|e^{i\delta_p^{ref}}$) to the component oscillation perpendicular to the plane of incidence ($\left|E_s^{ref}\right|e^{i\delta_s^{ref}}$), both normalized to their initial (incidence) values ($\left|E_p^{inc}\right|e^{i\delta_p^{inc}}$ and $\left|E_s^{inc}\right|e^{i\delta_s^{inc}}$, respectively). Then, parameter $tan(\Psi)$ corresponds to a ratio of normalized reflected amplitudes $\frac{r_p}{r_s}$ and Δ to a phase shift upon reflection (Eq. 2)

$$\rho \equiv \frac{\left|E_p^{ref}\right|}{\left|E_p^{inc}\right|}\frac{\left|E_s^{inc}\right|}{\left|E_s^{ref}\right|}\frac{e^{i\delta_p^{ref}}}{e^{i\delta_p^{inc}}}\frac{e^{i\delta_s^{inc}}}{e^{i\delta_s^{ref}}} = \frac{r_p}{r_s}e^{i(\Delta_p-\Delta_s)} = \tan(\Psi)e^{i\Delta} \tag{2}$$

To determine real physical properties of the studied material (e.g., optical constants and thicknesses of layers, uniformity, or roughness), the model-based analysis of $\Psi(\lambda)$ and $\Delta(\lambda)$ must be performed. However, to get correct results, a model corresponding closely to the real sample must be set, keeping as few unknown parameters as possible. Typically, layer-by-layer sample examination must be performed before the multi-layer study. Subsequent analysis and evaluation of the physical correctness of the results may be complicated (Jellison 2005).

The great advantage of spectroscopic ellipsometry is a non-destructive and non-contact character of the measurements with potentially high sensitivity down to sub-nm thickness level of the determination. In the research of biointerfaces, spectroscopic ellipsometry was used to monitor effects like adsorption, molecular interactions at interfaces, kinetics, or layer composition (Arwin 2005; Elwing 1998; Goyal and Subramanian 2010; Hinrichs

and Eichhorn 2018; Yin et al. 2011). However, using ellipsometry in the research of the biomolecular thin layers is hampered by the absence of a well-established methodologies for ellipsometric measurements in aqueous solutions.

In this work, ellipsometric measurements were used for polymer brush coating characterization and swelling research (Víšová et al. 2020c) (APPENDIX VI). Moreover, the ellipsometric skills were practiced and the methodology for dry sample measurements were prepared during the studies on the optical parameters of thin layers of Cr and NiFe (Hashim et al. 2020) (APPENDIX VIII). The measurements were performed using spectroscopic ellipsometers SE 850 (Sentech, Germany) and VASE (J.A.Woollam, Lincoln, USA). For measurements in a water environment, custom-made cell-holder and cell with incorporated sample holder were developed at the Institute of Physics of the Czech Academy of Sciences (Prague, Czech Republic) (Figure 22).

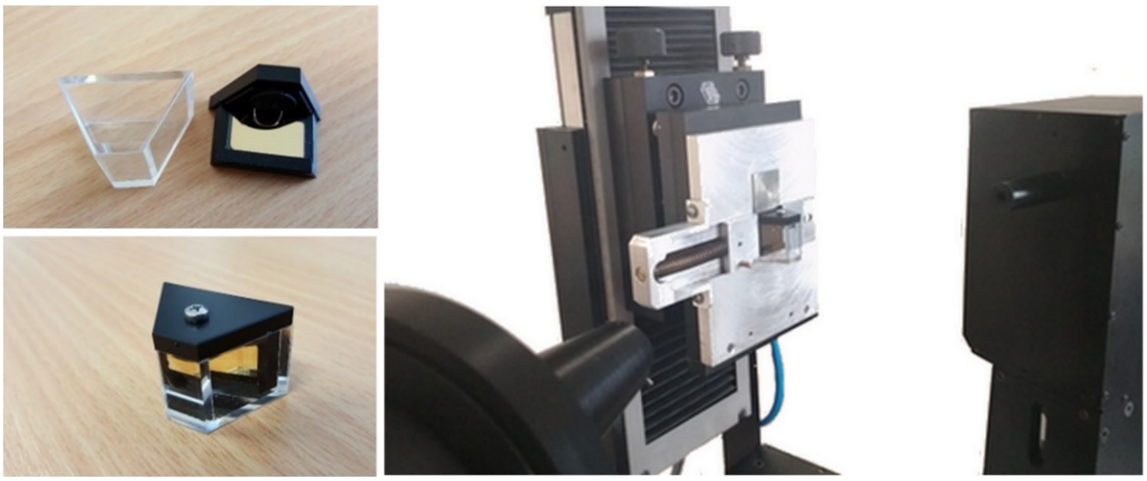

Figure 22: *Custom-made cell (left) and cell holder (right) for VASE ellipsometer (right) (Víšová et al. 2020c).*

4.3. Quartz crystal microbalance (QCM)

The QCM is an acoustic sensor probing in real-time the changes in the resonant frequency of the piezoelectric crystal resonator. Typically, the alternating current is applied to the piezoelectric crystal (usually quartz) using a pair of golden electrodes, to induced oscillations at the resonant frequency. The typical resonant frequencies used in biomolecular research are ~ 5–10 MHz and are inversely proportional to the thickness of the crystal.

For uniform, thin and rigid film of mass Δm adsorbed on the QCM crystal with sensitive area A, thickness d, and density ρ_Q in air, the change in frequency Δf follows theoretical equation (Sauerbrey 1959)

$$\Delta f = -\frac{f \Delta m}{\rho_Q A d} = -C_f \varphi \tag{3}$$

The sensitivity factor $C_f = -\frac{f^2}{d f \rho_Q}$ is a constant for the crystal of given parameters and φ is a change of mass per unit area.

However, such linear dependency of Δf on Δm is not valid in liquids, where the interface layer is created by flexible, soft, and viscoelastic films. Due to mechanical losses, the liquid environment causes the dissipation of oscillation energy. QCM-D method excites resonant frequency oscillations of the crystal by a short impulse of the driving voltage and subsequently the voltage decay is recorded as a function of time. By fitting the decay curve as exponentially dampened sinusoidal wave $A(t)$

$$A(t) = A_0 e^{t/\tau} \sin(2\pi f t + \varphi) \tag{4}$$

for A_0, is an amplitude, τ is a decay time constant, f resonant frequency, and φ phase angle, the frequency and dissipation can be obtained at the same time, being a function of the film thickness, density, viscosity or elasticity.

Using the viscoelastic Voight model, Voinova et al. showed for a viscoelastic layer of thickness h, viscosity η and elastic shear modulus μ on a QCM crystal with the thickness h_0, density ρ_0, and angular frequency of oscillations ω under a bulk Newtonian liquid with viscosity η_L and viscous penetration depth of the shear wave in the bulk liquid δ_L, that Δf and ΔD are proportional to viscoelastic properties of the system as follows in Equation 5 and Equation 6 (Voinova et al. 1999).

$$\Delta f \approx -\frac{1}{2\pi\rho_0 h_0}\left\{\frac{\eta_L}{\delta_L} + h\rho\omega - 2h\left(\frac{\eta_L}{\delta_L}\right)^2 \frac{\eta\omega^2}{\mu^2 + \omega^2\eta^2}\right\} \quad (5)$$

$$\Delta D \approx -\frac{1}{2\pi f\rho_0 h_0}\left\{\frac{\eta_L}{\delta_L} + 2h\left(\frac{\eta_L}{\delta_L}\right)^2 \frac{\mu\omega}{\mu^2 + \omega^2\eta^2}\right\} \quad (6)$$

Recording the Δf and ΔD at multiple overtones of a fundamental resonance frequency of the QCM crystal and using different mathematical models, the physical characteristics of the adsorbed layer, such as adsorbed layer mass, thickness, density, shear elasticity, viscosity, and kinetics of the viscoelastic film can be obtained (Domack et al. 1997; Muramatsu and Kimura 1992; Rodahl et al. 1997; Wu et al. 2015).

In this work (i) the QCM device developed at the Institute of Physics of the Czech Academy of Sciences (Prague, Czech Republic) combined with openQCM Q-1 (Novaetech, Italy) and tailored microfluidic system, and (ii) a custom-made two-channel apparatus consisting of portable QCM Analyzer (KEVA, Brno, Czech Republic) and a microfluidic-based crystal holder were used for polymer brush coating characterization and biosensor development. Au-coated QCM crystals with the resistance of max. 30 Ω and frequency range around 10 MHz were used for polymer-brush coated sensor preparation (Víšová et al. 2020c) (APPENDIX VI, APPENDIX XII, APPENDIX XIX).

4.4. Infrared spectroscopy

A wide range of vibrational methods is a great tool for the characterization of biomaterials on a molecular level (Barth 2007; Fabian and Mäntele 2001; Schrader 2008). Adsorption of infrared light (IR) with frequencies matching the frequencies of some vibrational modes of molecules brings deep information about molecular structure and creates the finger-print-like character of the infrared absorption spectra (Socrates 2004). Even though IR spectroscopy brings valuable insight into molecular structure, it is not a feasible method for the analysis of complex samples or aqueous-based solutions.

In this work, IR spectroscopy was used for polymer and copolymer brush structure characterization and probing of the molecular changes caused by functionalization (Lísalová et al. 2017; Vaisocherová-Lísalová et al. 2016a) (APPENDIX IX, APENDIX IV, APENDIX III). The infrared spectrometer used was the Thermo Scientific™ Nicolet™ iS50 FTIR Spectrometer equipped with the PEM module for polarization modulation-infrared reflection-absorption spectroscopy (*PM-IRRAS*) feasible for measuring of the ultrathin layers on mirror-like substrates, and Thermo Scientific™ Smart SAGA™ accessory for very thin film layer analysis under grazing angle of incidence.

4.5. Contact angle measurements

Contact angle measurement allows a quantitative determination of wetting of the surface by a liquid. The angle is defined as the angle formed by the liquid at the surface / gas (air) / liquid interface. Physico-chemical properties of all three components and roughness and structure of the surface are influencing the results. The traditional definition of the contact angle was given by Young who proposed the contact angle as a result of the equilibrium of a drop resting on a plane solid surface under the action of three surface tensions — at the interface of liquid / vapor, solid / liquid, and solid / vapor (Zisman 1964). Typically, the surface is considered to be hydrophilic for the contact angle

θ < 90°, hydrophobic for θ > 90°, and super-hydrophobic for θ > 150° (Figure 23) (Law 2014).

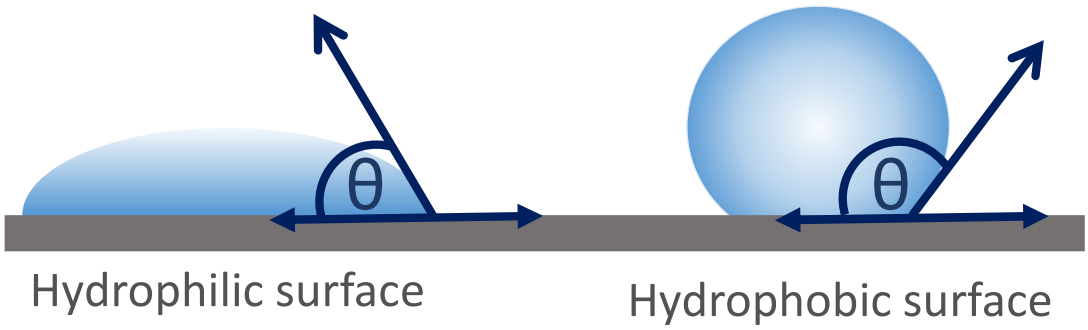

Figure 23: *Drop of water on a surface for probing the wetting characteristics. Dark blue arrows depict interface tensions modulating drop shape. Left: Water drop on a hydrophilic surface, contact angle ϑ is rather small. Right: Water drop on a hydrophobic surface, contact angle is high.*

The contact angle can be probed using static (sessile drop) or dynamic measurements. The sessile drop experiment is done by simply placing a drop of liquid on the surface and is suitable for smooth and homogenous surfaces. During dynamic angle measurement, the advancing and receding angles are recorded while the drop volume (and so the contact line) is increasing and decreasing, respectively. The contact angle hysteresis gives information about chemical and topographical inhomogeneities, swelling, surface rearrangement, or alternations caused by the solvent presence. In this work, both methods were used for polymer brush coating characterization (Vaisocherová-Lísalová et al. 2016a; Víšová et al. 2020b) (APPENDIX III, APPENDIX V) measured by Contact angle goniometer OCA 20 (DataPhysics Instruments, Germany) equipped with SCA 21 software.

4.6. Other techniques

Among other techniques used for surface characterization in the presented work, scanning electron microscopy (SEM) and atomic force microscopy (AFM) were used for detailed surface imaging. Both methods have a great resolution, however, measuring in a native environment (aqueous-based solutions) is limited and demanding.

Electron microscopy was used for nanoparticle characterization and bacteria imaging. Samples were fixed by glutaraldehyde fixation method and then dehydrated either by simple drying or using the critical point drying procedure. Dual Beam Scanning Electron Microscope (Versa 3D DualBeam™ (FEI Company, USA) and e_LiNE plus system (Raith, Germany) were employed for the measurements.

AFM scanning was performed using Dimension Icon (Bruker, USA) at the Institute of Physics of the Czech Academy of Sciences (Prague, Czech Republic) for polymer brush surface characterization, and Dimension FastScan Bio (Bruker, USA) in semi-contact PeakForce Tapping mode at Masaryk University in Brno for studies of bacteria surface-attachment and bacteriophage-bacteria interactions. More details can be found in the publication in preparation (APPENDIX XI)

Fluorescent microscopy was employed to imaging cells and protein fouling on different ultra-low fouling coatings. The high-resolution spinning disk confocal microscopy (Spin SR, Olympus) was used for fluorescent measurements presented here. The details of the experiments are summarized in the appropriate publications. (Víšová et al. 2020a; Víšová et al. 2020b; Víšová et al. 2020c) (APPENDIX V, APPENDIX VI, APPENDIX VII).

PART III

RESULTS

5. Probing of the antifouling polymer brush properties

5.1. Optimization of polymer brush coatings preparation

A set of different types of antifouling polymer brushes was prepared to study the interactions among antifouling polymer brush coatings and biological systems. (For more details on the state-of-art of the antifouling polymer brushes see Chapter 3.2.2.4). Three different zwitterionic and one non-ionic acrylamide and methacrylamide-based monomers with different physico-chemical properties (CBAA, CBMAA, SBMAA, and HPMAA, (Figure 24)) were used for homopolymer or copolymer brushes preparation. The advanced copolymer brush structures were patented and published (for more details see Chapter 5.3).

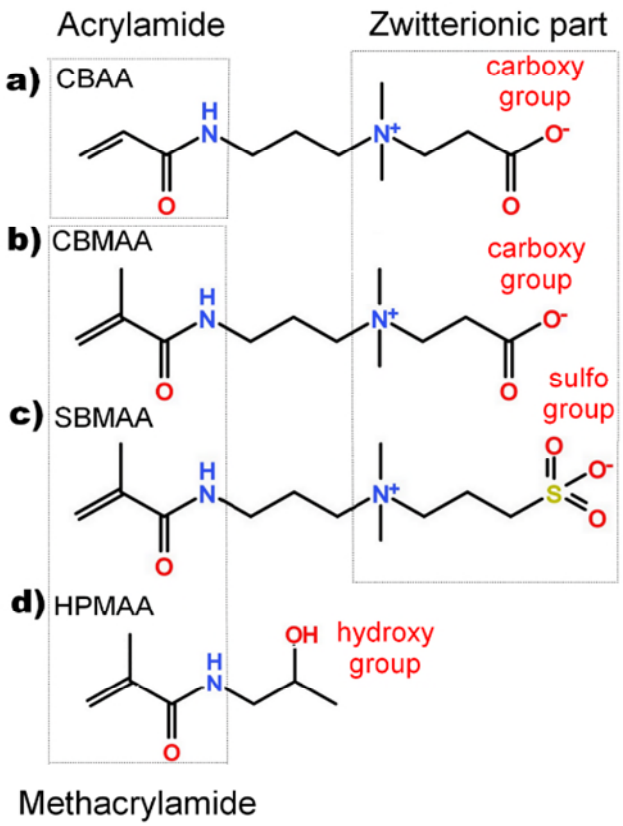

Figure 24: *Scheme of the zwitterionic and non-ionic monomers used for polymer brushes preparation (Višová et al. 2020c).*

Two methods of polymerization were employed. Typically, polymer brush coatings on gold or glass surfaces were prepared by optimized “grafting from” method, the surface-initiated atom transfer radical polymerization (SI-ATRP) (Figure 25). Moreover, reversible addition-fragmentation chain transfer (RAFT) was studied for the preparation of polymer brush chains with reactive groups for polymer-biomolecules conjugation.

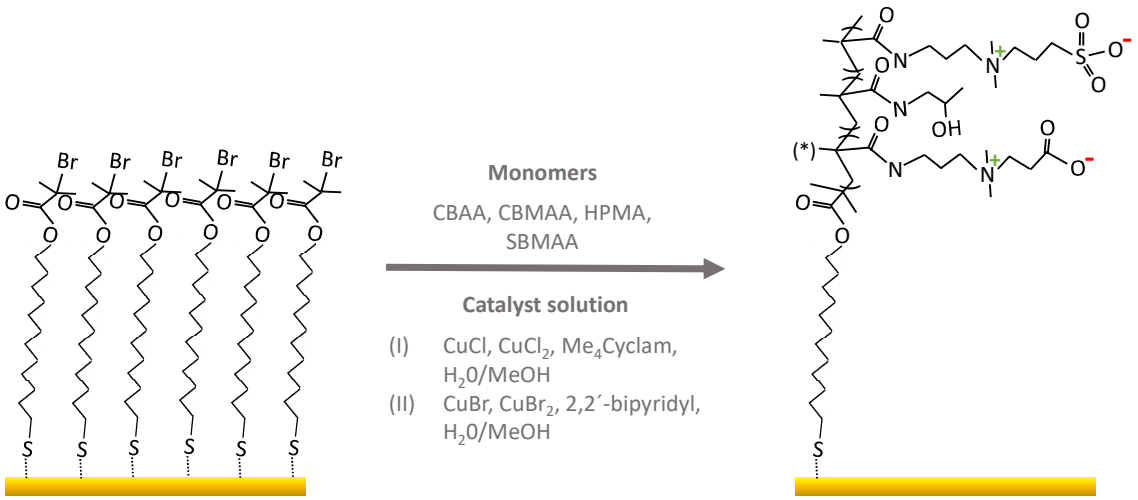

Figure 25: *Synthesis of homo- or copolymer brushes via SI-ATRP. The golden surface coated with SAM layer of Br-initiators is incubated with catalyst solution and a mix of monomers according to the intended coating composition. In pCBAA the methyl group from pCBMAA marked (*) is replaced with H.*

In general, RAFT and SI-ATRP methods are described in detail elsewhere (Barbey et al. 2009). Briefly, RAFT polymerization was performed according to the previously published method (Rodriguez-Emmenegger et al. 2011d), using 4,4-azobis(4-cyanopentanoic) acid as initiator and 4-cyano-4-(phenylcarbonothioylthio) pentanoic acid as raft agent (CTA). The type of the solvent and the CTA:initiator ratio was optimized according to the application (intended polymer chain molecular weight and monomer-type used). The polymerization solution was then dialyzed against Milli-Q water for 72 h and the final product was characterized using IR spectroscopy and gel permeation chromatography. Additional modifications were subsequently applied to introduce the groups for polymer

chain attachment. The set of NHS- or SH-ended pCBAA in a range of sizes of 5 kDa–30 kDa and a copolymer structure p(SBMAA-*ran*-CBMAA-*ran*-HPMAA) (for more details on the copolymer see Chapter 5.3) were prepared by an optimized RAFT procedure.

The SI-ATRP process (especially the initiation efficiency and rate of the polymerization), and the resulting properties of the polymer brush coatings (e.g., thickness or grafting density) prepared by SI-ATRP are dependent on parameters such as time of polymerization, types of catalysts, monomers, and their molar ratios, or the solvent polarity in the polymerization solution (Horn and Matyjaszewski 2013; Mastan et al. 2016; Matyjaszewski et al. 1999; Yan et al. 2016). While optimizing all mentioned parameters, two different catalytic solutions were studied in this work. First, CuBr, $CuBr_2$, and 2,2'-bipyridyl were successfully used for the preparation of thick and dense pCBAA coatings (Vaisocherová-Lísalová et al. 2016b; Vaisocherova et al. 2015b) (APPENDIX I, APPENDIX II). However, the solution was very sensitive to residual oxygen. Later, the solution of CuCl, $CuCl_2$, and Me_4Cyclam was used for the preparation of all types of polymer brush coatings reported here (Lísalová et al. 2017; Vaisocherová-Lísalová et al. 2016a; Víšová et al. 2020a; Víšová et al. 2020b; Víšová et al. 2020c) (APPENDIX III, APPENDIX IV, APPENDIX V, APPENDIX VI, APPENDIX VII).

To simplify the demanding preparation of polymer brush coatings by SI-ATRP, the new laboratory for polymer brush coatings preparation and a custom-made polymerization apparatus was built at the Institute of Physics during the course of the study. The apparatus consists of a multipath vacuum line for the work in the inert atmosphere (easy and repeatable switch between vacuum or nitrogen / argon atmosphere) and a multi-reactor carousel with replaceable reactors for effective preparation of up to 140 coated chips of different sizes, shapes, and substrates (SPR chips, QCM crystals) in up to 7 different polymerization solutions of a minimal volume, simultaneously (Figure 26).

The optimized SI-ATRP approaches were used for preparation of polymer brush coatings of a variety of physico-chemical properties for further research. More details on the individual coatings, their parameters, and the description of optimized procedures of preparation can be found further in Chapter 5, Chapter 6, and in relevant publications.

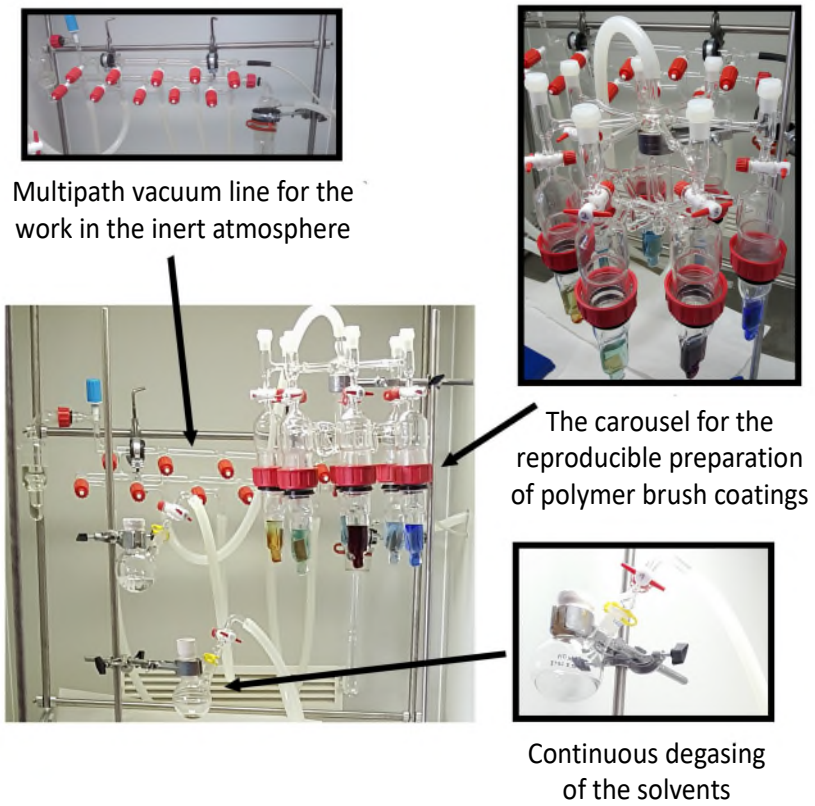

Figure 26: *The SI-ATRP apparatus at the Institute of Physics of the Czech Academy of Sciences (Prague, Czech Republic) for reproducible and effective polymer brush coating preparation.*

5.2. Influence of functionalization on polymer brush fouling resistance

The effects of the molecular mechanisms involved in functionalization of ultra-low fouling carboxy-functional coatings on the BE capacity and especially on the resistance to fouling were investigated extensively during the course of this work. In (Lísalová et al. 2017) (APPENDIX IV) it was shown, that despite the general opinion, hydrolysis is not effective enough to restore the polymer brush structure after EDC/NHS or EDC/sulfoNHS activation (see also Chapter 2.2.2.2), impairing the post-modified resistance of the coating.

Specifically, the SPR data showed relatively high fouling levels from undiluted blood plasma after EDC/NHS activation and hydrolysis-based deactivation using different deactivation buffers, reaction times, and procedures. The optimized deactivation procedure using 30 min of hydrolysis-based deactivation of activated pCBMAA in the deactivation buffer (10 mM sodium borate + 10 mM imidazole + 10 mM NaCl, pH 8.0) led to the fouling levels from the undiluted blood plasma of ~ 18–25 ng/cm^2 compared to the levels of ~ 0–5 ng/cm^2 on the non-activated surface (Figure 27A). The XPS measurements confirmed that only about 63 % of active sulfo-NHS esters were hydrolyzed back to carboxy groups after 30 min of hydrolysis. Moreover, IR spectroscopy revealed another important aspect of the EDC-based activation — the ratio between bands assigned to ionized COO^- and nonionized COOH significantly differ after EDC/NHS activation and deactivation by hydrolysis compared to non-activated coating, possibly impairing the zwitterionic character of the post-modified structure (Figure 27B). Experimental details and more results on the topic can be found in (Lísalová et al. 2017) (APPENDIX IV).

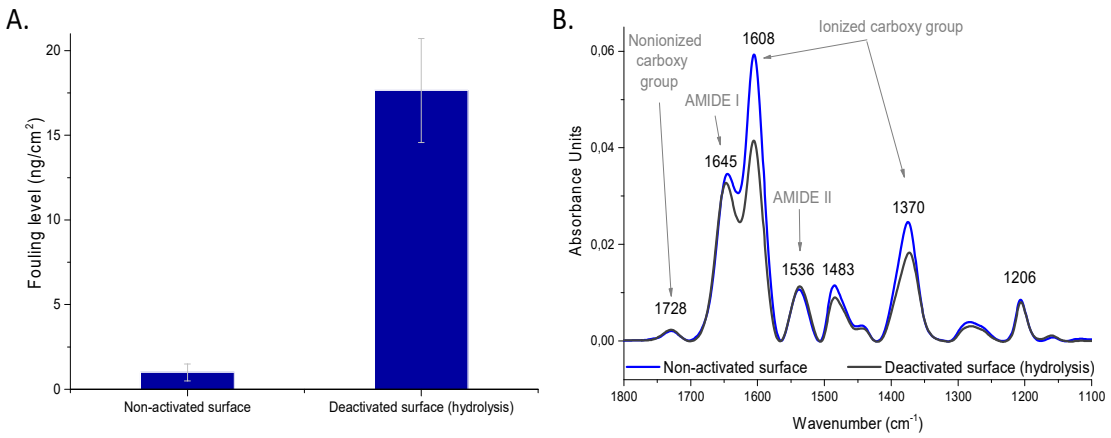

Figure 27: *Representative data show disruption of the p(CB)-brush structure and impairment of the resistance after activation and deactivation by 30 min of hydrolysis in deactivation buffer. A: Non-activated, and activated/deactivated by hydrolysis pCBMAA coatings were exposed to undiluted human blood plasma. The fouling level was assessed by SPR. B: Infrared absorption spectra of non-activated and activated/deactivated by hydrolysis pCBMAA brushes. The decrease in the bands of 1608 cm^{-1} and 1370 cm^{-1} (bands of ionized carboxy group) before activation and after deactivation is apparent.*

To restore post-modified brush properties more effectively, the deactivation of EDC/NHS activated p(CB)-brushes based on covalent attachment of small primary amine and carboxy groups containing molecules was suggested. In the typical SPR fouling experiment studying the p(CB)-brush resistance recovery (Figure 28), p(CB)-brush was mounted in SPR and washed with ultrapure water (Q-water) (for 5 min). Afterwards, the carboxy groups of the p(CB)-brush were turned into active esters using 0.1 M EDC and 0.5 M NHS aqueous solution (20 min). Then, the BE in optimized immobilization buffer was added (20 min), followed by the deactivation agent (30 min). Between all mentioned steps, 2 min long control injections of Q-water were performed. Subsequent measurements of the fouling from complex samples (e.g., undiluted blood plasma) consisted of the injection of PBS buffer for up to 10 min followed by the incubation with complex sample (10 min) and washing with PBS (10 min). The fouling level was determined as the difference between the two PBS baselines. Typically, the higher ionic strength PBS (750 mM NaCl) was

introduced for 5 min followed by PBS again, to wash off all weakly electrostatically bound material and to specify firmly attached nonspecific mass only.

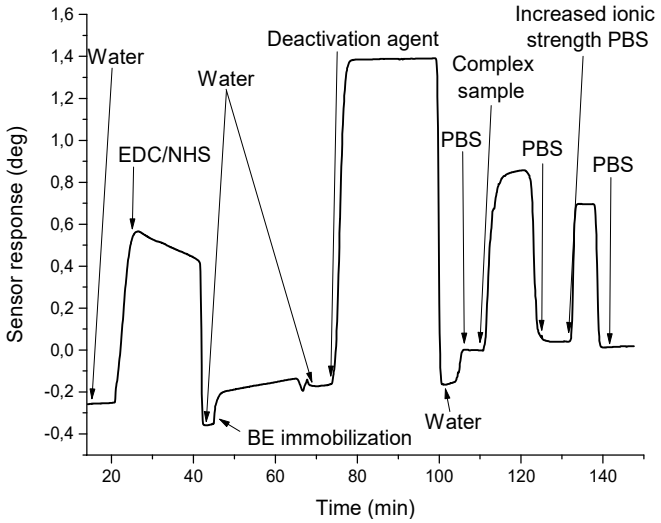

Figure 28: *Typical SPR sensorgram of the experiment to evaluate the performance of the deactivation method.*

The screening of the deactivation of p(CB)-brushes by covalent attachment of the deactivating agents under optimized conditions was performed. Figure 29A shows the set of the deactivating molecules; they were chosen to have a carboxy group, primary amine for covalent attachment, and different lengths of aliphatic chain. Figure 29B shows SPR fouling measurements on p(CB)-brush coating after activation and deactivation by covalent attachment of the respective molecules from Figure 29A. For comparison, hydrolysis-based deactivation is included. With the increasing length of the aliphatic chain the fouling increases (Figure 29B). The best performing non-ethoxy-based deactivation agent was reported to be glycine (1 M glycine, pH 7). The additional improvement of the resistance recovery can be achieved by adding an ethoxy group to increase the hydrophilicity of the resulting deactivated structure [(2-aminoethoxy) acetic acid, AEAA)].

Infrared spectra showed an improvement in ionized carboxy group band recovery after deactivation by a reaction of active esters with glycine molecule. After activation, the ionized carboxy group band at 1608 cm^{-1} decreased to 60 % of the original band of the

non-activated coating. After covalent attachment of glycine, the band recovers to 90 % of the original value, compared to 70 % recovery using hydrolysis-based deactivation (Figure 30). Moreover, in (APPENDIX IX) the IR spectroscopy confirmed, that AEAA restores the ionic form of the carboxy group even more effectively compared to glycine.

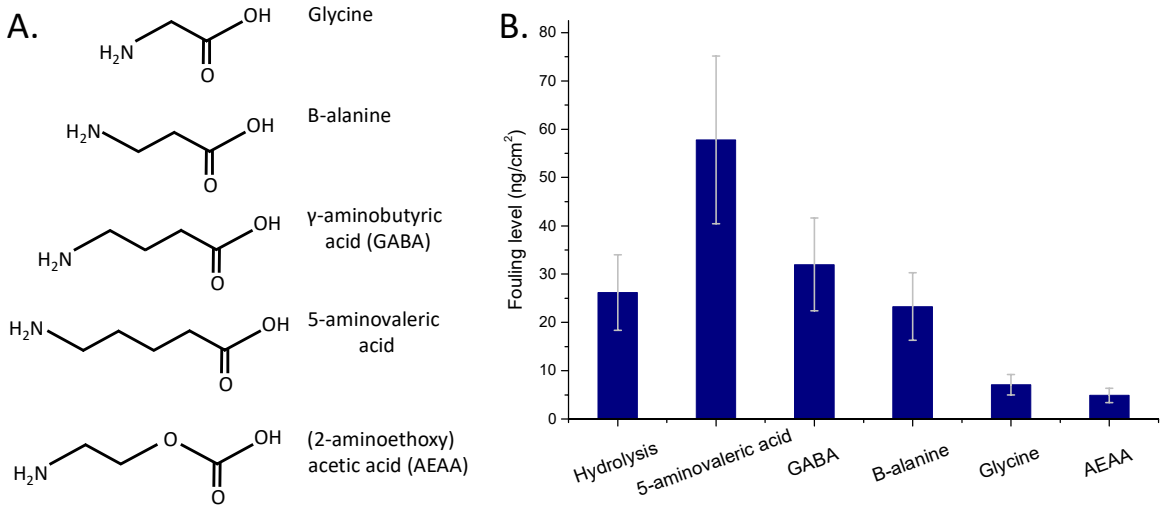

Figure 29: *p(CB)-brush deactivation by covalent attachment of primary amine-containing small carboxy-ended molecules. A: Structures of the deactivating agents used. B: Fouling levels on the activated and deactivated pCBMAA using different deactivation agents measured by SPR.*

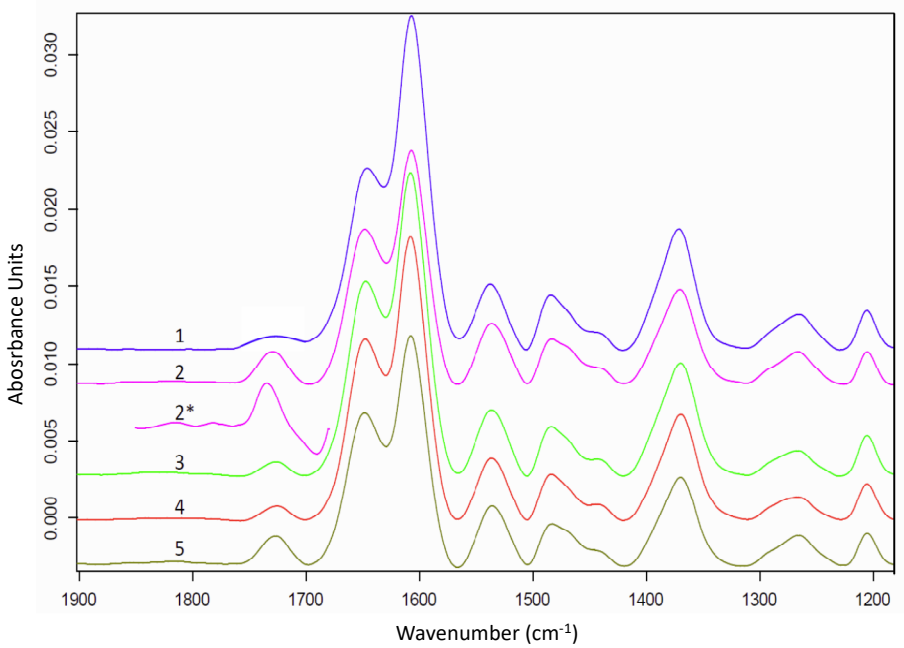

Figure 30: *PM-IRRAS spectra of pCBMAA (1) before activation, (2) after EDC/NHS-based activation, (3) after activation and deactivation with glycine, (4) after activation and deactivation by hydrolysis, (5) after deactivation with ethanolamine. (2*) depicts a part of the difference-spectrum (2)-(1) (Lísalová et al. 2017) (APPENDIX IV).*

It was demonstrated that only the covalent coupling of optimized amino acid-based agents (such as glycine or AEAA) to active NHS esters in the p(CB)-brush substantially improved resistance of activated/deactivated, or BE-functionalized p(CB)-brushes to plasma fouling, while the biorecognition activity stays impaired. These findings were published in (Lísalová et al. 2017) (APPENDIX IV) and are subjects of the patent applications (APPENDIX XIII and APPENDIX XIV).

The successful deactivation procedure has to recover the neutral zwitterionic structure of the functionalized polymer brush, which is a key prerequisite for its antifouling properties. In general, the balance between negative and positive charges is disrupted either through the consumption of carboxy groups for the conjugation with BE, the net charge of the BE itself, or impairing of zwitterionicity of betaines caused by molecular changes in the brush structure after activation (Lísalová et al. 2017) (APPENDIX IV).

To compensate for these effects, improve resistance, and recover the functionalized p(CB)-brush neutral net charge, the advanced deactivation by covalent attachment of a mixture of low molecular-weight molecules bearing primary amines and additional negatively charged moieties was suggested. Besides the two previously studied carboxy-terminated compounds — glycine and AEAA, the two permanently negatively charged agents, 2-aminoethyl hydrogen sulfate (D1), and aminomethanesulfonic acid (D2) were employed (Figure 31). The mixture with the optimized ratio of permanent negative charges along with carboxy groups allows to optimize the charge balance of the surface and restore its post-functionalized resistance to fouling. The deactivation of the pCBAA homopolymer and pCBMAA-based copolymer was tested using SPR fouling experiments (Figure 32) and IR spectroscopy.

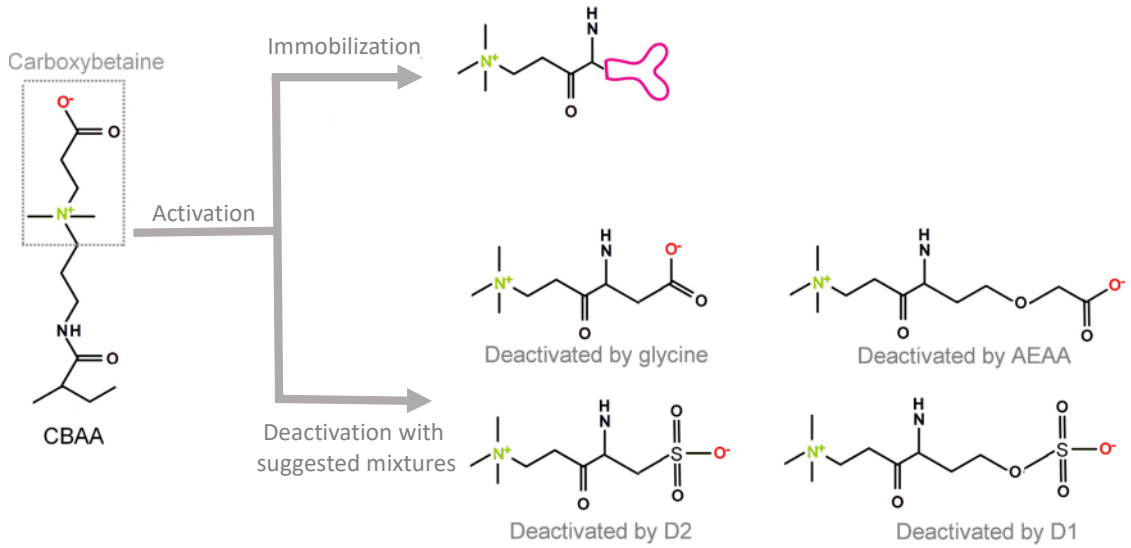

Figure 31: *CBAA monomer unit before activation (left), the detail of the structure after BE immobilization (right top), and products of deactivation by glycine, AEAA, D1, and D2. Positively charged atoms are marked green, negatively charged atoms are red.*

The Figure 32 shows fouling levels after pCBAA deactivation with selected deactivation mixtures (complete data can be found in (APPENDIX IX). Compared to the fouling level after glycine-based deactivation, a significant improvement (7.5 times reduction of the

fouling level to 3.8 ng/cm^2) was observed after the addition of a very small amount of negative permanent charge of D1 (4 %) (96G:4D1). However, the higher content of D1 impairs the resistance again.

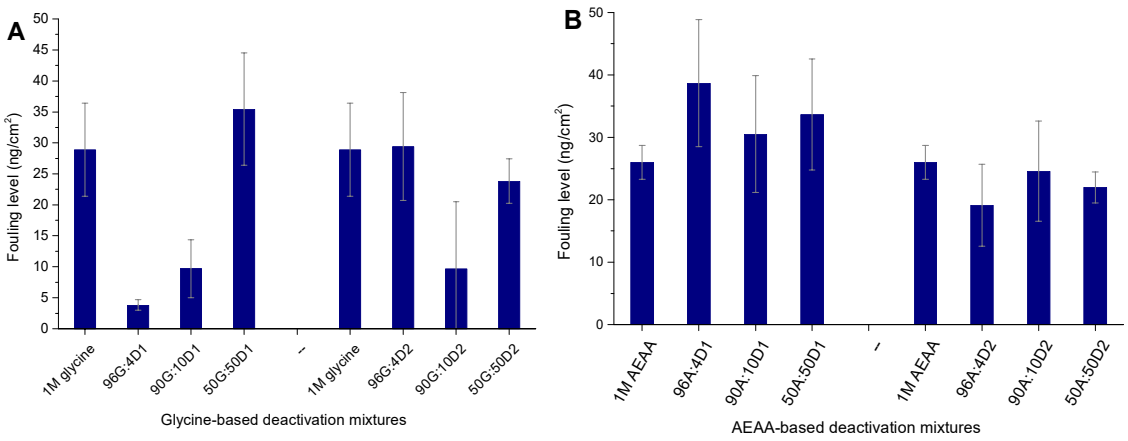

Figure 32: *Fouling levels on IgG-functionalized and deactivated pCBAA after exposure to undiluted human plasma. A: Glycine-based mixtures were used for surface deactivation. 96G:4D1/4D2 = 960 mM G + 40 mM D1 or 40 mM D2, 90G:10D1/D2 = 900 mM G + 100 mM D1 or 100 mM D2, 50G:50D1/D2 = 500 mM G + 500 mM D1 or 500 mM D2. B: AEAA-based mixtures were used for surface deactivation. 96A:4D1/4D2 = 960 mM A + 40 mM D1 or 40 mM D2, 90A:10D1/D2 = 900 mM A + 100 mM D1 or 100 mM D2, 50A:50D1/D2 = 500 mM A + 500 mM D1 or 500 mM D2.*

The IR spectra analysis revealed an expected decrease in absorption of ionized carboxyl after all deactivation procedures, however, strong bands of sulfate group at 1253 cm^{-1}, 1229 cm^{-1}, and 1010 cm^{-1}, and sulfo group at 1230 cm^{-1}, and 1010 cm^{-1} appear after D1-, or D2-based deactivation, confirming the attachment of D1, and D2, respectively. The extra permanent negative charge in the deactivated structure addresses the misbalance of the charge density caused by functionalization, restoring more effectively fouling resistance. Moreover, the deactivation method is generic, the same trends were observed for the p(CB)-copolymer brush (the magnitude of the change was proportional to the amount of carboxy groups in the structure).

The biorecognition capabilities of the anti-bacterial IgG antibody-functionalized pCBAA biochip for the detection of *E. coli* H157:O7 from crude food sample (minced meat) employing new optimized deactivation procedures were explored. To assure the best comparability with the state-of-art deactivation methods, the glycine-based procedure was used along with the new suggested mixtures. Using 90G:10D2 mixture or AEAA deactivation solution, the fouling from minced meat on the functionalized coating was suppressed to 2.1 ng/cm^2 and 1.0 ng/cm^2, respectively, compared to fouling level on glycine-deactivated coatings (10.1 ng/cm^2). The limit of detection was improved by two orders of magnitude, compared to glycine-based deactivation. All the data and more information can be found in a submitted paper (APPENDIX IX)

The proposed deactivation strategy using the tailored composition of a deactivation mixture brings an attractive way to recover the p(CB)-based brush resistance to fouling after functionalization and tune its post-modified characteristics (such as surface net charge). Moreover, we showed that such an approach is generic and can be used to improve fouling resistance of any p(CB)-brush coating, which makes it a very promising tool for high-performance label-free biosensor applications, as well as for fields including studies on cell interactions with surface and cell-on-chip technologies.

5.3. Tailoring of the new antifouling functionalizable polymer brush structures

Functional polymer coatings that combine the high resistance to nonspecific fouling from complex media with bioactive element (BE) immobilization capacity represent an emerging class of new functional materials for a number of biological, bioanalytical, and biosensor technologies and create an important platform for studies of biomolecular interactions in native complex conditions (Banerjee et al. 2011). The state-of-art pCBAA zwitterionic polymer brushes showing superior resistance and high BEs loading capacity, however, suffer from the resistance impairment after EDC/NHS functionalization (Chapter 5.2) and relative sensitivity to different physico-chemical properties of the complex samples (Chapter 3.2.2.4). During the course of this thesis, we have developed, patented, and published/prepared for publication two types of new copolymer brush coatings with lower susceptibility to functionalization-based impairment and improved antifouling properties.

A random copolymer brush structure combining high resistance of hydroxy-ended pHPMAA and feasible functionalization of carboxy-ended pCBMAA was introduced in (Rodriguez-Emmenegger et al. 2016; Vaisocherová-Lísalová et al. 2016a) (APPENDIX III) (Figure 33). The p(CBMAA-*ran*-HPMAA) coatings were prepared via the SI-ATRP method (Chapter 5.1, Figure 25). Due to the similar polymerization rates of both monomers, the control over the surface molar content of the pCBMAA was achieved by simple tuning of the volume concentration of CBMAA in the polymerization feed (Figure 34).

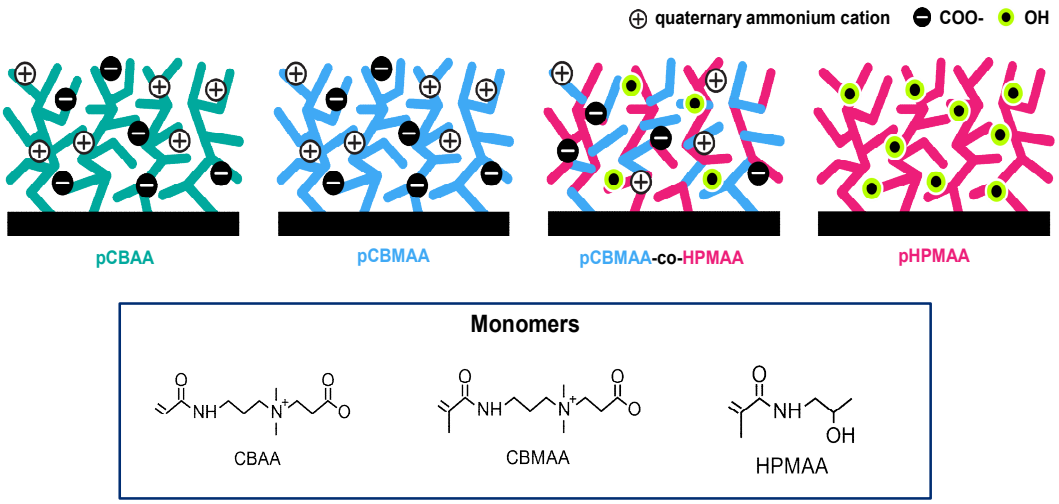

Figure 33: *Scheme of the zwitterionic CB-based and non-ionic antifouling homo- and copolymer brushes.*

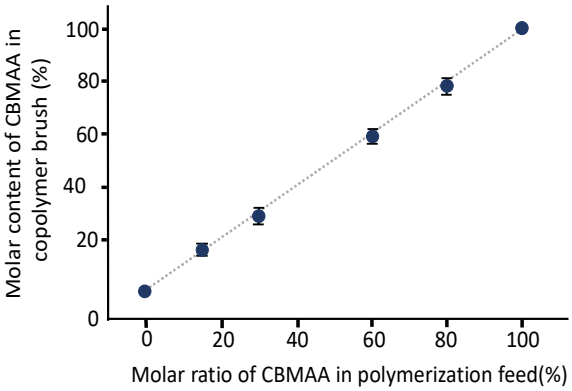

Figure 34: *Dependence of the surface molar content of CBMAA in copolymer brush on CBMAA molar ratio in polymerization solution determined from PM-IRRAS spectra.*

The fine-tuning of the CBMAA content in the copolymer structure allows tailoring the physico-chemical properties of the coating. With increasing content of hydrophilic carboxy-ended CBMAA the overall hydrophilicity (Figure 35) and BE-loading capacity increase. However, due to the susceptibility of the resistance of p(CB) to

functionalization-based impairment (Chapter 4.2), the fouling level increases at the same time (Figure 36).

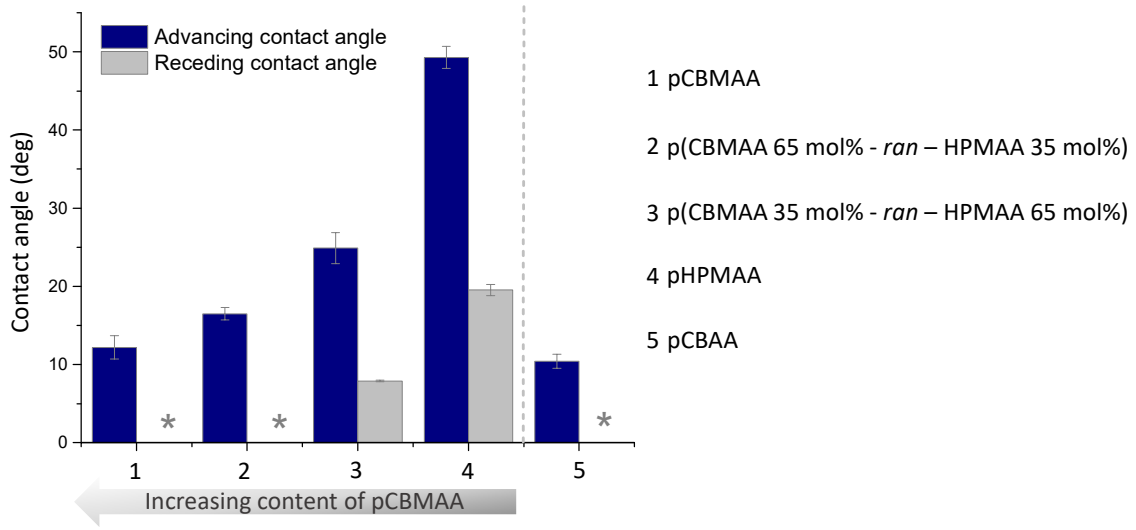

Figure 35: *Dynamic contact angle characterisation of a set of random copolymer p(CBMAA-ran-HPMAA) with increasing content of pCBMAA (0–100 mol%). pCBAA is shown for comparison. Receding angles marked by asterisk could not be determined due to a very high wettability.*

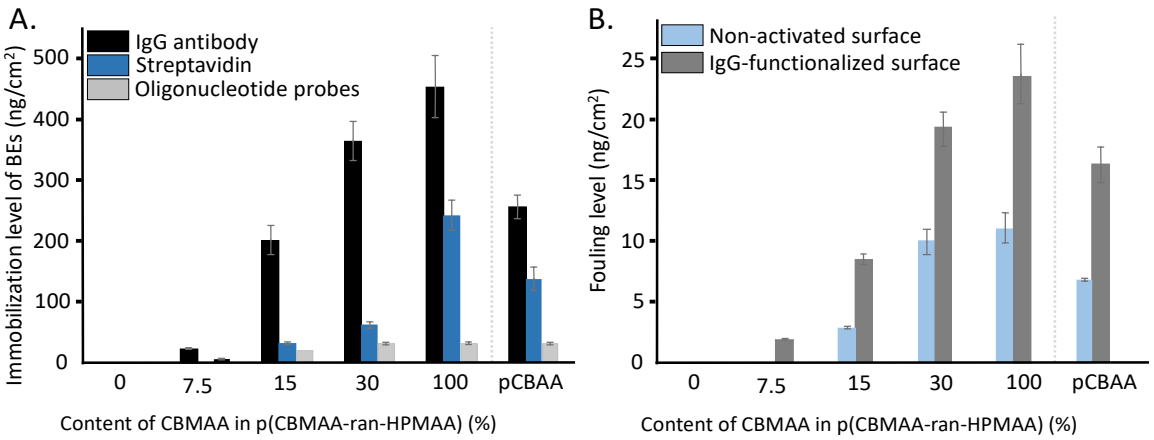

Figure 36: *The characterization of p(CBMAA-ran-HPMAA) brush properties in dependency on the content of pCBMAA in the structure. A: Level of immobilization increases with increasing CBMAA content. B: Fouling level increases with increasing CBMAA content. pCBAA is depicted in A and B as a reference state-of-art antifouling polymer brush coating (Vaisocherová-Lísalová et al. 2016a) (APPENDIX III).*

The easy tailoring of the p(CBMAA-*ran*-HPMAA) brush fouling resistance, BE loading capacity, level of hydrophilicity, and level of zwitterionicity creates the tunable platform for applications in high-performance biosensors or research of biomolecular and biological interactions near surfaces with different properties. In particular, p(CBMAA-*ran*-HPMAA) brush biocompatibility (Víšová et al. 2020b) (APPENDIX V) makes it a great tool for living cell studies. More details on p(CBMAA-*ran*-HPMAA) preparation and characterization can be found in (Vaisocherová-Lísalová et al. 2016a; Víšová et al. 2020a; Víšová et al. 2020b) (APPENDIX III, APPENDIX VII, APPENDIX V).

Based on the research on p(CBMAA-*ran*-HPMAA) copolymer brush and the research on the pCB deactivation issues, new functionalizable antifouling polymer brush material with an optimized architecture based on a statistical distribution of CBMAA, HPMAA and SBMAA were designed. The addition of a small amount of SBMAA, which in contrast to carboxybetaine bears permanent negative charge, helps to optimize the charge state after functionalization. The fouling levels from undiluted plasma were compared for anti-bacterial antibody-functionalized pCBAA, p(CBMAA/15mol%-*ran*-HPMAA/85mol%), and poly(SBMAA/3mol%-*ran*-CBMAA/15mol%-*ran*-HPMAA/82mol%) deactivated using AEAA-based deactivation procedure (see chapter 5.2), showing increasing tendency in resistance of more advanced structures (14.5 ng/cm^2, 7.9 ng/cm^2 and 4.5 ng/cm^2 from undiluted blood plasma, respectively). Moreover, the composition of the terpolymer brush can be adjusted for a specific application. The negatively charged short amino-modified oligonucleotide probes were successfully immobilized on the p(SBMAA/0.5mol%-*ran*-CBMAA/15mol%-*ran*-HPMAA/84.5mol%), showing a fouling level of 0 ng/cm^2, compared to 3 ng/cm^2 of the p(CBMAA/15mol%-*ran*-HPMAA/85mol%). When positively charged BE is immobilized, the higher amount of permanent negative charge can be used with advantage – the p(SBMAA/30mol%-*ran*-CBMAA/15mol%-*ran*-HPMAA/55mol%) exhibited fouling level of 6 ng/cm^2, compared to 11.7 ng/cm^2 of the p(CBMAA/15mol%-*ran*-HPMAA/85mol%). The new structure is the subject to the patent applications (APPENDIX XV and APPENDIX XVII).

The composition of the random copolymers p(CBMAA-*ran*-HPMAA), and p(SBMAA-*ran*-CBMAA-*ran*-HPMAA) can be easily tuned to maintain sufficient binding capacity, while

enhancing post-functionalization antifouling properties. Moreover, physico-chemical properties of the coatings, such as hydrophilicity, rigidity or ionicity can be simply adjusted. Such antifouling functional platforms with tunable properties are promising tools for many biological and biomedical applications, such as cell research or biosensors applications. Some of the applications of both copolymer structures are further described in Chapter 6.

5.4. Polymer brush preconditioning and swelling studies

For a deeper understanding of the superior fouling resistance properties of ultra-low fouling polymer brush coatings, the environment-dependent structural changes of zwitterionic and non-ionic polymer brushes were studied. The model set of homopolymer brushes with the comparable architecture of the polymer backbone, varying in monomer structure and functional groups represents a series of different surface physico-chemical properties (Figure 24). Particularly, pCBAA and pCBMAA allow a comparison of the role of acrylamide and methacrylamide backbones, respectively, and pCBMAA, pSBMAA, and pHPMAA reflect the role of different functional groups (i.e. carboxy-, sulfo- and hydroxy groups, respectively) in environment-evoked structural changes and shifts in polymer brush properties.

To describe the structural changes in the polymer brush layer, spectroscopic ellipsometry was employed. The ellipsometric spectra of dried and wet coatings were recorded using optimized hardware for measuring thin layers in an aqueous environment (Figure 22, Chapter 4.2) developed at the Institute of Physics of the Czech Academy of Sciences (Prague, Czech Republic).

Typically, the empirical Cauchy or advanced Cauchy-Urbach, or Sellmaier models have been used in literature for fitting the ellipsometric data of dielectric transparent molecular layers (Furchner et al. 2013; Kroning et al. 2015; Tang et al. 2001; Wiarachai et al. 2016). However, for zwitterionic brushes having a more complex structure, the simple parameters of these models were found to be insufficient to obtain a best-fit in full measured energy region (especially in a higher energy range) (Figure 37). Moreover, no universal fitting model was found to describe sufficiently all polymer brushes under study. Therefore, the models using a more complex parametrization were suggested and optimized for every polymer brush type separately. Specifically, a single-oscillator (Tauc-Lorentz) model was employed in pCBAA and pSBMAA brushes, and a double-oscillator (Gaussians) model in pCBMAA and pHPMAA brushes of the thickness of 60-130 nm. The analysis of the thicker brushes of pCBAA (more than 200 nm) revealed the graded refractive index distribution decreasing monotonically away from the surface (Figure 38).

Examples of the fitted spectra of all four polymer brushes and more details about experiments can be found in Supporting Information in (Víšová et al. 2020c) (APPENDIX VI)

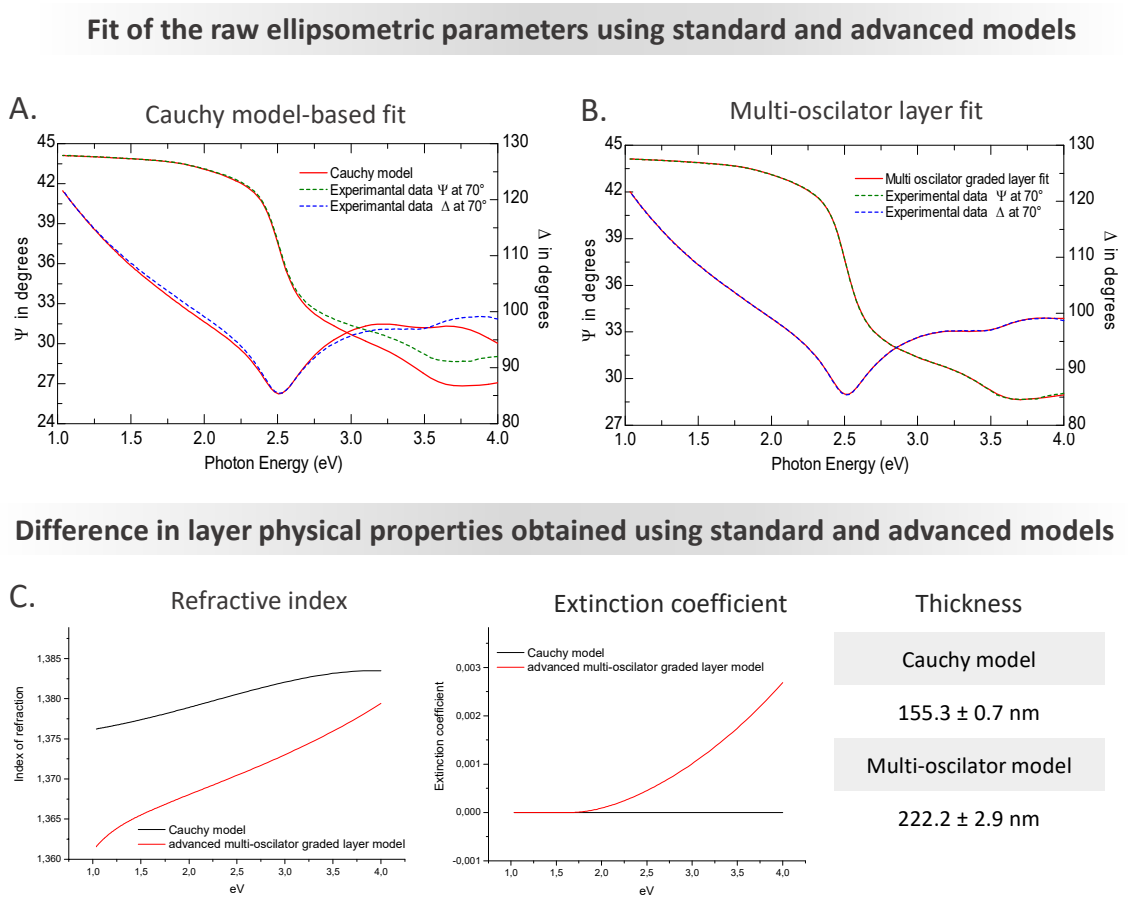

Figure 37: *The pCBAA brush ellipsometric data measured in water environment fitted using standard Cauchy model (A), and optimized advanced multi-oscillator model suggested in the study (B). Bottom line (C) compares physical parameters obtained from applied models.*

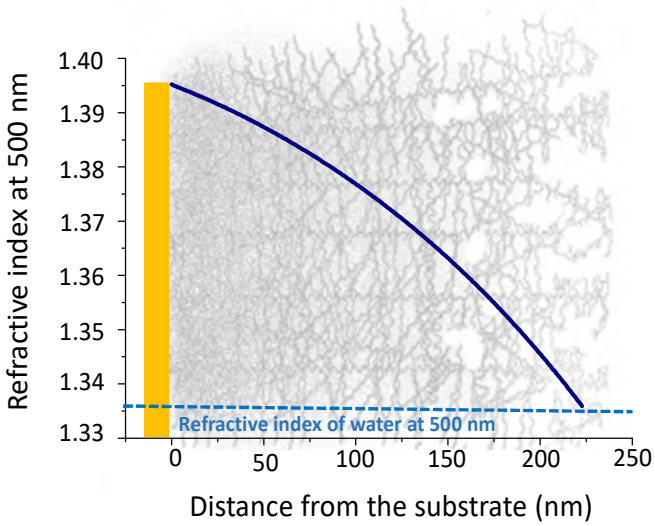

Figure 38: *Refractive index dependency (at 500 nm) on the distance from the substrate for pCBAA with the thickness of 232 nm in water. Background: scheme of the polymer brush with graded density of polymer chains decreasing with the distance from the gold substrate.*

The changes in the effective thickness and refractive index of homopolymer brushes regarding the monovalent and bivalent ionic strength of the environment were studied using spectroscopic ellipsometry. Interestingly, with increasing ionic strength in the aqueous buffer (HEPES), all zwitterionic coatings exhibited an increase in effective thickness, whereas the effective thickness of non-ionic pHPMAA systematically decreased (Figure 39). Carboxy-functional zwitterionic coatings (pCBAA, pCBMAA) responded about 3 times more intensively to monovalent (NaCl) than bivalent ($MgCl_2$) ions presence. On the other hand, the thicknesses of both pHPMAA and pSBMAA brushes were only weakly affected by ion type.

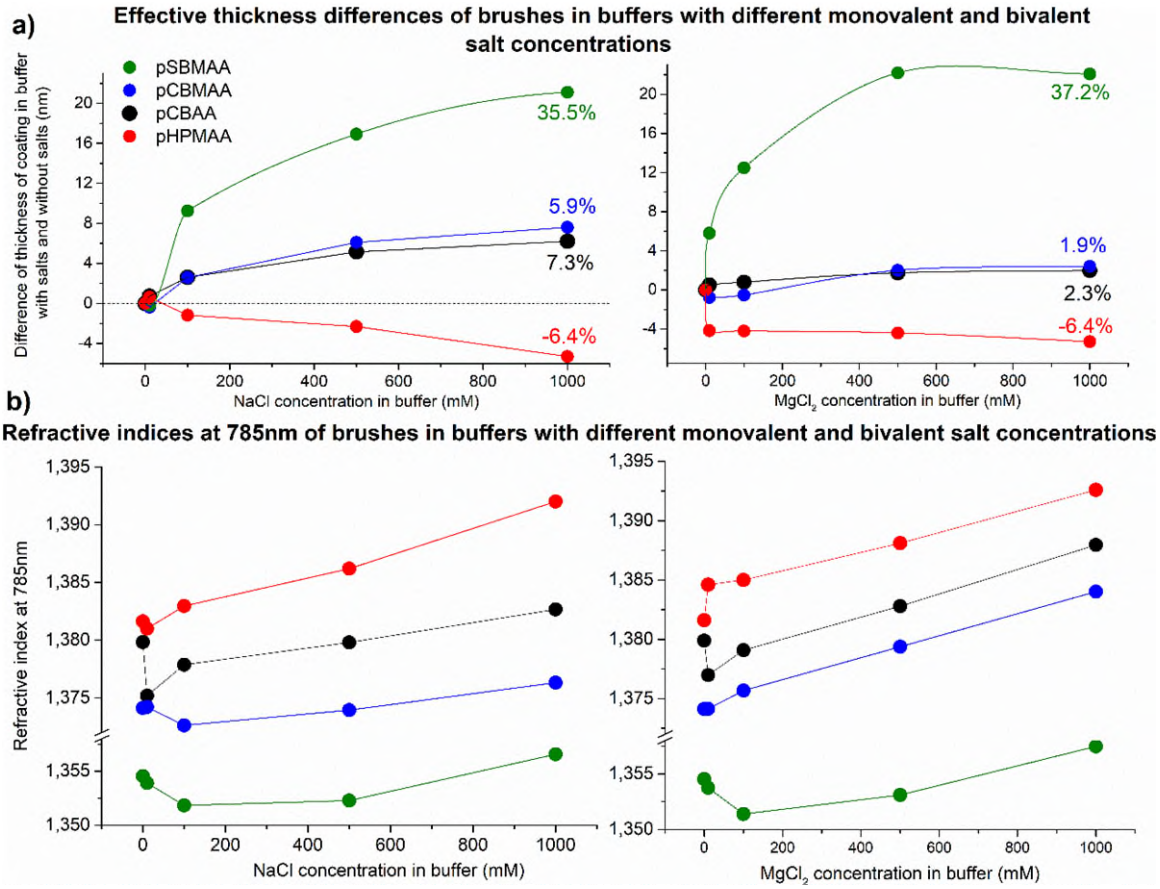

Figure 39: *Changes in the effective thickness (a) and refractive index at 785 nm (b) of polymer brushes at varying ionic strength of monovalent (left column) and bivalent (right column) ions. The %-increase depicted in (a) is calculated as a change of thickness in 1M salt regarding the thickness in non-salt environment (Víšová et al. 2020c)*

Interestingly, data from ellipsometry showed, that for all studied types of brushes, with increasing ionic strength and increasing thickness, the refractive index slightly increased as well. Moreover, QCM experiments argued, that the salt ions were bounded in the polymer structures (data and discussion in greater detail can be found in (Víšová et al. 2020c) (APPENDIX VI). Based on the ellipsometric and QCM experiments, the hypothesis of polymer brush swelling was suggested (Figure 40). While non-ionic pHPMAA responded to an increase in ionic strength by shrinking attributed to dehydration, and only a small amount of salt ions were bounded in the structure, zwitterionic materials exhibited much more complex behavior. For the zwitterionic brush with lower packing density, the polymer chains were likely more coil-like near the surface in the environment with no added salts. Around 10 mM of the salt, the chains started to uncoil as the electrostatic interactions between chains were shielded. The "unbound" structure increased in thickness, but decreased in refractive index and increased in the QCM signal. Above

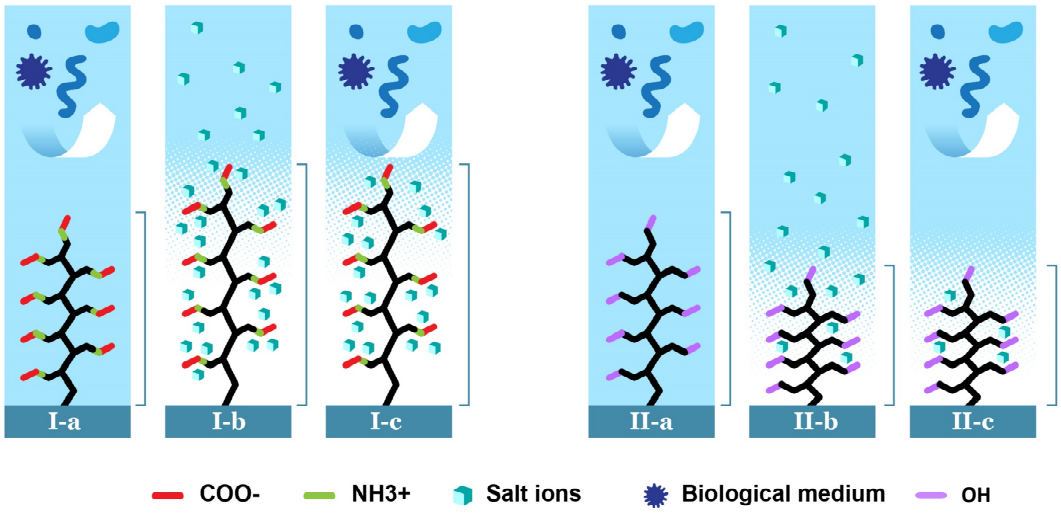

Figure 40: *Scheme of the swelling hypothesis. Left: antifouling zwitterionic polymer brush (I-a) introduced to higher ionic strength environment exhibited increase in thickness and refractive index, caused by bounding salt ions in the structure and shielding of intra-polymer brush interactions (I-b). Right: antifouling non-ionic polymer brush (II-a) introduced to higher ionic strength environment exhibited shrinking assigned mainly to dehydration (II-b). For both types of brushes, such changes may influence the polymer brush fouling resistance (I-c and II-c). Design of the figure: Daniel Špaček, neuroncollective.com.*

100 mM salt, the effect of binding salt ions in the structure counterweighted the effect of chains straightening, increasing thickness, refractive index, and decreasing QCM signal.

The structural changes in antifouling polymer brushes described above were shown to influence the fouling resistance. The polymer brush coatings were incubated in solutions of different salt ion concentrations for 20 min and then immediately exposed to undiluted human blood plasma. The fouling level was observed by fluorescent microscopy, as it is not a swelling-sensitive method (Figure 41). Interestingly, the optimal NaCl concentration for preconditioning of methacrylamide-based brushes was found to be 500 mM, while acrylamide-based brush showed the optimal preconditioning concentration to be around 100 mM. Even though, the pCBMAA is considered to be slightly less resistant to fouling from undiluted blood plasma than pCBAA (see also Chapter 3.2.2.4), the fouling levels on the preconditioned pCBAA and pCBMAA using optimal NaCl concentrations are comparable. However, pCBAA reports higher resistance to undiluted blood plasma under physiological conditions (~ 150 mM).

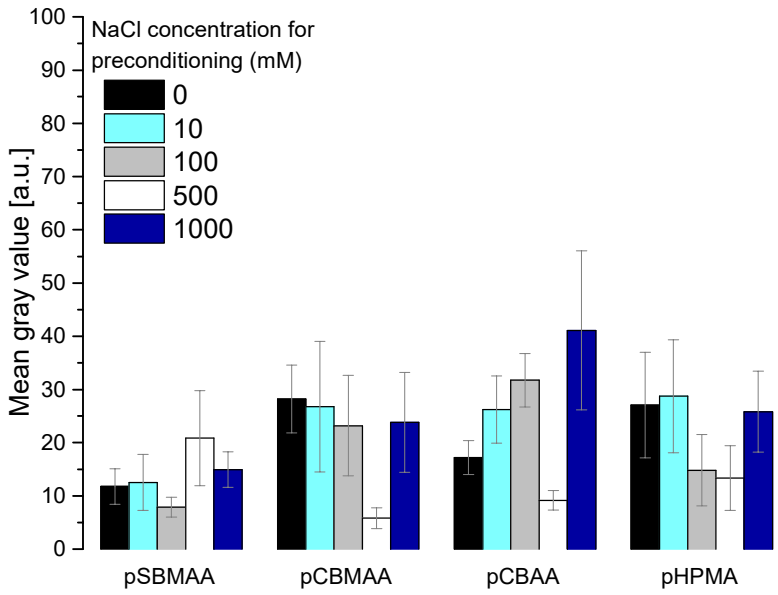

Figure 41: *Fouling from undiluted blood plasma on homopolymer brushes pre-incubated in different ionic strength environments measuered by fluorescent microscopy (Višová et al. 2020c).*

To describe the preconditioning of the polymer brush coatings in greater detail, the reversibility of hydration of polymer brush coatings after drying followed by rehydration, and the influence of drying-induced changes on fouling resistance were studied. All brushes exhibited a slight decrease in refractive index (Figure 42 A) and increase in wet effective thickness (Figure 42 B) after rehydration compared to non-dried structures. This suggests a higher level of hydration in the rehydrated layer, compared to the non-dried coatings. These results were supported by SPR measurements – the fouling level from undiluted blood plasma was significantly decreased after polymer brush rehydration (Figure 42 C; for more details on the influence of hydration on the fouling resistance see Chapter 3.2.1.).

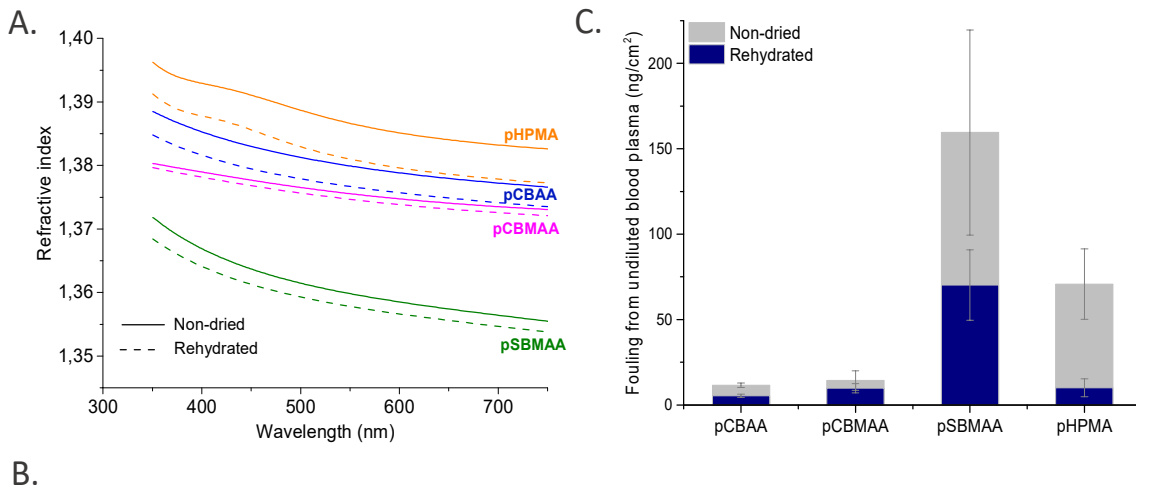

Table: Wet effective thickness of different homopolymers before drying and after drying / rehydration measured by ellipsometry

Wet thickness	pCBAA	pCBMAA	pSBMAA	pHPMAA
Non-dried (nm)	119.0 ± 0.1	119.2 ± 0.2	67.3 ± 0.8	82.5 ± 0.4
After rehydration (nm)	125.4 ± 0.2	122.1 ± 0.2	73.6 ± 1.1	85.7 ± 0.2

Figure 42: *Influence of drying-based preconditioning on the polymer brush structure, and the fouling level from undiluted blood plasma. The properties of non-dried and after-drying rehydrated homopolymers in water was measured by spectroscopic ellipsometry A: Refractive index changes B: The effective thickness changes. D: Fouling levels from undiluted blood plasma measured by SPR. (Višová et al. 2020c)*

The study on preconditioning (Víšová et al. 2020c) (APPENDIX VI) describes the response of the structure and properties of antifouling polymer brush coatings to changes of ionic strength of their environment and drying with subsequent rehydration. It was shown, that simple preconditioning can significantly influence antifouling resistance, introducing a simple way of polymer brush resistance tailoring and highlighting the importance of an in-depth understanding for processes occurring in the brush layers in relevant environments.

6. Antifouling polymer brushes: applications

6.1. Antifouling polymer brush coatings in cell research

6.1.1. Antifouling coatings as tunable platforms for cell-surface interaction studies

The cell-surface interactions describe a complex relationship between surface properties, protein adsorption, and cell adhesion and function. The physico-chemical properties of the interface influencing cell adhesion and response are for example roughness and topography, surface stiffness, biochemical cues and functional groups, charge, or wettability (Alves et al. 2010; Oliveira et al. 2014; Schweikl et al. 2007; Stevens and George 2005; Van Kooten et al. 1992; Van Wachem et al. 1987; van Wachem et al. 1985). Therefore, well-defined antifouling polymer brush coatings guaranteeing negligible nonspecific protein adsorption, biocompatibility, and sufficient level of functional groups for further functionalization represent an attractive approach to elucidate the effects of surface physico-chemical properties on cellular behavior and create a promising platform for studies of highly specific surface-cell interactions.

In (Víšová et al. 2020b) (APPENDIX V), the set of well-defined antifouling polymer brushes with tailored physico-chemical properties was employed to study the effect of wettability, surface charge, and swelling of antifouling platforms on the cell growth, shape, and cytoskeleton distribution. In particular, using of the human hepatocellular carcinoma cell line (Huh7), the tendency of the cell growth, cellular shaping, cytoskeleton distribution, and clustering upon contact with the p(CBMAA-*ran*-HPMAA) with different amount of pCBMAA (0–100 mol%) and pCBAA was analyzed using the high-resolution spinning disk confocal microscopy.

After 4 days of incubation of Huh7 cells on antifouling coatings, cells were viable but were not fully adhered to any type of brushes — they could be easily washed out from the brush structure using mild solutions such as PBS or water. The lowest cell settlement was observed for the highest amounts of pHPMAA in the structure [pHPMAA and p(CBMAA/35mol%-*ran*-HPMAA/65mol%)] and it slightly increased with the increasing

amount of pCBMAA. The highest settlement was found on pCBAA, but still an order of magnitude lower than that observed using a solution-based positive control. The same trend was described by studying cluster formation and the shape of the cells (Figure 43). For pHPMAA, the lowest cluster area and strictly round shape of cells were detected, while pCBAA showed the highest cluster area and the cells became more irregular in shape with the cytoskeleton distribution exhibiting a prerequisite of the cell adhesion pattern.

Comparing such observation with Figure 35, the increasing wettability of antifouling polymer brushes may induce increasing settlement of cells with more irregular shapes and higher cluster area. However, a significant difference in the cell shape was observed between pCBAA and pCBMAA, both showing extremely high wettability. Only the cells on pCBAA exhibited growth and shape patterns indicating well-spread cells, whereas growth on pCBMAA resulted in a decrease in cell spreading with more rounded morphology and peripheral cytoskeleton distribution.

The fouling studies of the coatings used for the cell adhesion research showed no detectable fouling neither from undiluted human blood plasma nor cell-free culture medium, however, a certain degree of fouling from the cells in the culture medium was observed. This may suggest, that the high surface resistance to nonspecific protein adsorption may not be a sufficient prerequisite to prevent cell adhesion or vice versa (Ostuni et al. 2001; Pape et al. 2017) and that as one of the critical parameters, wettability should be considered.

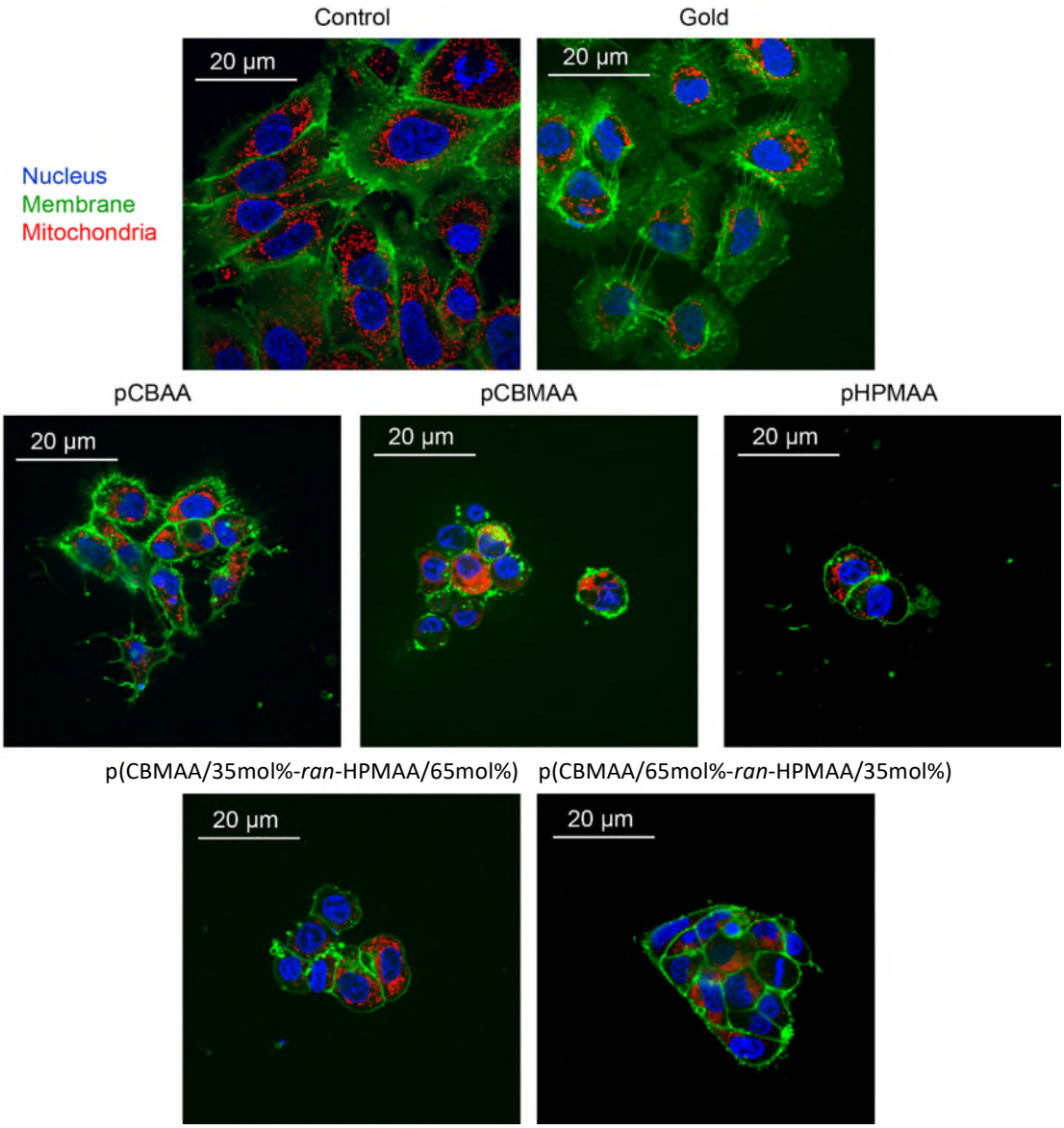

Figure 43: *Analysis of cellular shape influenced by antifouling polymer brush background. Cells were seeded on different substrates for 4 days and labeled with MitoTracker Red (red dye), Hoechst 33342 nuclear stain (blue dye). Cell membranes were labeled with CellMask™ Green (green dye) (Víšová et al. 2020b).*

To demonstrate the applicability of antifouling coatings in cell-surface interaction research, the study on RGD-induced yes associated protein (YAP) connected mechanotransduction in cells was conducted (Víšová et al. 2020a) (APPENDIX VII). The RGD-peptides are known to promote cell adhesion through specific integrin interaction, triggering a certain mechanical stress response in cells (Hersel et al. 2003). Such surface-mediated stress response may be detectable by probing the YAP translocation in Huh7 cells.

The set of RGD-functionalized p(CB)-based antifouling brushes was employed as a smooth approach to control the level of extracellular mechanical stress. The antifouling background diminished nonspecific interactions of cells and cell culture media with the surface and can accurately tailor the cell-surface interactions by creating a controlled cell-surface interface.

Two different strategies to prepare a surface with varying concentrations of RGD peptide were performed (Figure 44). First, carboxy-functional coatings pCBAA (or carboxy-ended OEG-SAMs as a reference surface) were functionalized using solutions with different concentrations of RGD-peptides (Figure 44-A1 and 44-A2). Second, a gradient of surface carboxy groups (Figure 44-B1 and 44-B2) was prepared by using p(CBMAA-*ran*-HPMAA) with varying ratio of carboxy-functional and hydroxy-functional monomer units (or OEG SAM coatings as a reference surface).

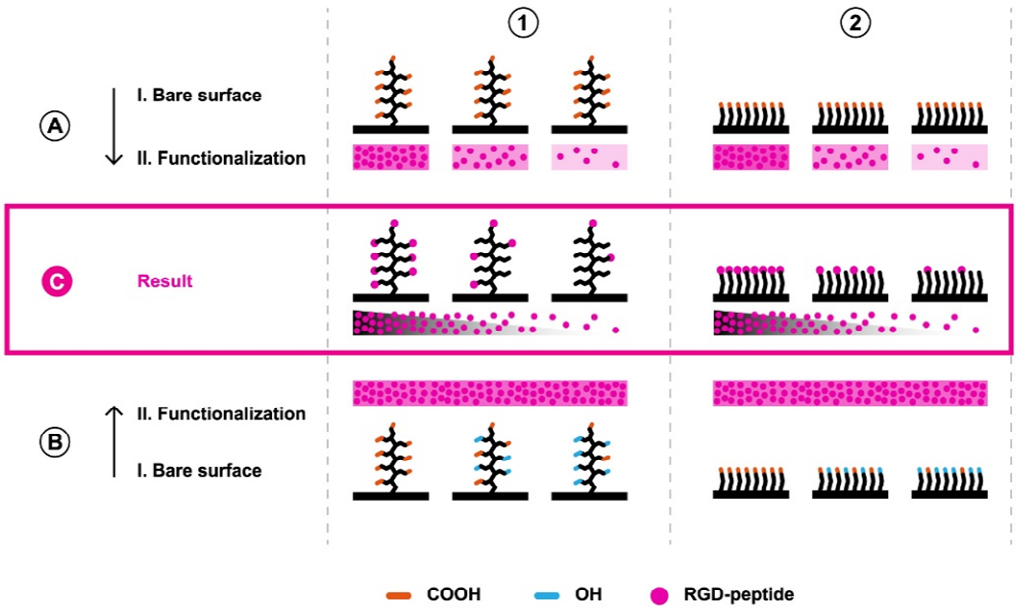

Figure 44: *Functionalization strategies to prepare coatings with varying concentrations of RGD peptide. RGD-functionalized variable sets of p(CB)-coatings (C1) and OEG SAM coatings (C2) were prepared using two different approaches. (A) Activated only-carboxy-functional coatings were exposed to varying concentrations of RGD-peptide solutions. (B) A set of coatings with varying ratios of carboxy groups in relation to non-reactive hydroxy groups was exposed to a high concentration of RGD-peptide after activation (Višová et al. 2020a) (APPENDIX VII).*

Functionalized coatings with different amounts of RGD-peptide and different levels of resistance to fouling were exposed to Huh7 cells for 3 days. While functionalized antifouling p(CB)-based brushes showed a clear dependency of cell growth on the RGD-peptide immobilized level, there was no dependency found for OEG SAM coatings, highlighting the importance of antifouling background in cell-surface interaction research (Figure 45).

.

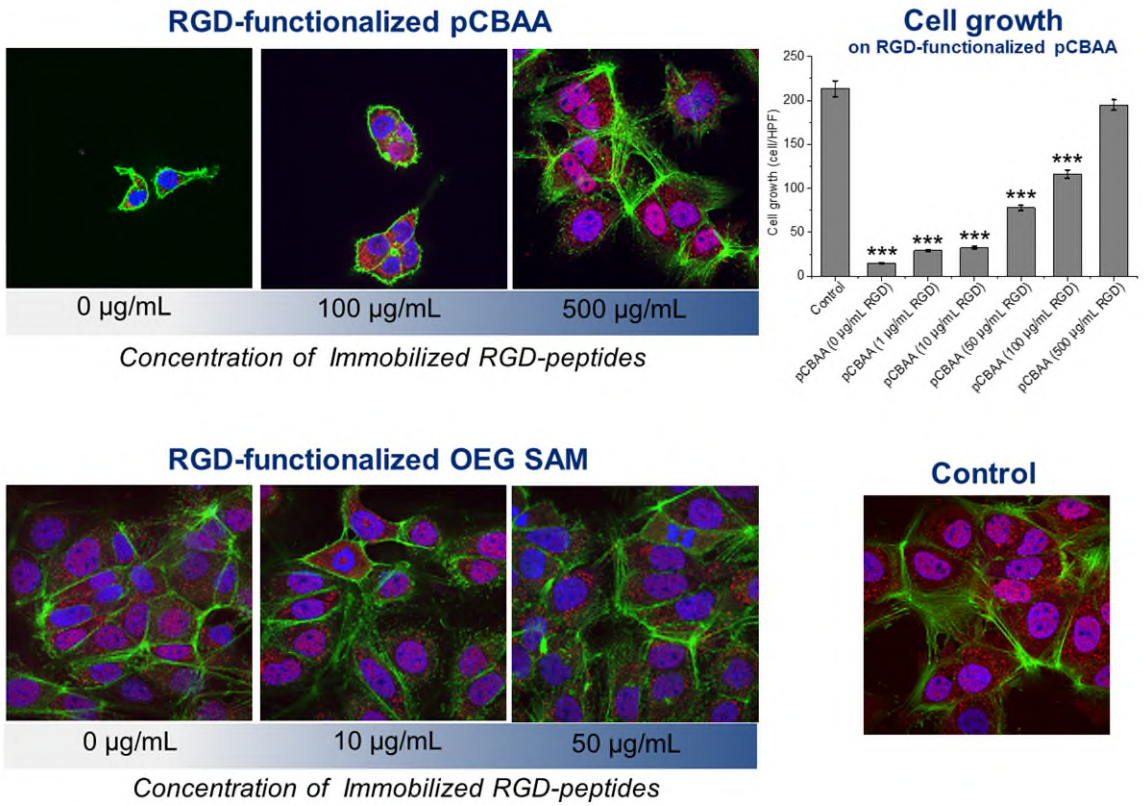

Figure 45: *Huh7 cells on RGD-functionalized only-carboxy-ended coatings. Staining: YAP (red), F-actin (green), nucleus (blue). Upper line: RGD-functionalized pCBAA (0, 100, 500µg/mL) and plot of the dependency of the cell growth (number of cells per high-power field) on the RGD-peptide concentration. One-way analysis of variance with Newman-Keuls test was performed, data are expressed as means ± SEM, ***P < 0.001. Bottom line: OEG SAM coatings (no dependency found) and control for experiments (Víšová et al. 2020a) (APPENDIX VII).*

The colocalization of YAP in the nucleus was determined for all sets of prepared functionalized coatings that are supposed to induce different levels of RGD-dependent surface-driven stress (Figure 46).

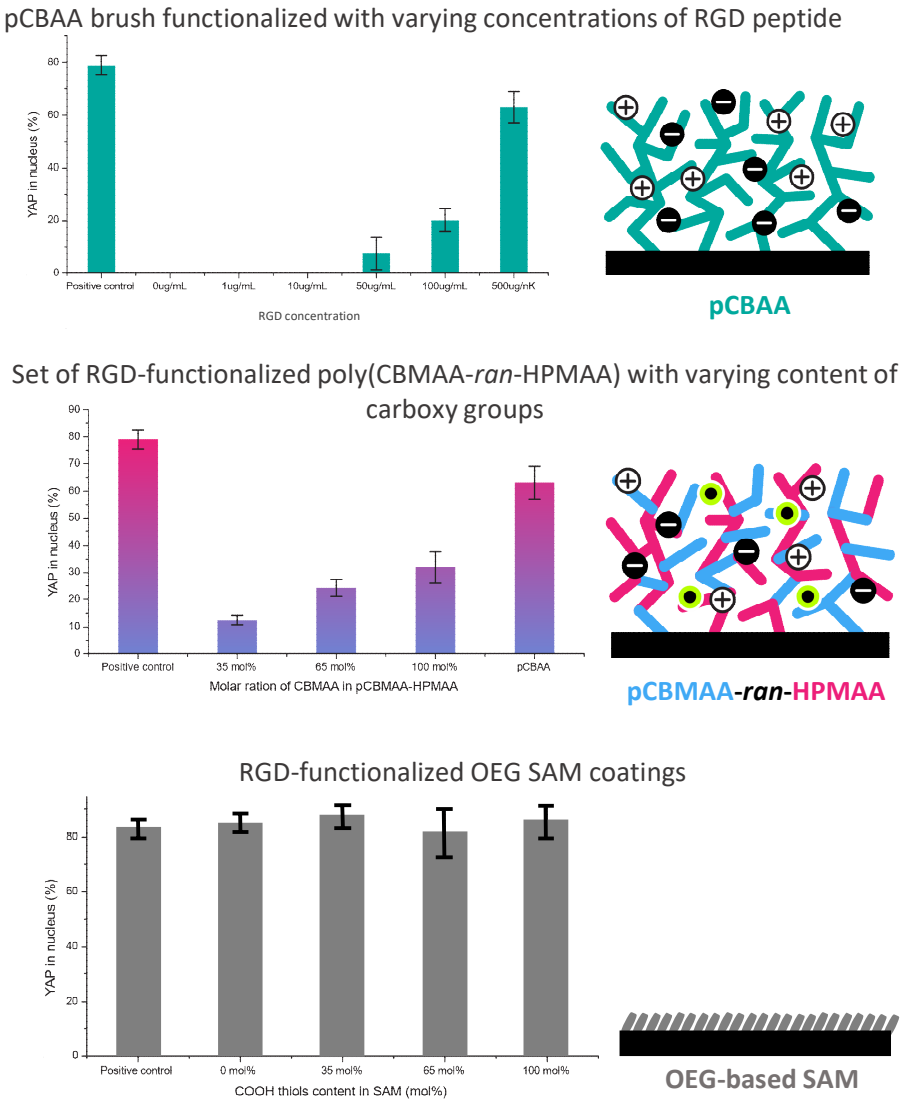

Figure 46: *Yap colocalization in the nucleus in cells growing on different RGD-functionalized surfaces. Top: antifouling pCBAA coatings functionalized with different amounts of RGD-peptide. Middle: Set of RGD-functionalized copolymer p(CBMAA-ran-HPMAA) antifouling coatings with increasing content of pCBMAA. Bottom: RGD-functionalized mix of carboxy- and hydroxyl group ended OEG SAM with varying content of carboxy group.*

Figure 46 and (Víšová et al. 2020a) (APPENDIX VII) clearly show the importance of antifouling background for research of surface-driven cell responses. While cells on p(CB)-

based RGD-functionalized coatings exhibited clear dependency of YAP colocalization in the nucleus on RGD-amount immobilized on the surface, both low-fouling OEG SAM-based methods failed. Moreover, comparing the colocalization of YAP in the nucleus in cells growing on antifouling carboxy-ended RGD-functional homopolymers pCBAA and pCBMAA, the difference is apparent (Figure 46 – Middle). In (Víšová et al. 2020b) (APPENDIX V) the higher tendency of the F-actin cytoskeleton to spread on pCBAA compared to pCBMAA was demonstrated. However, F-actin polymerization was reported to induce the increase of YAP level in the nucleus (Low et al. 2014; Moroishi et al. 2015). These findings suggest, that other physico-chemical properties of the surface (not only resistance to fouling and biocompatibility) should be taken into account while explaining cell behavior, bringing more possibilities for finer tuning of the required amount of the stress level.

These observations highlight the tailored antifouling functionalizable coatings as essential tools in surface-driven cellular response studies.

6.1.2. Antifouling coatings in bacteria – bacteriophage interaction research

Nowadays, antibiotic resistance is of great concern, as the number of multidrug-resistant bacterial strains increases (Nikaido 2009; Sultan et al. 2018). A promising alternative could be phage-based therapy, which possesses highly specific bacteriophage antimicrobial activity that is not subject to the development of the resistance (Sulakvelidze et al. 2001; Wittebole et al. 2014). However, bacteriophage – cell interactions and especially the discovery of new bacteriophage species are still subjects of ongoing researches.

We suggested the functionalizable antifouling coatings as a platform for bacteriophage – cell interaction studies. In principle, two strategies employing antifouling coatings were explored using SPR. (i) Immobilization of bacteriophage on the antifouling surface and subsequent detection of bacteria using a phage as BE. (ii) Immobilization of bacteria on the antifouling surface, and subsequent interaction with bacteriophages (or another lytic agent). While the first approach may be interesting for the field of biosensors, the second

approach may be a feasible tool for fast and high throughput screening of bacteriophages interactions with bacteria in native conditions.

As the first step, the real-time study on a model host-phage pair of *S. aureus* RN4220 Δ*tarM* and Phage vB_SauP_P68 (P68) was performed to characterize bacterial lysis using standard surfaces. As a reference, the antibacterial enzyme Lysostafin was studied. The advanced AFM methodology for real-time imaging of bacterial lysis on the single-cell level in the native conditions of the growth medium is reported in a publication in preparation (APPENDIX XI).

The preliminary data show successful employment of antifouling coatings in strategies (i) and (ii): (i) The pCBAA coating was EDC/NHS activated and the bacteriophage P68 was successfully immobilized using an optimized procedure followed by AEAA-based deactivation. Then, different concentrations of *S. aureus* RN4220 Δ*tarM* in Tris-based buffer were detected (Figure 47).

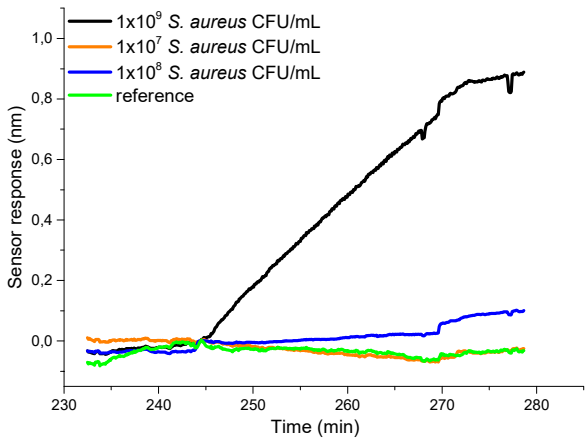

Figure 47: *Example of SPR detection of S.aureus using phage P68 - functionalized antifouling coating. The reference channel is bacteriophage AS3 - functionalized and 1 x 10^8 CFU/mL of S.aureus was injected.*

(ii) The lysis of *S. aureus* RN4220 Δ*tarM* and *S. aureus* 2124 epidermidis immobilized on pCBAA was induced by Lysostafin and observed in real-time by SPR.

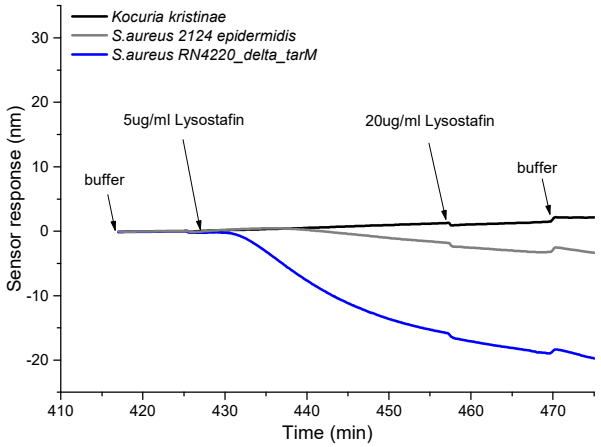

Figure 48: *Example of lysis of S. aureus RN4220 ΔtarM and S. aureus 2124 epidermidis with Lysostafin detected by SPR. In the reference channel, the Lysostafin-resistant Kocuria kristinae was immobilized.*

The preliminary results indicate that antifouling functionalizable brushes may be a useful tool for further research of bacteriophage – bacteria interactions in real-world complex samples. The potential of the coating in such field will be further studied.

6.2. Antifouling coatings in biosensors

6.2.1. Food safety applications

Foodborne illnesses are a significant threat to public health worldwide — every year, millions of foodborne illness outbreaks influence hundreds of millions of people. For successful recovery of infected patients and cost reduction, the time needed for pathogen identification and quantification is crucial.

The universal biochip technology for real-time multi-detection of pathogens in tens of minutes, without a need for sample incubation or filtration, based on antifouling functionalizable coatings was developed (Figure 49). In the course of this work, the SPR and QCM real-time detection of foodborne pathogens *E. coli* O157:E7 and *Salmonella typhimurium* was performed in different crude food samples.

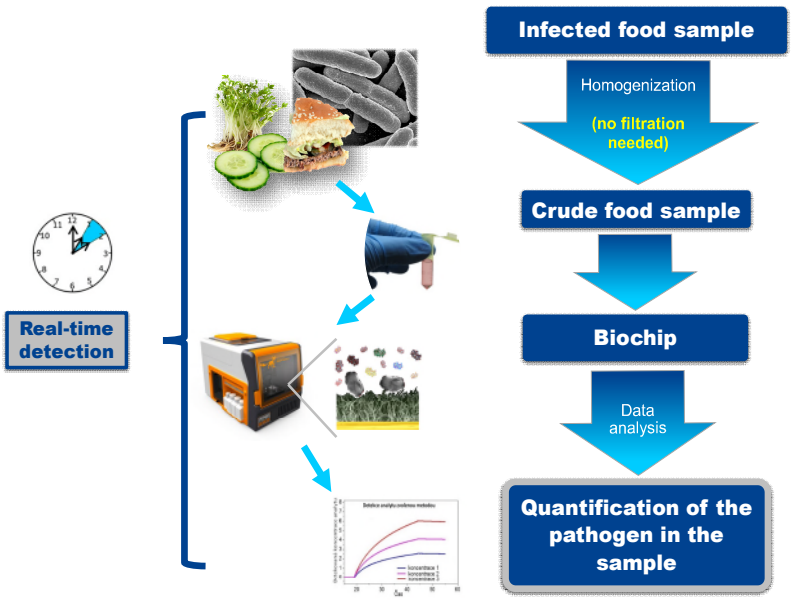

Figure 49: *The scheme of antifouling biochip-based detection. The food sample is simply homogenized and without a need for cultivation or filtration introduced on the biochip. In few minutes the data can be analysed and the pathogen is quantified.*

A three-step detection assay was typically employed using antifouling coatings functionalized with anti-bacterial antibody deactivated by simple hydrolysis (see Chapter 4.2). The assay was performed as follows: (i) primary detection of bacteria in crude food sample after sample injection was followed by (ii) the injection of a biotinylated anti-bacteria antibody and finally (iii) the signal was enhanced using streptavidin-coated spherical gold nanoparticles (Figure 50).

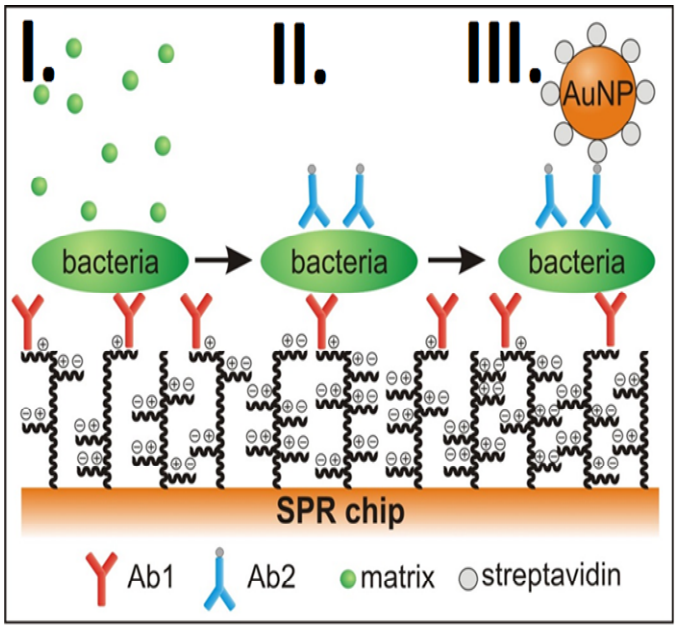

Figure 50: *The scheme of the three-step bacteria detection assay in crude food samples. I. The bacteria spiked crude food sample is injected on the functionalized antifouling biochip surface followed by primary detection. II. Biotinylated anti-bacterial antibody is reacting with captured bacteria. III. The detection signal is enhanced using streptavidin-coated gold nanoparticles (Vaisocherová-Lísalová et al. 2016b) (APPENDIX II).*

The assay was performed using SPR on antifouling pCBAA coating, showing LOD for *E. coli* in hamburger and cucumber samples to be 17 CFU/mL and 57 CFU/mL, respectively, and for Salmonella 12×10^3 CFU/mL and 7.4×10^3 CFU/mL, respectively (Vaisocherová-Lísalová et al. 2016b) (APPENDIX II). A similar LOD was achieved using the same detection scheme on the optimized structure of p(CBMAA/15mol%-*ran*-HPMAA/85mol%), performing LOD of *E. coli* detection of 81 CFU/mL in cucumber (Vaisocherová-Lísalová et

al. 2016a) (APPENDIX III). However, only the deactivation by hydrolysis was performed in both cases. In (APPENDIX IX) the significant improvement in LOD of bacteria detection was reported using the optimized method of deactivation by covalent attachment of small deactivating agents, showing LOD of primary detection (only step (i) in Figure 50) of *E. coli* in minced meat sample to be ~ 10^2 CFU/mL. Up to one order of magnitude lower LOD of *Salmonella* in hamburger crude sample was achieved by employing the antibody-functionalized and AEAA deactivated p(CBAA) coating in QCM biosensor (APPENDIX XVIII).

6.2.2. Biosensors for medical applications

The success of most therapies lies in the early initiation of the treatment. Therefore, rapid detection of biomarkers of diseases in the early stages is crucial. However, bodily fluids show great complexity and diversity among donors, complicating the detection procedures by extra isolation or multiplications steps. Antifouling functionalizable coating-based biosensors may bring a great advantage of zero-fouling background enabling fast and reliable detection directly from undiluted bodily fluids.

MicroRNA (miRNA) is a short non-coding RNA regulating gene expression and so influencing all cellular machinery. There is an increasing number of works correlating circulating miRNA to the pathogenesis of most human malignancies and their prognosis (Calin and Croce 2006; Esquela-Kerscher and Slack 2006; Lu et al. 2005). In the (Vaisocherova et al. 2015b) (APPENDIX I) the biosensor based on the SPR imaging for rapid and multiplexed detection of miRNA directly from erythrocyte lysate, without the need for extraction or pre-amplification was reported.

Amino-modified short DNA probes complementary to half of the sequence of the detected miRNA were immobilized using EDC/NHS activation on pCBAA brush, followed by hydrolysis-based deactivation. Then, the erythrocyte sample was pre-mixed with the short biotinylated DNA probe complementary to the second part of the miRNA sequence (Figure 51). Subsequently, the sample was introduced to the surface for sandwich-type hybridization (Figure 51-I), followed by signal amplification by streptavidin-functionalized gold nanoparticles (Figure 51-II).

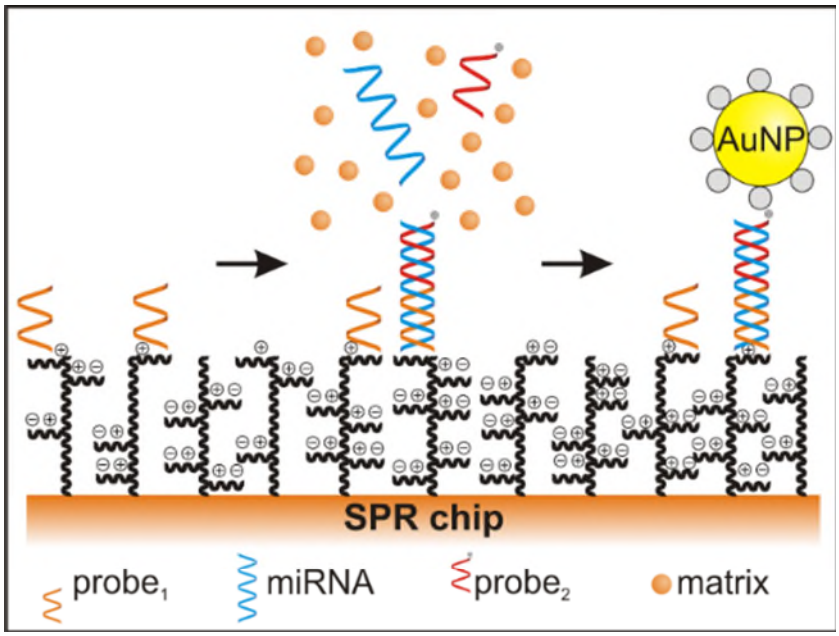

Figure 51: *The scheme of the two-step miRNA detection assay in erythrocyte lysate sample. I. The miRNA contained erythrocyte sample mixed with short biotinylated DNA probe (complementary to a part of miRNA sequence) was injected on the functionalized antifouling biochip surface, followed by sandwich-type hybridisation with the immobilized probe. II. The detection signal is enhanced using streptavidin-coated gold nanoparticles (Vaisocherova et al. 2015b) (APPENDIX I).*

The developed SPRi biosensor allowed the detection of sub-picomolar concentrations of different miRNAs from ~ 90% erythrocyte lysate sample in less than 45 min. Further, the biosensor was used for the screening of endogenous levels of miRNAs miR-16, miR-181, miR-34a, and miR-125b in samples from patients with myelodysplastic syndrome, compared to a normal sample (from a donor with no myelodysplastic syndrome diagnosis). The results and more discussion can be found in (Vaisocherova et al. 2015b) (APPENDIX I).

The worldwide pandemic outbreak of the SARS-CoV-2 virus burdens the health care systems significantly and hampers the economy all over the world. Nowadays, the hot topic helping fight pandemic is the fast and reliable detection of the virus that would prevent its spreading.

A new portable and easy-to-use multichannel QCM-based sensor with a tailored microfluidics system allows fast (~ 10 min), reliable, sensitive, and repeatable quantitative detection of SARS-COV-2 virus in a wide range of different clinical samples with minimum pre-treatment steps. Such a new biosensor employing the p(SBMAA-*ran*-CBMAA-*ran*-HPMAA) copolymer brush-based biochip technology (see Chapter 4.3) is reported in (APPENDIX XII, APPENDIX XIX) (Figure 52).

The cell-expressed high-affinity anti-nucleocapsid protein N of SARS-CoV-2 antibody was immobilized using EDC/NHS activation on the advanced polymer brush coating, followed by AEAA deactivation. The fouling resistance was proved for oropharyngeal, nasopharyngeal, stool, and throat swabs, showing a wide range of different samples for potential detection of the virus. The calibration curve measured in spiked cell medium shows the LOD of 6.7×10^3 PFU/mL (plaque-forming units) (APPENDIX XII), which is a clinically relevant value (Wölfel et al. 2020). Moreover, a comparative QCM and RT-qPCR study was performed analysing naturally-contaminated clinical nasopharyngeal swabs from healthy and infected donors. The qualitative agreement for all studied samples wasachieved, demonstrating the real potential of the QCM biosensor for clinical applications (APPENDIX XII).

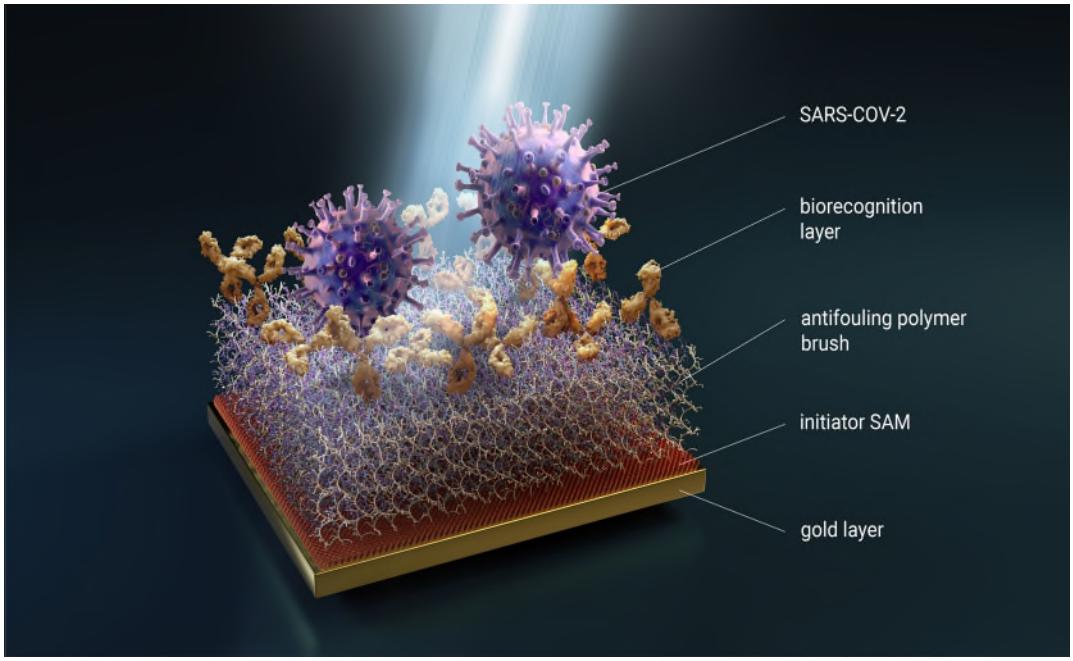

Figure 52: *Illustration of antifouling biochip-based detection of SARS-COV-2. Design of the figure: Daniel Špaček, neuroncollective.com.*

Conclusion

In this doctoral dissertation thesis, we focused on the processes influencing the performance of functional antifouling polymer brush coatings, tuning and optimizing their binding capacity, functionalization procedures, and fouling resistance when incubated with real-world biological samples.

It was shown that a change in the properties of polymer brushes can occur not only as a result of chemical interventions in their structure but also by purely physical effects, such as repeated drying and swelling and the presence of salts in the environment. Spectroscopic ellipsometry and QCM have shown that zwitterionic polybetaine brushes (pCBAA, pCBMAA, pSBMAA) swell with increasing salt concentration while binding the salt ions into the structure, while nonionic pHPMAA shrinks. Such structural changes were shown to influence the coating resistance and can be used for preconditioning polymer brushes to increase the resistance. While for pCBAA the optimum NaCl concentration of the environment before the complex sample introduction is around 100 mM, i.e. close to physiological conditions, pCBMAA requires a higher concentration of 500 mM NaCl. Moreover, the polymer brush coatings exhibited higher swelling after drying and rehydration compared to non-dried coatings, significantly improving the fouling resistance. Thus, it is suggested that the repeated shrinkage and relaxation of the chains allow a more advantageous arrangement to be established.

It was also reported that functionalization of poly(carboxybetaine)-based brushes, i.e., immobilization of the biorecognition elements, can lead to a disruption of the chain arrangement and substantial changes of surface physicochemical properties such as charge state, resulting in a deterioration of antifouling properties. To address the issue, the advanced deactivation procedure was introduced. The active esters remaining after EDC/NHS activation were deactivated with (2-aminoethoxy) acetic acid, AEAA, or with a tailored mixture of permanently charged deactivating agents, aminomethanesulfonic acid, or 2-aminoethyl hydrogen sulfate, and carboxy ended small molecules (e.g., glycine or AEAA). The tuning with mixed reagents resulted in a significant improvement in

antifouling properties and biorecognition capabilities compared to commonly used glycine and many other studied deactivation procedures.

Reflecting functionalization-related resistance impairment studies, two advanced copolymer brush architectures were developed. The approach of copolymerization of functionalizable poly(carboxybetaine methacrylamide), pCBMAA, with non-reactive poly (*N*-(2-hydroxypropyl methacrylamide), pHPMAA, is newly shown in the presented work. Nonionic pHPMAA itself has excellent antifouling properties and, as a non-reactive component, serves to control the amount of carboxyl groups in a tunable manner, i.e. to reduce the chemical intervention with the brush structure to an acceptable extent. The composition of this random copolymer can be tuned to maintain sufficient binding capacity and excellent antifouling properties even at high HPMAA contents. By adding a suitable amount of the zwitterionic SBMAA compound bearing the permanently ionized sulfo group into the copolymer structure, the post-modified resistance is more effectively recovered. Even a very small amount of SBMAA in terpolymer p(SBMAA-*ran*-CBMAA-*ran*-HPMAA) brings a significant improvement in the properties of the functionalized platform (e.g. resistance to undiluted blood plasma).

The results of the fundamental research obtained in this work was further used in several applications. It was demonstrated that newly developed antifouling polymer brushes can be used as tunable platforms for mechanotransduction controlling and cell response manipulation, highlighting the antifouling background as an essential prerequisite for cellular response studies. Preliminary data suggested that such platforms can be useful in cell-virus interaction research as well.

Antifouling functional polymer brushes and optimized functionalization procedures were employed in the development of advanced biochip technologies for food safety and biosensors for medical applications. Without the need for cultivation, incubation, or filtration, bacteria *E. coli* and *Salmonella* were detected from crude hamburger, cucumber, or minced meat samples in less than 30 min with LODs sufficient for the minimal infective doses detection. The detection assay for the screening of multiple miRNAs of the clinically relevant concentrations directly from the erythrocyte lysate using one biochip in less than 45 min was developed. Moreover, a novel QCM-based biosensor with advanced functional antifouling polymer brush biochip technology for rapid, cheap,

and point-of-care detection of coronavirus SARS-CoV-2 directly from complex cell lysate samples or bodily fluids in clinically relevant concentrations is under development.

The results obtained in the course of this work contributed to 8 papers published in peer-reviewed journals, 4 manuscripts submitted or in preparation, ~16 conference contributions, several invited lectures, and 7 outcomes of the applied research in a form of patent applications and functional samples.

References

Adamczyk, Z., 2003. Particle adsorption and deposition: role of electrostatic interactions. Advances in Colloid and Interface Science 100-102, 267-347.

Ahmad, M., Helms, V., Lengauer, T., Kalinina, O.V., 2015. How Molecular Conformational Changes Affect Changes in Free Energy. J. Chem. Theory Comput. 11(7), 2945-2957.

Al-Rawashdeh, N.A.F., Azzam, W., 2011. Gold nanoparticles chemisorbed by a terphenyldithiol self-assembled monolayer for fabrication of a protein biosensor. Res. Chem. Intermed. 37(7), 759-770.

Alemán, E.A., Pedini, H.S., Rueda, D., 2009. Covalent-Bond-Based Immobilization Approaches for Single-Molecule Fluorescence. Chembiochem : a European journal of chemical biology 10(18), 2862-2866.

Almonte, L., Lopez-Elvira, E., Baró, A.M., 2014. Surface-Charge Differentiation of Streptavidin and Avidin by Atomic Force Microscopy–Force Spectroscopy. ChemPhysChem 15(13), 2768-2773.

Alves, N.M., Pashkuleva, I., Reis, R.L., Mano, J.F., 2010. Controlling cell behavior through the design of polymer surfaces. Small 6(20), 2208-2220.

Amiji, M., Park, K., 1992. Prevention of protein adsorption and platelet adhesion on surfaces by PEO/PPO/PEO triblock copolymers. Biomaterials 13(10), 682-692.

Armstrong, J.K., 2009. The occurrence, induction, specificity and potential effect of antibodies against poly(ethylene glycol). Birkhauser Verlag Ag, Basel.

Arnold, F., 1991. Metal-Affinity Separations: A New Dimension in Protein Processing. Bio/technology (Nature Publishing Company) 9, 151-156.

Arwin, H., 2005. Ellipsometry in Life Sciences. In: Tompkins, H.G., Irene, E.A. (Eds.), Handbook of Ellipsometry, pp. 799-855. William Andrew Publishing, Norwich, NY.

Aubé, A., Campbell, S., Schmitzer, A.R., Claing, A., Masson, J.-F., 2017. Ultra-low fouling methylimidazolium modified surfaces for the detection of HER2 in breast cancer cell lysates. Analyst 142(13), 2343-2353.

Auer, S., Azizi, L., Faschinger, F., Blazevic, V., Vesikari, T., Gruber, H.J., Hytonen, V.P., 2017. Stable immobilisation of His-tagged proteins on BLI biosensor surface using cobalt. Sens. Actuator B-Chem. 243, 104-113.

Azzaroni, O., Brown, A.A., Huck, W.T.S., 2007. Tunable Wettability by Clicking Counterions Into Polyelectrolyte Brushes. Adv. Mater. 19(1), 151-154.

Bae, Y.M., Oh, B.-K., Lee, W., Lee, W.H., Choi, J.-W., 2005. Study on orientation of immunoglobulin G on protein G layer. Biosensors and Bioelectronics 21(1), 103-110.

Bajpai, A.K., Shukla, S.K., Bhanu, S., Kankane, S., 2008. Responsive polymers in controlled drug delivery. Progress in Polymer Science 33(11), 1088-1118.

Baldrich, E., Restrepo, A., O'Sullivan, C.K., 2004. Aptasensor Development: Elucidation of Critical Parameters for Optimal Aptamer Performance. Analytical Chemistry 76(23), 7053-7063.

Bandyopadhyay, D., Prashar, D., Luk, Y.Y., 2011. Anti-Fouling Chemistry of Chiral Mono layers: Enhancing Biofilm Resistance on Racemic Surface. Langmuir 27(10), 6124-6131.

Banerjee, I., Pangule, R.C., Kane, R.S., 2011. Antifouling coatings: recent developments in the design of surfaces that prevent fouling by proteins, bacteria, and marine organisms. Adv Mater 23(6), 690-718.

Barbey, R.l., Lavanant, L., Paripovic, D., Schuwer, N., Sugnaux, C., Tugulu, S., Klok, H.-A., 2009. Polymer Brushes via Surface-Initiated Controlled Radical Polymerization: Synthesis, Characterization, Properties, and Applications. Chemical Reviews 109(11), 5437-5527.

Barth, A., 2007. Infrared spectroscopy of proteins. Biochimica et Biophysica Acta (BBA) - Bioenergetics 1767(9), 1073-1101.

Bazin, I., Tria, S.A., Hayat, A., Marty, J.-L., 2017. New biorecognition molecules in biosensors for the detection of toxins. Biosensors and Bioelectronics 87, 285-298.
Beers, K.L., Boo, S., Gaynor, S.G., Matyjaszewski, K., 1999. Atom Transfer Radical Polymerization of 2-Hydroxyethyl Methacrylate. Macromolecules 32(18), 5772-5776.
Beigelman, L., McSwiggen, J.A., Draper, K.G., Gonzalez, C., Jensen, K., Karpeisky, A.M., Modak, A.S., Matulicadamic, J., Direnzo, A.B., Haeberli, P., Sweedler, D., Tracz, D., Grimm, S., Wincott, F.E., Thackray, V.G., Usman, N., 1995. CHEMICAL MODIFICATION OF HAMMERHEAD RIBOZYMES - CATALYTIC ACTIVITY AND NUCLEASE RESISTANCE. J. Biol. Chem. 270(43), 25702-25708.
Benesch, J., Svedhem, S., Svensson, S.C., Valiokas, R., Liedberg, B., Tengvall, P., 2001. Protein adsorption to oligo(ethylene glycol) self-assembled monolayers: experiments with fibrinogen, heparinized plasma, and serum. Journal of biomaterials science. Polymer edition 12(6), 581-597.
Berlinova, I.V., Dimitrov, I.V., Kalinova, R.G., Vladimirov, N.G., 2000. Synthesis and aqueous solution behaviour of copolymers containing sulfobetaine moieties in side chains. Polymer 41(3), 831-837.
Bertok, T., Šedivá, A., Filip, J., Ilcikova, M., Kasak, P., Velic, D., Jane, E., Mravcová, M., Rovenský, J., Kunzo, P., Lobotka, P., Šmatko, V., Vikartovská, A., Tkac, J., 2015. Carboxybetaine Modified Interface for Electrochemical Glycoprofiling of Antibodies Isolated from Human Serum. Langmuir 31(25), 7148-7157.
Bhattacharjee, S.M., Giacometti, A., Maritan, A., 2013. Flory theory for polymers. Journal of Physics: Condensed Matter 25(50), 503101.
Bhushan, B., 2018. Bio- and Inorganic Fouling. In: Bhushan, B. (Ed.), Biomimetics. Springer International Publishing, Cham.
Biesheuvel, P.M., van der Veen, M., Norde, W., 2005. A Modified Poisson−Boltzmann Model Including Charge Regulation for the Adsorption of Ionizable Polyelectrolytes to Charged Interfaces, Applied to Lysozyme Adsorption on Silica. The Journal of Physical Chemistry B 109(9), 4172-4180.
Bixler, G.D., Bhushan, B., 2012. Biofouling: lessons from nature. Philosophical Transactions of the Royal Society A: Mathematical, Physical and Engineering Sciences 370(1967), 2381-2417.
Björck, L., 1988. Protein L. A novel bacterial cell wall protein with affinity for Ig L chains. Journal of immunology (Baltimore, Md. : 1950) 140(4), 1194-1197.
Blaney, B.L., Ewing, G.E., 1976. Van Der Waals Molecules. Annual Review of Physical Chemistry 27(1), 553-584.
Block, H., Maertens, B., Spriestersbach, A., Brinker, N., Kubicek, J., Fabis, R., Labahn, J., Schafer, F., 2009. IMMOBILIZED-METAL AFFINITY CHROMATOGRAPHY (IMAC): A REVIEW. In: Burgess, R.R., Deutscher, M.P. (Eds.), Guide to Protein Purification, Second Edition, pp. 439-473. Elsevier Academic Press Inc, San Diego.
Bolduc, O.R., Clouthier, C.M., Pelletier, J.N., Masson, J.F., 2009. Peptide Self-Assembled Monolayers for Label-Free and Unamplified Surface Plasmon Resonance Biosensing in Crude Cell Lysate. Analytical Chemistry 81(16), 6779-6788.
Bolduc, O.R., Pelletier, J.N., Masson, J.-F.o., 2010. SPR Biosensing in Crude Serum Using Ultralow Fouling Binary Patterned Peptide SAM. Analytical Chemistry 82(9), 3699-3706.
Bontempo, D., Heredia, K.L., Fish, B.A., Maynard, H.D., 2004. Cysteine-reactive polymers synthesized by atom transfer radical polymerization for conjugation to proteins. Journal of the American Chemical Society 126(47), 15372-15373.
Bradbury, A.R.M., Sidhu, S., Dubel, S., McCafferty, J., 2011. Beyond natural antibodies: the power of in vitro display technologies. Nature Biotechnology 29(3), 245-254.
Brambilla, D., Sola, L., Chiari, M., 2021. Advantageous antibody microarray fabrication through DNA-directed immobilization: A step toward use of extracellular vesicles in diagnostics. Talanta 222, 121542.
Brandes, N., Welzel, P.B., Werner, C., Kroh, L.W., 2006. Adsorption-induced conformational changes of proteins onto ceramic particles: Differential scanning calorimetry and FTIR analysis. Journal of Colloid and Interface Science 299(1), 56-69.

Brault, N.D., Sundaram, H.S., Huang, C.-J., Li, Y., Yu, Q., Jiang, S., 2012. Two-Layer Architecture Using Atom Transfer Radical Polymerization for Enhanced Sensing and Detection in Complex Media. Biomacromolecules 13(12), 4049-4056.
Brittain, W.J., Minko, S., 2007. A structural definition of polymer brushes. Journal of Polymer Science Part A: Polymer Chemistry 45(16), 3505-3512.
Brown, A.A., Khan, N.S., Steinbock, L., Huck, W.T.S., 2005. Synthesis of oligo(ethylene glycol) methacrylate polymer brushes. European Polymer Journal 41(8), 1757-1765.
Browne, W.R., 2008. Photochemistry of immobilized photoactive compounds. Coordination Chemistry Reviews 252(23), 2470-2479.
Budkov, Y.A., Kiselev, M.G., 2017. Flory-type theories of polymer chains under different external stimuli. Journal of Physics: Condensed Matter 30(4), 043001.
Buijs, J., Norde, W., Lichtenbelt, J.W.T., 1996. Changes in the Secondary Structure of Adsorbed IgG and F(ab')2 Studied by FTIR Spectroscopy. Langmuir 12(6), 1605-1613.
Cai, B.J., Wang, S.T., Huang, L., Ning, Y., Zhang, Z.Y., Zhang, G.J., 2014. Ultrasensitive Label-Free Detection of PNA-DNA Hybridization by Reduced Graphene Oxide Field-Effect Transistor Biosensor. Acs Nano 8(3), 2632-2638.
Calin, G.A., Croce, C.M., 2006. MicroRNA signatures in human cancers. Nat. Rev. Cancer 6(11), 857-866.
Camci-Unal, G., Annabi, N., Dokmeci, M.R., Liao, R., Khademhosseini, A., 2014. Hydrogels for cardiac tissue engineering. NPG Asia Materials 6(5), e99-e99.
Campos, L.M., Killops, K.L., Sakai, R., Paulusse, J.M.J., Damiron, D., Drockenmuller, E., Messmore, B.W., Hawker, C.J., 2008. Development of Thermal and Photochemical Strategies for Thiol−Ene Click Polymer Functionalization. Macromolecules 41(19), 7063-7070.
Campuzano, S., Orozco, J., Kagan, D., Guix, M., Gao, W., Sattayasamitsathit, S., Claussen, J.C., Merkoci, A., Wang, J., 2012. Bacterial Isolation by Lectin-Modified Microengines. Nano Letters 12(1), 396-401.
Cao, B., Tang, Q., Li, L., Humble, J., Wu, H., Liu, L., Cheng, G., 2013. Switchable Antimicrobial and Antifouling Hydrogels with Enhanced Mechanical Properties. Advanced Healthcare Materials 2(8), 1096-1102.
Caruso, F., Rodda, E., Furlong, D.F., Niikura, K., Okahata, Y., 1997. Quartz crystal microbalance study of DNA immobilization and hybridization for nucleic acid sensor development. Analytical Chemistry 69(11), 2043-2049.
Casals, E., Pfaller, T., Duschl, A., Oostingh, G.J., Puntes, V., 2010. Time Evolution of the Nanoparticle Protein Corona. ACS Nano 4(7), 3623-3632.
Caswell, K.K., Wilson, J.N., Bunz, U.H.F., Murphy, C.J., 2003. Preferential End-to-End Assembly of Gold Nanorods by Biotin−Streptavidin Connectors. Journal of the American Chemical Society 125(46), 13914-13915.
Catimel, B., Scott, A.M., Lee, F.T., Hanai, N., Ritter, G., Welt, S., Old, L.J., Burgess, A.W., Nice, E.C., 1998. Direct immobilization of gangliosides onto gold-carboxymethyldextran sensor surfaces by hydrophobic interaction: applications to antibody characterization. Glycobiology 8(9), 927-938.
Cieplak, M., Kutner, W., 2016. Artificial Biosensors: How Can Molecular Imprinting Mimic Biorecognition? Trends in Biotechnology 34(11), 922-941.
Cline, G.W., Hanna, S.B., 1988. Kinetics and mechanisms of the aminolysis of N-hydroxysuccinimide esters in aqueous buffers. The Journal of Organic Chemistry 53(15), 3583-3586.
Connal, L.A., Kinnane, C.R., Zelikin, A.N., Caruso, F., 2009. Stabilization and Functionalization of Polymer Multilayers and Capsules via Thiol−Ene Click Chemistry. Chemistry of Materials 21(4), 576-578.
Corkhill, P.H., Jolly, A.M., Ng, C.O., Tighe, B.J., 1987. Synthetic hydrogels: 1. Hydroxyalkyl acrylate and methacrylate copolymers - water binding studies. Polymer 28(10), 1758-1766.

Cox, J.D., Curry, M.S., Skirboll, S.K., Gourley, P.L., Sasaki, D.Y., 2002. Surface passivation of a microfluidic device to glial cell adhesion: a comparison of hydrophobic and hydrophilic SAM coatings. Biomaterials 23(3), 929-935.
Crivianu-Gaita, V., Thompson, M., 2016. Aptamers, antibody scFv, and antibody Fab' fragments: An overview and comparison of three of the most versatile biosensor biorecognition elements. Biosensors and Bioelectronics 85, 32-45.
Cui, M., Song, Z.L., Wu, Y.M., Guo, B., Fan, X.J., Luo, X.L., 2016. A highly sensitive biosensor for tumor maker alpha fetoprotein based on poly(ethylene glycol) doped conducting polymer PEDOT. Biosensors & bioelectronics 79, 736-741.
Cummings, R.D., Etzler, M.E., 2009. Antibodies and Lectins in Glycan Analysis. In: Cummings, R.D., Esko, J.D., Hudson H;, F., Stanley, P., Carolyn R;, B., Hart, G.W., Marilynn E;, E. (Eds.), Essentials of Glycobiology, 2 ed. Cold Spring Harbor Laboratory Press, New York.
Currie, E.P., Norde, W., Stuart, M.A., 2003. Tethered polymer chains: surface chemistry and their impact on colloidal and surface properties. Advances in Colloid and Interface Science 100, 205-265.
Dalsin, J.L., Hu, B.-H., Lee, B.P., Messersmith, P.B., 2003. Mussel Adhesive Protein Mimetic Polymers for the Preparation of Nonfouling Surfaces. Journal of the American Chemical Society 125(14), 4253-4258.
Dalsin, J.L., Lin, L., Tosatti, S., Vörös, J., Textor, M., Messersmith, P.B., 2005. Protein Resistance of Titanium Oxide Surfaces Modified by Biologically Inspired mPEG−DOPA. Langmuir 21(2), 640-646.
Davis, F., Higson, S.P.J., 2005. Structured thin films as functional components within biosensors. Biosensors and Bioelectronics 21(1), 1-20.
de Gennes, P.G., 1980. Conformations of Polymers Attached to an Interface. Macromolecules 13(5), 1069-1075.
Decher, G., 1997. Fuzzy Nanoassemblies: Toward Layered Polymeric Multicomposites. Science 277(5330), 1232-1237.
Deng, L., Mrksich, M., Whitesides, G.M., 1996. Self-assembled monolayers of alkanethiolates presenting tri(propylene sulfoxide) groups resist the adsorption of protein. Journal of the American Chemical Society 118(21), 5136-5137.
Desseaux, S., Klok, H.-A., 2015. Fibroblast adhesion on ECM-derived peptide modified poly(2-hydroxyethyl methacrylate) brushes: Ligand co-presentation and 3D-localization. Biomaterials 44, 24-35.
Domack, A., Prucker, O., Rühe, J., Johannsmann, D., 1997. Swelling of a polymer brush probed with a quartz crystal resonator. Physical Review E 56(1), 680-689.
Dommerholt, J., Rutjes, F.P.J.T., van Delft, F.L., 2016. Strain-Promoted 1,3-Dipolar Cycloaddition of Cycloalkynes and Organic Azides. Top Curr Chem (Cham) 374(2), 16-16.
Douglas, T., Young, M., 1998. Host–guest encapsulation of materials by assembled virus protein cages. Nature 393(6681), 152-155.
Du, X., Li, J., Welle, A., Li, L., Feng, W., Levkin, P.A., 2015. Reversible and Rewritable Surface Functionalization and Patterning via Photodynamic Disulfide Exchange. Adv. Mater. 27(34), 4997-5001.
Du, Y.J., Brash, J.L., 2003. Synthesis and characterization of thiol-terminated poly(ethylene oxide) for chemisorption to gold surface. Journal of Applied Polymer Science 90(2), 594-607.
Ducker, W.A., Mastropietro, D., 2016. Forces between extended hydrophobic solids: Is there a long-range hydrophobic force? Current Opinion in Colloid & Interface Science 22, 51-58.
Dür;, S., Thomason;, J.C., 2010. Biofouling. Blackwell Publishing Ltd.
Duverger, E., Frison, N., Roche, A.-C., Monsigny, M., 2003. Carbohydrate-lectin interactions assessed by surface plasmon resonance. Biochimie 85(1), 167-179.
Ederth, T., Claesson, P., Liedberg, B., 1998. Self-Assembled Monolayers of Alkanethiolates on Thin Gold Films as Substrates for Surface Force Measurements. Long-Range Hydrophobic Interactions and Electrostatic Double-Layer Interactions. Langmuir 14(17), 4782-4789.

Eliasson, M., Olsson, A., Palmcrantz, E., Wiberg, K., Inganäs, M., Guss, B., Lindberg, M., Uhlén, M., 1988. Chimeric IgG-binding receptors engineered from staphylococcal protein A and streptococcal protein G. J. Biol. Chem. 263(9), 4323-4327.
Elwing, H., 1998. Protein absorption and ellipsometry in biomaterial research. Biomaterials 19(4-5), 397-406.
Elwing, H., Welin, S., Askendal, A., Nilsson, U., LundstrÖm, I., 1987. A wettability gradient method for studies of macromolecular interactions at the liquid/solid interface. Journal of Colloid and Interface Science 119(1), 203-210.
Endo, T., Kerman, K., Nagatani, N., Takamura, Y., Tamiya, E., 2005. Label-free detection of peptide nucleic acid-DNA hybridization using localized surface plasmon resonance based optical biosensor. Analytical Chemistry 77(21), 6976-6984.
Epstein, A.K., Wong, T.-S., Belisle, R.A., Boggs, E.M., Aizenberg, J., 2012. Liquid-infused structured surfaces with exceptional anti-biofouling performance. Proceedings of the National Academy of Sciences 109(33), 13182-13187.
Esquela-Kerscher, A., Slack, F.J., 2006. Oncomirs - microRNAs with a role in cancer. Nat. Rev. Cancer 6(4), 259-269.
Fabian, H., Mäntele, W., 2001. Infrared Spectroscopy of Proteins. Handbook of Vibrational Spectroscopy.
Faiz, S., Zahoor, A.F., 2016. Ring opening of epoxides with C-nucleophiles. Molecular Diversity 20(4), 969-987.
Fan, X.W., Lin, L.J., Messersmith, P.B., 2006a. Cell fouling resistance of polymer brushes grafted from Ti substrates by surface-initiated polymerization: Effect of ethylene glycol side chain length. Biomacromolecules 7(8), 2443-2448.
Fan, Y., Shang, X., Liu, Z., Wu, L., 2006b. Regio- and Diastereoselective Ring-Opening Reaction of Epoxides with Nitric Oxide. Synthetic Communications 36(21), 3149-3152.
Faucheux, N., Schweiss, R., Lutzow, K., Werner, C., Groth, T., 2004. Self-assembled monolayers with different terminating groups as model substrates for cell adhesion studies. Biomaterials 25(14), 2721-2730.
Feng, X.J., Jiang, L., 2006. Design and creation of superwetting/antiwetting surfaces. Adv. Mater. 18(23), 3063-3078.
Ferapontova, E.E., Grigorenko, V.G., Egorov, A.M., Borchers, T., Ruzgas, T., Gorton, L., 2001. Mediatorless biosensor for H2O2 based on recombinant forms of horseradish peroxidase directly adsorbed on polycrystalline gold. Biosensors & bioelectronics 16(3), 147-157.
Flory, P.J., 1949. THE CONFIGURATION OF REAL POLYMER CHAINS. J. Chem. Phys. 17(3), 303-310.
Fu, J.L., Liu, M.H., Liu, Y., Woodbury, N.W., Yan, H., 2012. Interenzyme Substrate Diffusion for an Enzyme Cascade Organized on Spatially Addressable DNA Nanostructures. Journal of the American Chemical Society 134(12), 5516-5519.
Furchner, A., Bittrich, E., Uhlmann, P., Eichhorn, K.J., Hinrichs, K., 2013. In-situ characterization of the temperature-sensitive swelling behavior of poly(N-isopropylacrylamide) brushes by infrared and visible ellipsometry. Thin Solid Films 541, 41-45.
Garay, R.P., El-Gewely, R., Armstrong, J.K., Garratty, G., Richette, P., 2012. Antibodies against polyethylene glycol in healthy subjects and in patients treated with PEG-conjugated agents. Expert Opin. Drug Deliv. 9(11), 1319-1323.
Garcia-Gradilla, V., Orozco, J., Sattayasamitsathit, S., Soto, F., Kuralay, F., Pourazary, A., Katzenberg, A., Gao, W., Shen, Y.F., Wang, J., 2013. Functionalized Ultrasound-Propelled Magnetically Guided Nanomotors: Toward Practical Biomedical Applications. Acs Nano 7(10), 9232-9240.
Gidi, Y., Bayram, S., Ablenas, C.J., Blum, A.S., Cosa, G., 2018. Efficient One-Step PEG-Silane Passivation of Glass Surfaces for Single-Molecule Fluorescence Studies. ACS applied materials & interfaces 10(46), 39505-39511.

Glinel, K., Jonas, A.M., Jouenne, T., Leprince, J.r.m., Galas, L., Huck, W.T.S., 2008. Antibacterial and Antifouling Polymer Brushes Incorporating Antimicrobial Peptide. Bioconjugate Chemistry 20(1), 71-77.
Gorb, S.N., 2009. Functional Surfaces in Biology. Springer Netherlands.
Goyal, D.K., Subramanian, A., 2010. In-situ protein adsorption study on biofunctionalized surfaces using spectroscopic ellipsometry. Thin Solid Films 518(8), 2186-2193.
Gragson, D.E., Richmond, G.L., 1997. Comparisons of the Structure of Water at Neat Oil/Water and Air/Water Interfaces As Determined by Vibrational Sum Frequency Generation. Langmuir 13(18), 4804-4806.
Guo, S.S., Janczewski, D., Zhu, X.Y., Quintana, R., He, T., Neoh, K.G., 2015. Surface charge control for zwitterionic polymer brushes: Tailoring surface properties to antifouling applications. Journal of Colloid and Interface Science 452, 43-53.
Hahn, M.S., Taite, L.J., Moon, J.J., Rowland, M.C., Ruffino, K.A., West, J.L., 2006. Photolithographic patterning of polyethylene glycol hydrogels. Biomaterials 27(12), 2519-2524.
Haines, J., Alexander, M., 1975. Microbial degradation of polyethylene glycols. Applied microbiology 29(5), 621-625.
Hairul Bahara, N.H., Tye, G.J., Choong, Y.S., Ong, E.B.B., Ismail, A., Lim, T.S., 2013. Phage display antibodies for diagnostic applications. Biologicals 41(4), 209-216.
Halperin, A., Kröger, M., 2009. Ternary Protein Adsorption onto Brushes: Strong versus Weak. Langmuir 25(19), 11621-11634.
Hamidi, M., Azadi, A., Rafiei, P., 2008. Hydrogel nanoparticles in drug delivery. Advanced Drug Delivery Reviews 60(15), 1638-1649.
Han, L., Yan, L., Wang, K., Fang, L., Zhang, H., Tang, Y., Ding, Y., Weng, L.-T., Xu, J., Weng, J., Liu, Y., Ren, F., Lu, X., 2017. Tough, self-healable and tissue-adhesive hydrogel with tunable multifunctionality. NPG Asia Materials 9(4), e372-e372.
Han, S., Kim, C., Kwon, D., 1997. Thermal/oxidative degradation and stabilization of polyethylene glycol. Polymer 38(2), 317-323.
Harder, P., Grunze, M., Dahint, R., Whitesides, G.M., Laibinis, P.E., 1998. Molecular conformation in oligo(ethylene glycol)-terminated self-assembled monolayers on gold and silver surfaces determines their ability to resist protein adsorption. Journal of Physical Chemistry B 102(2), 426-436.
Hashim, H., Kozhaev, M., Kapralov, P., Panina, L., Belotelov, V., Visova, I., Chvostova, D., Dejneka, A., Shpetnyi, I., Latyshev, V., Vorobiov, S., Komanicky, V., 2020. Controlling the Transverse Magneto-Optical Kerr Effect in Cr/NiFe Bilayer Thin Films by Changing the Thicknesses of the Cr Layer. Nanomaterials 10(2), 10.
Haupt, K., Mosbach, K., 2000. Molecularly Imprinted Polymers and Their Use in Biomimetic Sensors. Chemical Reviews 100(7), 2495-2504.
He, H., Zhou, L., Wang, Y., Li, C., Yao, J., Zhang, W., Zhang, Q., Li, M., Li, H., Dong, W.-f., 2015. Detection of trace microcystin-LR on a 20MHz QCM sensor coated with in situ self-assembled MIPs. Talanta 131, 8-13.
He, Y., Chang, Y., Hower, J.C., Zheng, J., Chen, S., Jiang, S., 2008. Origin of repulsive force and structure/dynamics of interfacial water in OEG-protein interactions: A molecular simulation study. Physical Chemistry Chemical Physics 10(36), 5539-5544.
Hennink, W.E., van Nostrum, C.F., 2012. Novel crosslinking methods to design hydrogels. Advanced Drug Delivery Reviews 64, 223-236.
Hermanson, G.T., 2013. Bioconjugate Techniques, Third ed. Academic Press, Boston.
Herrwerth, S., Eck, W., Reinhardt, S., Grunze, M., 2003. Factors that Determine the Protein Resistance of Oligoether Self-Assembled Monolayers − Internal Hydrophilicity, Terminal Hydrophilicity, and Lateral Packing Density. Journal of the American Chemical Society 125(31), 9359-9366.

Hersel, U., Dahmen, C., Kessler, H., 2003. RGD modified polymers: biomaterials for stimulated cell adhesion and beyond. Biomaterials 24(24), 4385-4415.
Hideshima, S., Hinou, H., Ebihara, D., Sato, R., Kuroiwa, S., Nakanishi, T., Nishimura, S.I., Osaka, T., 2013. Attomolar Detection of Influenza A Virus Hemagglutinin Human H1 and Avian H5 Using Glycan-Blotted Field Effect Transistor Biosensor. Analytical Chemistry 85(12), 5641-5644.
Hinrichs, K., Eichhorn, K.-J., 2018. Ellipsometry of functional organic surfaces and films. Springer.
Hlady, V., Buijs, J., 1996. Protein adsorption on solid surfaces. Current Opinion in Biotechnology 7(1), 72-77.
Ho, A.H.-P., Wu, S.-Y., Kong, S.-K., Zeng, S., Yong, K.-T., 2017. SPR Biosensors. In: Ho, A.H.-P., Kim, D., Somekh, M.G. (Eds.), Handbook of Photonics for Biomedical Engineering, pp. 123-145. Springer Netherlands, Dordrecht.
Hoarau, M., Badieyan, S., Marsh, E.N.G., 2017. Immobilized enzymes: understanding enzyme – surface interactions at the molecular level. Organic & Biomolecular Chemistry 15(45), 9539-9551.
Hoare, T.R., Kohane, D.S., 2008. Hydrogels in drug delivery: Progress and challenges. Polymer 49(8), 1993-2007.
Hoffman, A.S., 2012. Hydrogels for biomedical applications. Advanced Drug Delivery Reviews 64, 18-23.
Holmlin, R.E., Chen, X.X., Chapman, R.G., Takayama, S., Whitesides, G.M., 2001. Zwitterionic SAMs that resist nonspecific adsorption of protein from aqueous buffer. Langmuir 17(9), 2841-2850.
Homola, J., 2003. Present and future of surface plasmon resonance biosensors. Anal. Bioanal. Chem. 377(3), 528-539.
Homola, J., 2006. Electromagnetic Theory of Surface Plasmons. In: Homola, J. (Ed.), Surface Plasmon Resonance Based Sensors, pp. 3-44. Springer Berlin Heidelberg, Berlin, Heidelberg.
Homola, J., Dostalek, J., Chen, S.F., Rasooly, A., Jiang, S.Y., Yee, S.S., 2002. Spectral surface plasmon resonance biosensor for detection of staphylococcal enterotoxin B in milk. International Journal of Food Microbiology 75(1-2), 61-69.
Homola, J., Yee, S.S., Gauglitz, G., 1999. Surface plasmon resonance sensors: review. Sens. Actuator B-Chem. 54(1-2), 3-15.
Hong, L., Wang, Z., Wei, X., Shi, J., Li, C., 2020. Antibodies against polyethylene glycol in human blood: A literature review. Journal of Pharmacological and Toxicological Methods 102, 106678.
Horáček, J., Skládal, P., 2000. Effect of organic solvents on immunoassays of environmental pollutants studied using a piezoelectric biosensor. Analytica Chimica Acta 412(1), 37-45.
Horak, D., 1992. PREPARATION AND PROPERTIES OF POLY (2-HYDROXYETHYL METHACRYLATES). Chem. Listy 86(5), 359-374.
Horn, M., Matyjaszewski, K., 2013. Solvent Effects on the Activation Rate Constant in Atom Transfer Radical Polymerization. Macromolecules 46(9), 3350-3357.
Howarter, J.A., Youngblood, J.P., 2007. Self-Cleaning and Anti-Fog Surfaces via Stimuli-Responsive Polymer Brushes. Adv. Mater. 19(22), 3838-3843.
Hoyos-Nogues, M., Gil, F.J., Mas-Moruno, C., 2018. Antimicrobial Peptides: Powerful Biorecognition Elements to Detect Bacteria in Biosensing Technologies. Molecules 23(7), 24.
Hsiue, G.-H., Guu, J.-A., Cheng, C.-C., 2001. Poly(2-hydroxyethyl methacrylate) film as a drug delivery system for pilocarpine. Biomaterials 22(13), 1763-1769.
Hu, Z.B., Cai, T., Chi, C.L., 2010. Thermoresponsive oligo(ethylene glycol)-methacrylate- based polymers and microgels. Soft Matter 6(10), 2115-2123.
Huang, B., Hu, X., Hu, X., Wang, N., Yang, K., Xiao, Z., Wu, P., 2017a. Synthesis and characterization of a novel inorganic-organic hybrid material based on polyoxometalates and dicyclohexylcarbodiimide. Journal of Molecular Structure 1149, 42-47.
Huang, L., Muyldermans, S., Saerens, D., 2010. Nanobodies (R): proficient tools in diagnostics. Expert Rev. Mol. Diagn. 10(6), 777-785.

Huang, W., Huang, J.J., Xu, C.H., Gu, S.J., Xu, W.L., 2014. Surface functionalization of cellulose membrane via heterogeneous "click" grafting of zwitterionic sulfobetaine. Polym. Bull. 71(10), 2559-2569.
Huang, Y., Wu, X., Tian, T., Zhu, Z., Lin, H., Yang, C., 2017b. Target-responsive DNAzyme hydrogel for portable colorimetric detection of lanthanide(III) ions. Science China Chemistry 60(2), 293-298.
Huber, F., Berwanger, J., Polesya, S., Mankovsky, S., Ebert, H., Giessibl, F.J., 2019. Chemical bond formation showing a transition from physisorption to chemisorption. Science 366(6462), 235-238.
Huckaby, J.T., Lai, S.K., 2018. PEGylation for enhancing nanoparticle diffusion in mucus. Advanced Drug Delivery Reviews 124, 125-139.
Huie, J.C., 2003. Guided molecular self-assembly: a review of recent efforts. Smart Materials and Structures 12(2), 264-271.
Chadtová Song, X., Gedeonová, E., Homola, J., 2019. Surface plasmon resonance biosensor for the ultrasensitive detection of bisphenol A. Anal. Bioanal. Chem. 411(22), 5655-5658.
Chaiet, L., Wolf, F.J., 1964. The properties of streptavidin, a biotin-binding protein produced by Streptomycetes. Archives of Biochemistry and Biophysics 106, 1-5.
Chaki, N.K., Vijayamohanan, K., 2002. Self-assembled monolayers as a tunable platform for biosensor applications. Biosensors & bioelectronics 17(1-2), 1-12.
Chan;, J., Wong;, S., 2010. Biofouling: Types, Impact and Anti-Fouling. Nova Science Publishers, Inc.
Chandradoss, S.D., Haagsma, A.C., Lee, Y.K., Hwang, J.-H., Nam, J.-M., Joo, C., 2014. Surface Passivation for Single-molecule Protein Studies. JoVE(86), e50549.
Chang, Y., Liao, S.C., Higuchi, A., Ruaan, R.C., Chu, C.W., Chen, W.Y., 2008. A Highly stable nonbiofouling surface with well-packed grafted zwitterionic polysulfobetaine for plasma protein repulsion. Langmuir 24(10), 5453-5458.
Chao, H., Bautista, D.L., Litowski, J., Irvin, R.T., Hodges, R.S., 1998. Use of a heterodimeric coiled-coil system for biosensor application and affinity purification. Journal of Chromatography B: Biomedical Sciences and Applications 715(1), 307-329.
Chen, G., Zhang, K., Luo, B., Hong, W., Chen, J., Chen, X., 2019a. Plasmonic-3D photonic crystals microchip for surface enhanced Raman spectroscopy. Biosensors and Bioelectronics 143, 111596.
Chen, H., Zhang, M., Yang, J., Zhao, C., Hu, R., Chen, Q., Chang, Y., Zheng, J., 2014. Synthesis and Characterization of Antifouling Poly(N-acryloylaminoethoxyethanol) with Ultralow Protein Adsorption and Cell Attachment. Langmuir 30(34), 10398-10409.
Chen, S., Li, L., Zhao, C., Zheng, J., 2010. Surface hydration: Principles and applications toward low-fouling/nonfouling biomaterials. Polymer 51(23), 5283-5293.
Chen, S., Liu, L.Y., Jiang, S.Y., 2006. Strong resistance of oligo(phosphorylcholine) self-assembled monolayers to protein adsorption. Langmuir 22(6), 2418-2421.
Chen, T., Yang, H., Wu, X., Yu, D., Ma, A., He, X., Sun, K., Wang, J., 2019b. Ultrahighly Charged Amphiphilic Polymer Brushes with Super-Antibacterial and Self-Cleaning Capabilities. Langmuir 35(8), 3031-3037.
Cheng, J., Teply, B.A., Sherifi, I., Sung, J., Luther, G., Gu, F.X., Levy-Nissenbaum, E., Radovic-Moreno, A.F., Langer, R., Farokhzad, O.C., 2007. Formulation of functionalized PLGA-PEG nanoparticles for in vivo targeted drug delivery. Biomaterials 28(5), 869-876.
Chirila, T.V., Constable, I.J., Crawford, G.J., Vijayasekaran, S., Thompson, D.E., Chen, Y.-C., Fletcher, W.A., Griffin, B.J., 1993. Poly(2-hydroxyethyl methacrylate) sponges as implant materials: in vivo and in vitro evaluation of cellular invasion. Biomaterials 14(1), 26-38.
Chirila, T.V., Hicks, C.R., Dalton, P.D., Vijayasekaran, S., Lou, X., Hong, Y., Clayton, A.B., Ziegelaar, B.W., Fitton, J.H., Platten, S., Crawford, G.J., Constable, I.J., 1998. Artificial cornea. Progress in Polymer Science 23(3), 447-473.
Chou, Y.-N., Wen, T.-C., Chang, Y., 2016a. Zwitterionic surface grafting of epoxylated sulfobetaine copolymers for the development of stealth biomaterial interfaces. Acta Biomaterialia 40, 78-91.

Chou, Y.N., Sun, F., Hung, H.C., Jain, P., Sinclair, A., Zhang, P., Bai, T., Chang, Y., Wen, T.C., Yu, Q.M., Jiang, S.Y., 2016b. Ultra-low fouling and high antibody loading zwitterionic hydrogel coatings for sensing and detection in complex media. Acta Biomaterialia 40, 31-37.
Iliuk, A.B., Hu, L., Tao, W.A., 2011. Aptamer in Bioanalytical Applications. Analytical Chemistry 83(12), 4440-4452.
Iqbal, S.S., Mayo, M.W., Bruno, J.G., Bronk, B.V., Batt, C.A., Chambers, J.P., 2000. A review of molecular recognition technologies for detection of biological threat agents. Biosensors and Bioelectronics 15(11), 549-578.
Israelachvili, J., Pashley, R., 1982. The hydrophobic interaction is long range, decaying exponentially with distance. Nature 300(5890), 341-342.
Israelachvili, J.N., 2011a. 15 - Solvation, Structural, and Hydration Forces. In: Israelachvili, J.N. (Ed.), Intermolecular and Surface Forces (Third Edition), pp. 341-380. Academic Press, San Diego.
Israelachvili, J.N., 2011b. Chapter 13 - Van der Waals Forces between Particles and Surfaces. In: Israelachvili, J.N. (Ed.), Intermolecular and Surface Forces (Third Edition), pp. 253-289. Academic Press, San Diego.
Issa, A.A., Luyt, A.S., 2019. Kinetics of Alkoxysilanes and Organoalkoxysilanes Polymerization: A Review. Polymers 11(3).
Iwasawa, T., Wash, P., Gibson, C., Rebek, J., Jr., 2007. Reaction of an Introverted Carboxylic Acid with Carbodiimide. Tetrahedron 63(28), 6506-6511.
Jain, P., Sun, L., Dai, J., Baker, G.L., Bruening, M.L., 2007. High-capacity purification of His-tagged proteins by affinity membranes containing functionalized polymer brushes. Biomacromolecules 8(10), 3102-3107.
Jefferis, R., 2009. Recombinant antibody therapeutics: the impact of glycosylation on mechanisms of action. Trends in Pharmacological Sciences 30(7), 356-362.
Jellison, G.E., 2005. 3 - Data Analysis for Spectroscopic Ellipsometry. In: Tompkins, H.G., Irene, E.A. (Eds.), Handbook of Ellipsometry, pp. 237-296. William Andrew Publishing, Norwich, NY.
Jesionowski, T., Zdarta, J., Krajewska, B., 2014. Enzyme immobilization by adsorption: a review. Adsorpt.-J. Int. Adsorpt. Soc. 20(5-6), 801-821.
Jewett, J.C., Bertozzi, C.R., 2010. Cu-free click cycloaddition reactions in chemical biology. Chemical Society reviews 39(4), 1272-1279.
Jiang, S., Cao, Z., 2010. Ultralow-Fouling, Functionalizable, and Hydrolyzable Zwitterionic Materials and Their Derivatives for Biological Applications. Adv. Mater. 22(9), 920-932.
Jiang, Y., Shi, M.L., Liu, Y., Wan, S., Cui, C., Zhang, L.Q., Tan, W.H., 2017. Aptamer/AuNP Biosensor for Colorimetric Profiling of Exosomal Proteins. Angew. Chem.-Int. Edit. 56(39), 11916-11920.
Jo, S., Park, K., 2000. Surface modification using silanated poly(ethylene glycol)s. Biomaterials 21(6), 605-616.
Jung, S.-Y., Lim, S.-M., Albertorio, F., Kim, G., Gurau, M.C., Yang, R.D., Holden, M.A., Cremer, P.S., 2003. The Vroman Effect: A Molecular Level Description of Fibrinogen Displacement. Journal of the American Chemical Society 125(42), 12782-12786.
Jung, Y., Lee, J.M., Jung, H., Chung, B.H., 2007. Self-Directed and Self-Oriented Immobilization of Antibody by Protein G−DNA Conjugate. Analytical Chemistry 79(17), 6534-6541.
Kam, N.W.S., Liu, Z., Dai, H.J., 2005. Functionalization of carbon nanotubes via cleavable disulfide bonds for efficient intracellular delivery of siRNA and potent gene silencing. Journal of the American Chemical Society 127(36), 12492-12493.
Kanduč, M., Schlaich, A., Schneck, E., Netz, R.R., 2016. Water-Mediated Interactions between Hydrophilic and Hydrophobic Surfaces. Langmuir 32(35), 8767-8782.
Karczmarczyk, A., Dubiak-Szepietowska, M., Vorobii, M., Rodriguez-Emmenegger, C., Dostalek, J., Feller, K.H., 2016. Sensitive and rapid detection of aflatoxin M1 in milk utilizing enhanced SPR and p(HEMA) brushes. Biosensors & bioelectronics 81, 159-165.

Karlsson, R., Michaelsson, A., Mattsson, L., 1991. Kinetic-Analysis of Monoclonal Antibody-Antigen Interactions with a New Biosensor Based Analytical System. Journal of Immunological Methods 145(1-2), 229-240.
Kaur, G., Saha, S., Tomar, M., Gupta, V., 2016. Influence of immobilization strategies on biosensing response characteristics: A comparative study. Enzyme Microb. Technol. 82, 144-150.
Kausar, A., 2017. Survey on Langmuir–Blodgett Films of Polymer and Polymeric Composite. Polymer-Plastics Technology and Engineering 56(9), 932-945.
Kawai, F., 2002. Microbial degradation of polyethers. Applied Microbiology and Biotechnology 58(1), 30-38.
Keefe, A.D., Pai, S., Ellington, A., 2010. Aptamers as therapeutics. Nature Reviews Drug Discovery 9(7), 537-550.
Kihlberg, B.M., Sjoholm, A.G., Bjorck, L., Sjobring, U., 1996. Characterization of the binding properties of protein LG, an immunoglobulin-binding hybrid protein. Eur. J. Biochem. 240(3), 556-563.
Kim, J., Cho, J., Seidler, P.M., Kurland, N.E., Yadavalli, V.K., 2010. Investigations of Chemical Modifications of Amino-Terminated Organic Films on Silicon Substrates and Controlled Protein Immobilization. Langmuir 26(4), 2599-2608.
Kim, J.C., Kim, M., Jung, J., Kim, H., Kim, I.J., Kim, J.R., Ree, M., 2012a. Biocompatible characteristics of sulfobetaine-containing brush polymers. Macromol. Res. 20(7), 746-753.
Kim, M., Kim, J.C., Rho, Y., Jung, J., Kwon, W., Kim, H., Ree, M., 2012b. Bacterial adherence on self-assembled films of brush polymers bearing zwitterionic sulfobetaine moieties. Journal of Materials Chemistry 22(37), 19418-19428.
Kim, S.A., Kim, S.J., Byun, K.M., Lee, S.H., Park, T.H., Kim, S.G., Shuler, M.L., Ieee, 2009. Avian Influenza-DNA Hybridization Detection using Wavelength Interrogation-based Surface Plasmon Resonance Biosensor. Ieee, New York.
Kingshott, P., Griesser, H.J., 1999. Surfaces that resist bioadhesion. Current Opinion in Solid State and Materials Science 4(4), 403-412.
Kirk, J.T., Brault, N.D., Baehr-Jones, T., Hochberg, M., Jiang, S., Ratner, D.M., 2013. Zwitterionic polymer-modified silicon microring resonators for label-free biosensing in undiluted human plasma. Biosensors & bioelectronics 42, 100-105.
Kiselev, A.V., 1965. Non-specific and specific interactions of molecules of different electronic structures with solid surfaces. Discussions of the Faraday Society 40(0), 205-218.
Klomp, G.F., Hashiguchi, H., Ursell, P.C., Takeda, Y., Taguchi, T., Dobelle, W.H., 1983. Macroporous hydrogel membranes for a hybrid artificial pancreas. II. Biocompatibility. Journal of Biomedical Materials Research 17(5), 865-871.
Knudsen, S.M., Lee, J., Ellington, A.D., Savran, C.A., 2006. Ribozyme-Mediated Signal Augmentation on a Mass-Sensitive Biosensor. Journal of the American Chemical Society 128(50), 15936-15937.
Kotlarek, D., Vorobii, M., Ogieglo, W., Knoll, W., Rodriguez-Emmenegger, C., Dostalek, J., 2019. Compact Grating-Coupled Biosensor for the Analysis of Thrombin. ACS sensors.
Kratschmer, C., Levy, M., 2017. Effect of Chemical Modifications on Aptamer Stability in Serum. Nucleic Acid Therapeutics 27(6), 335-344.
Krebs, B., Rauchenberger, R., Reiffert, S., Rothe, C., Tesar, M., Thomassen, E., Cao, M., Dreier, T., Fischer, D., Höß, A., Inge, L., Knappik, A., Marget, M., Pack, P., Meng, X.-Q., Schier, R., Söhlemann, P., Winter, J., Wölle, J., Kretzschmar, T., 2001. High-throughput generation and engineering of recombinant human antibodies. Journal of Immunological Methods 254(1), 67-84.
Kröger, D., Liley, M., Schiweck, W., Skerra, A., Vogel, H., 1999. Immobilization of histidine-tagged proteins on gold surfaces using chelator thioalkanes. Biosensors and Bioelectronics 14(2), 155-161.
Kroning, A., Furchner, A., Aulich, D., Bittrich, E., Rauch, S., Uhlmann, P., Eichhorn, K.-J., Seeber, M., Luzinov, I., Kilbey, S.M., Lokitz, B.S., Minko, S., Hinrichs, K., 2015. In Situ Infrared Ellipsometry for

Protein Adsorption Studies on Ultrathin Smart Polymer Brushes in Aqueous Environment. ACS applied materials & interfaces 7(23), 12430-12439.
Kruger, K., Grabowski, P.J., Zaug, A.J., Sands, J., Gottschling, D.E., Cech, T.R., 1982. Self-splicing RNA: Autoexcision and autocyclization of the ribosomal RNA intervening sequence of tetrahymena. Cell 31(1), 147-157.
Kruis, I.C., Lowik, D., Boelens, W.C., van Hest, J.C.M., Pruijn, G.J.M., 2016. An integrated, peptide-based approach to site-specific protein immobilization for detection of biomolecular interactions. Analyst 141(18), 5321-5328.
Kuang, H., Chen, W., Xu, D.H., Xu, L.G., Zhu, Y.Y., Liu, L.Q., Chu, H.Q., Peng, C.F., Xu, C.L., Zhu, S.F., 2010. Fabricated aptamer-based electrochemical "signal-off" sensor of ochratoxin A. Biosensors & bioelectronics 26(2), 710-716.
Kuzyk, A., Schreiber, R., Fan, Z.Y., Pardatscher, G., Roller, E.M., Hogele, A., Simmel, F.C., Govorov, A.O., Liedl, T., 2012. DNA-based self-assembly of chiral plasmonic nanostructures with tailored optical response. Nature 483(7389), 311-314.
Lai, M., Cai, K., Zhao, L., Chen, X., Hou, Y., Yang, Z., 2011. Surface Functionalization of TiO2 Nanotubes with Bone Morphogenetic Protein 2 and Its Synergistic Effect on the Differentiation of Mesenchymal Stem Cells. Biomacromolecules 12(4), 1097-1105.
Lang, N.D., Holloway, S., Nørskov, J.K., 1985. Electrostatic adsorbate-adsorbate interactions: The poisoning and promotion of the molecular adsorption reaction. Surf. Sci. 150(1), 24-38.
Lange, S.C., van Andel, E., Smulders, M.M.J., Zuilhof, H., 2016. Efficient and Tunable Three-Dimensional Functionalization of Fully Zwitterionic Antifouling Surface Coatings. Langmuir 32(40), 10199-10205.
Latham, M.P., Kay, L.E., 2012. Is buffer a good proxy for a crowded cell-like environment? A comparative NMR study of calmodulin side-chain dynamics in buffer and E. coli lysate. PloS one 7(10), e48226-e48226.
Lauga, E., Brenner, M., Stone, H., 2007. Microfluidics: The No-Slip Boundary Condition. In: C.;, T., A.L.;, Y., J.F.;, F. (Eds.), Springer Handbook of Experimental Fluid Mechanics. Springer, Berlin, Heidelberg.
Law, K.-Y., 2014. Definitions for hydrophilicity, hydrophobicity, and superhydrophobicity: getting the basics right. ACS Publications.
Leckband, D.E., Schmitt, F.J., Israelachvili, J.N., Knoll, W., 1994. Direct Force Measurements of Specific and Nonspecific Protein Interactions. Biochemistry 33(15), 4611-4624.
Lee, B.S., Chi, Y.S., Lee, K.-B., Kim, Y.-G., Choi, I.S., 2007. Functionalization of poly(oligo(ethylene glycol) methacrylate) films on gold and Si/SiO2 for immobilization of proteins and cells: SPR and QCM studies. Biomacromolecules 8(12), 3922-3929.
Lee, H., Scherer, N.F., Messersmith, P.B., 2006. Single-molecule mechanics of mussel adhesion. Proceedings of the National Academy of Sciences 103(35), 12999-13003.
Leed, E.A., Sofo, J.O., Pantano, C.G., 2005. Electronic structure calculations of physisorption and chemisorption on oxide glass surfaces. Physical Review B 72(15), 155427.
Leigh, B.L., Cheng, E., Xu, L., Andresen, C., Hansen, M.R., Guymon, C.A., 2017. Photopolymerizable Zwitterionic Polymer Patterns Control Cell Adhesion and Guide Neural Growth. Biomacromolecules 18(8), 2389-2401.
Leng, C., Han, X., Shao, Q., Zhu, Y., Li, Y., Jiang, S., Chen, Z., 2014. In Situ Probing of the Surface Hydration of Zwitterionic Polymer Brushes: Structural and Environmental Effects. The Journal of Physical Chemistry C 118(29), 15840-15845.
Lequoy, P., Murschel, F., Liberelle, B., Lerouge, S., De Crescenzo, G., 2016. Controlled co-immobilization of EGF and VEGF to optimize vascular cell survival. Acta Biomaterialia 29, 239-247.
Lessel, M., Bäumchen, O., Klos, M., Hähl, H., Fetzer, R., Paulus, M., Seemann, R., Jacobs, K., 2015. Self-assembled silane monolayers: an efficient step-by-step recipe for high-quality, low energy surfaces. Surface and Interface Analysis 47(5), 557-564.

Li, C.Y., Wang, W.C., Xu, F.J., Zhang, L.Q., Yang, W.T., 2011. Preparation of pH-sensitive membranes via dopamine-initiated atom transfer radical polymerization. Journal of Membrane Science 367(1), 7-13.
Li, F., Chen, W., Zhang, S., 2008. Development of DNA electrochemical biosensor based on covalent immobilization of probe DNA by direct coupling of sol–gel and self-assembly technologies. Biosensors and Bioelectronics 24(4), 781-786.
Li, L., Chen, S., Zheng, J., Ratner, B.D., Jiang, S., 2005. Protein Adsorption on Oligo(ethylene glycol)-Terminated Alkanethiolate Self-Assembled Monolayers: The Molecular Basis for Nonfouling Behavior. The Journal of Physical Chemistry B 109(7), 2934-2941.
Li, L., Li, Y., Luo, X., Deng, J., Yang, W., 2010. Helical poly(N-propargylamide)s with functional catechol groups: Synthesis and adsorption of metal ions in aqueous solution. Reactive and Functional Polymers 70(12), 938-943.
Li, X.M., Song, S.Y., Pei, Y.X., Dong, H., Aastrup, T., Pei, Z.C., 2016. Oriented and reversible immobilization of His-tagged proteins on two- and three-dimensional surfaces for study of protein-protein interactions by a QCM biosensor. Sens. Actuator B-Chem. 224, 814-822.
Lim, C.Y., Owens, N.A., Wampler, R.D., Ying, Y., Granger, J.H., Porter, M.D., Takahashi, M., Shimazu, K., 2014. Succinimidyl Ester Surface Chemistry: Implications of the Competition between Aminolysis and Hydrolysis on Covalent Protein Immobilization. Langmuir 30(43), 12868-12878.
Lim, K., Chua, R.R.Y., Saravanan, R., Basu, A., Mishra, B., Tarnbyah, P.A., Ho, B., Leong, S.S.J., 2013. Immobilization Studies of an Engineered Arginine-Tryptophan-Rich Peptide on a Silicone Surface with Antimicrobial and Antibiofilm Activity. ACS applied materials & interfaces 5(13), 6412-6422.
Lim, S.I., Lukianov, C.I., Champion, J.A., 2017. Self-assembled protein nanocarrier for intracellular delivery of antibody. Journal of Controlled Release 249, 1-10.
Lin, P.-C., Weinrich, D., Waldmann, H., 2010. Protein Biochips: Oriented Surface Immobilization of Proteins. Macromolecular Chemistry and Physics 211(2), 136-144.
Lipman, N.S., Jackson, L.R., Trudel, L.J., Weis-Garcia, F., 2005. Monoclonal Versus Polyclonal Antibodies: Distinguishing Characteristics, Applications, and Information Resources. ILAR Journal 46(3), 258-268.
Lísalová, H., Brynda, E., Houska, M., Víšová, I., Mrkvová, K., Song, X.C., Gedeonová, E., Surman, F., Riedel, T., Pop-Georgievski, O., Homola, J., 2017. Ultralow-Fouling Behavior of Biorecognition Coatings Based on Carboxy-Functional Brushes of Zwitterionic Homo- and Copolymers in Blood Plasma: Functionalization Matters. Analytical Chemistry 89(6), 3524-3531.
Liu, H.F., Ma, J., Winter, C., Bayer, R., 2010. Recovery and purification process development for monoclonal antibody production. MAbs 2(5), 480-499.
Liu, Y., Deng, Y., Li, T.T., Chen, Z., Chen, H., Li, S., Liu, H.N., 2018. Aptamer-Based Electrochemical Biosensor for Mercury Ions Detection Using AuNPs-Modified Glass Carbon Electrode. J. Biomed. Nanotechnol. 14(12), 2156-2161.
Liu, Y., Lai, Y.X., Yang, G.J., Tang, C.L., Deng, Y., Li, S., Wang, Z.L., 2017. Cd-Aptamer Electrochemical Biosensor Based on AuNPs/CS Modified Glass Carbon Electrode. J. Biomed. Nanotechnol. 13(10), 1253-1259.
Löfblom, J., Feldwisch, J., Tolmachev, V., Carlsson, J., Ståhl, S., Frejd, F.Y., 2010. Affibody molecules: Engineered proteins for therapeutic, diagnostic and biotechnological applications. FEBS Letters 584(12), 2670-2680.
Long, R., 2013. Understanding the Electronic Structures of Graphene Quantum Dot Physisorption and Chemisorption onto the TiO2 (110) Surface: A First-Principles Calculation. ChemPhysChem 14(3), 579-582.
Low, B.C., Pan, C.Q., Shivashankar, G.V., Bershadsky, A., Sudol, M., Sheetz, M., 2014. YAP/TAZ as mechanosensors and mechanotransducers in regulating organ size and tumor growth. FEBS Letters 588(16), 2663-2670.
Lowe, S., O'Brien-Simpson, N.M., Connal, L.A., 2015. Antibiofouling polymer interfaces: poly(ethylene glycol) and other promising candidates. Polymer Chemistry 6(2), 198-212.

Lu, H.-C., Chen, H.-M., Lin, Y.-S., Lin, J.-W., 2008. A Reusable and Specific Protein A-Coated Piezoelectric Biosensor for Flow Injection Immunoassay. Biotechnology Progress 16(1), 116-124.
Lu, J., Getz, G., Miska, E.A., Alvarez-Saavedra, E., Lamb, J., Peck, D., Sweet-Cordero, A., Ebert, B.L., Mak, R.H., Ferrando, A.A., Downing, J.R., Jacks, T., Horvitz, H.R., Golub, T.R., 2005. MicroRNA expression profiles classify human cancers. Nature 435(7043), 834-838.
Lu, Y., Liu, J., 2006. Functional DNA nanotechnology: emerging applications of DNAzymes and aptamers. Current Opinion in Biotechnology 17(6), 580-588.
Luan, J.Y., Xu, T., Cashin, J., Morrissey, J.J., Kharasch, E.D., Singamaneni, S., 2018. Environmental Stability of Plasmonic Biosensors Based on Natural versus Artificial Antibody. Analytical Chemistry 90(13), 7880-7887.
Luderer, F., Walschus, U., 2005. Immobilization of oligonucleoticles for biochemical sensing by self-assembled monolayers: Thiol-organic bonding on gold and silanization on silica surfaces. In: Wittmann, C. (Ed.), Immobilisation of DNA on Chips I, pp. 37-56. Springer-Verlag Berlin, Berlin.
Luk, Y.-Y., Kato, M., Mrksich, M., 2000. Self-assembled monolayers of alkanethiolates presenting mannitol groups are inert to protein adsorption and cell attachment. Langmuir 16(24), 9604-9608.
Ma, H.W., Hyun, J.H., Stiller, P., Chilkoti, A., 2004. "Non-fouling" oligo(ethylene glycol)-functionalized polymer brushes synthesized by surface-initiated atom transfer radical polymerization. Adv. Mater. 16(4), 338-+.
Ma, L., Liu, J., 2020. Catalytic Nucleic Acids: Biochemistry, Chemical Biology, Biosensors, and Nanotechnology. iScience 23(1), 100815.
Ma, M.L., Hill, R.M., 2006. Superhydrophobic surfaces. Current Opinion in Colloid & Interface Science 11(4), 193-202.
Ma, P.C., Kim, J.K., Tang, B.Z., 2006. Functionalization of carbon nanotubes using a silane coupling agent. Carbon 44(15), 3232-3238.
Ma, S., Zhang, X., Yu, B., Zhou, F., 2019. Brushing up functional materials. NPG Asia Materials 11(1), 24.
Mahmoud, Z.N., Gunnoo, S.B., Thomson, A.R., Fletcher, J.M., Woolfson, D.N., 2011. Bioorthogonal dual functionalization of self-assembling peptide fibers. Biomaterials 32(15), 3712-3720.
Mallikaratchy, P., 2017. Evolution of Complex Target SELEX to Identify Aptamers against Mammalian Cell-Surface Antigens. Molecules 22(2).
Martelli, G., Zope, H.R., Bròvia Capell, M., Kros, A., 2013. Coiled-coil peptide motifs as thermoresponsive valves for mesoporous silica nanoparticles. Chemical Communications 49(85), 9932-9934.
Martínez-Jothar, L., Doulkeridou, S., Schiffelers, R.M., Sastre Torano, J., Oliveira, S., van Nostrum, C.F., Hennink, W.E., 2018. Insights into maleimide-thiol conjugation chemistry: Conditions for efficient surface functionalization of nanoparticles for receptor targeting. Journal of Controlled Release 282, 101-109.
Masson, J.-F., 2017. Surface Plasmon Resonance Clinical Biosensors for Medical Diagnostics. ACS sensors 2(1), 16-30.
Mastan, E., Xi, L., Zhu, S., 2016. Factors Affecting Grafting Density in Surface-Initiated ATRP: A Simulation Study. Macromolecular Theory and Simulations 25(3), 220-228.
Matyjaszewski, K., Miller, P.J., Shukla, N., Immaraporn, B., Gelman, A., Luokala, B.B., Siclovan, T.M., Kickelbick, G., Vallant, T., Hoffmann, H., Pakula, T., 1999. Polymers at Interfaces: Using Atom Transfer Radical Polymerization in the Controlled Growth of Homopolymers and Block Copolymers from Silicon Surfaces in the Absence of Untethered Sacrificial Initiator. Macromolecules 32(26), 8716-8724.
Mi, L., Jiang, S., 2014. Integrated Antimicrobial and Nonfouling Zwitterionic Polymers. Angewandte Chemie International Edition 53(7), 1746-1754.
Milner, S.T., Witten, T.A., Cates, M.E., 1988. Theory of the grafted polymer brush. Macromolecules 21(8), 2610-2619.

Minko, S., 2008. Grafting on Solid Surfaces: “Grafting to” and “Grafting from” Methods. In: Stamm, M. (Ed.), Polymer Surfaces and Interfaces: Characterization, Modification and Applications, pp. 215-234. Springer Berlin Heidelberg, Berlin, Heidelberg.
Miyadera, T., Kosower, E.M., 1972. Receptor site labeling through functional groups. 2. Reactivity of maleimide groups. Journal of medicinal chemistry 15(5), 534-537.
Mizutani, A., Kikuchi, A., Yamato, M., Kanazawa, H., Okano, T., 2008. Preparation of thermoresponsive polymer brush surfaces and their interaction with cells. Biomaterials 29(13), 2073-2081.
Montalbetti, C.A., Falque, V., 2005. Amide bond formation and peptide coupling. Tetrahedron 61(46), 10827-10852.
Montheard, J.-P., Chatzopoulos, M., Chappard, D., 1992. 2-Hydroxyethyl Methacrylate (HEMA): Chemical Properties and Applications in Biomedical Fields. Journal of Macromolecular Science, Part C 32(1), 1-34.
Morales, M.A., Halpern, J.M., 2018. Guide to Selecting a Biorecognition Element for Biosensors. Bioconjugate Chemistry 29(10), 3231-3239.
Moretta, R., Terracciano, M., Borbone, N., Oliviero, G., Schiattarella, C., Piccialli, G., Falanga, A.P., Marzano, M., Dardano, P., De Stefano, L., Rea, I., 2020. PNA-Based Graphene Oxide/Porous Silicon Hybrid Biosensor: Towards a Label-Free Optical Assay for Brugada Syndrome. Nanomaterials 10(11), 17.
Morlat, S., Gardette, J.-L., 2001. Phototransformation of water-soluble polymers. I: photo-and thermooxidation of poly (ethylene oxide) in solid state. Polymer 42(14), 6071-6079.
Moroishi, T., Hansen, C.G., Guan, K.L., 2015. The emerging roles of YAP and TAZ in cancer. Nature reviews. Cancer 15(2), 73-79.
Morpurgo, M., Bayer, E.A., Wilchek, M., 1999. N-hydroxysuccinimide carbonates and carbamates are useful reactive reagents for coupling ligands to lysines on proteins. J. Biochem. Biophys. Methods 38(1), 17-28.
Morris, T.A., Peterson, A.W., Tarlov, M.J., 2009. Selective Binding of RNase B Glycoforms by Polydopamine-Immobilized Concanavalin A. Analytical Chemistry 81(13), 5413-5420.
Mostafa, G.S., 2018. Convective Heat and Mass Transfer. CRC Press.
Müller, S., Strohbach, D., Wolf, J., 2006. Sensors made of RNA: tailored ribozymes for detection of small organic molecules, metals, nucleic acids and proteins. IEE Proceedings - Nanobiotechnology, pp. 31-40.
Muramatsu, H., Kimura, K., 1992. QUARTZ CRYSTAL DETECTOR FOR MICRORHEOLOGICAL STUDY AND ITS APPLICATION TO PHASE-TRANSITION PHENOMENA OF LANGMUIR-BLODGETT-FILMS. Analytical Chemistry 64(21), 2502-2507.
Muyldermans, S., 2013. Nanobodies: Natural Single-Domain Antibodies. In: Kornberg, R.D. (Ed.), Annual Review of Biochemistry, Vol 82, pp. 775-797. Annual Reviews, Palo Alto.
Nahar, P., Wali, N.M., Gandhi, R.P., 2001. Light-Induced Activation of an Inert Surface for Covalent Immobilization of a Protein Ligand. Analytical Biochemistry 294(2), 148-153.
Nelson, B.P., Grimsrud, T.E., Liles, M.R., Goodman, R.M., Corn, R.M., 2001. Surface Plasmon Resonance Imaging Measurements of DNA and RNA Hybridization Adsorption onto DNA Microarrays. Analytical Chemistry 73(1), 1-7.
Neto, C., Evans, D.R., Bonaccurso, E., Butt, H.-J., Craig, V.S.J., 2005. Boundary slip in Newtonian liquids: a review of experimental studies. Reports on Progress in Physics 68(12), 2859-2897.
Netzer, L., Sagiv, J., 1983. A new approach to construction of artificial monolayer assemblies. Journal of the American Chemical Society 105(3), 674-676.
Neves, M.A.D., Blaszykowski, C., Bokhari, S., Thompson, M., 2015. Ultra-high frequency piezoelectric aptasensor for the label-free detection of cocaine. Biosensors and Bioelectronics 72, 383-392.

Nguyen, B.H., Tran, L.D., Do, Q.P., Nguyen, H.L., Tran, N.H., Nguyen, P.X., 2013. Label-free detection of aflatoxin M1 with electrochemical Fe3O4/polyaniline-based aptasensor. Materials Science and Engineering: C 33(4), 2229-2234.
Nguyen, H.H., Park, J., Kang, S., Kim, M., 2015. Surface Plasmon Resonance: A Versatile Technique for Biosensor Applications. Sensors 15(5), 10481-10510.
Niazov, T., Pavlov, V., Xiao, Y., Gill, R., Willner, I., 2004. DNAzyme-functionalized Au nanoparticles for the amplified detection of DNA or telomerase activity. Nano Letters 4(9), 1683-1687.
Nie, W., Wang, Q., Zou, L., Zheng, Y., Liu, X., Yang, X., Wang, K., 2018. Low-Fouling Surface Plasmon Resonance Sensor for Highly Sensitive Detection of MicroRNA in a Complex Matrix Based on the DNA Tetrahedron. Analytical Chemistry.
Nielsen, P.E., 1997. Peptide nucleic acid (PNA) From DNA recognition to antisense and DNA structure. Biophysical Chemistry 68(1), 103-108.
Nikaido, H., 2009. Multidrug Resistance in Bacteria. Annual Review of Biochemistry 78(1), 119-146.
Nilson, B.H.K., Logdberg, L., Kastern, W., Bjorck, L., Akerstrom, B., 1993. PURIFICATION OF ANTIBODIES USING PROTEIN-L-BINDING FRAMEWORK STRUCTURES IN THE LIGHT-CHAIN VARIABLE DOMAIN. Journal of Immunological Methods 164(1), 33-40.
Noh, H., Vogler, E.A., 2007. Volumetric interpretation of protein adsorption: Competition from mixtures and the Vroman effect. Biomaterials 28(3), 405-422.
Norde, W., 1986. Adsorption of proteins from solution at the solid-liquid interface. Advances in Colloid and Interface Science 25, 267-340.
Norde, W., Gags, D., 2004. Interaction of bovine serum albumin and human blood plasma with PEO-tethered surfaces: Influence of PEO chain length, grafting density, and temperature. Langmuir 20(10), 4162-4167.
Northrop, B.H., Frayne, S.H., Choudhary, U., 2015. Thiol–maleimide “click” chemistry: evaluating the influence of solvent, initiator, and thiol on the reaction mechanism, kinetics, and selectivity. Polymer Chemistry 6(18), 3415-3430.
Okano, T., Yamada, N., Okuhara, M., Sakai, H., Sakurai, Y., 1995. Mechanism of Cell Detachment from Temperature-Modulated, Hydrophilic-Hydrophobic Polymer Surfaces. Biomaterials 16(4), 297-303.
Oliveira, S.M., Alves, N.M., Mano, J.F., 2014. Cell interactions with superhydrophilic and superhydrophobic surfaces. Journal of Adhesion Science and Technology 28(8-9), 843-863.
Orgeret-Ravanat, C., Gramain, P., Dejardin, P., Schmitt, A., 1988. Adsorption/desorption of a PEO-rich comb-like polymer at a silica/aqueous solution interface. Colloids and Surfaces 33(0), 109-119.
Ostovan, A., Ghaedi, M., Arabi, M., Yang, Q., Li, J.H., Chen, L.X., 2018. Hydrophilic Multitemplate Molecularly Imprinted Biopolymers Based on a Green Synthesis Strategy for Determination of B-Family Vitamins. ACS applied materials & interfaces 10(4), 4140-4150.
Ostuni, E., Chapman, R.G., Holmlin, R.E., Takayama, S., Whitesides, G.M., 2001. A survey of structure-property relationships of surfaces that resist the adsorption of protein. Langmuir 17(18), 5605-5620.
Otsuka, H., Nagasaki, Y., Kataoka, K., 2003. PEGylated nanoparticles for biological and pharmaceutical applications. Advanced Drug Delivery Reviews 55(3), 403-419.
Pan, J.M., Chen, W., Ma, Y., Pan, G.Q., 2018. Molecularly imprinted polymers as receptor mimics for selective cell recognition. Chemical Society reviews 47(15), 5574-5587.
Pape, A.C.H., Ippel, B.D., Dankers, P.Y.W., 2017. Cell and Protein Fouling Properties of Polymeric Mixtures Containing Supramolecular Poly(ethylene glycol) Additives. Langmuir 33(16), 4076-4082.
Parrillo, V., de los Santos Pereira, A., Riedel, T., Rodriguez-Emmenegger, C., 2017. Catalyst-free “click” functionalization of polymer brushes preserves antifouling properties enabling detection in blood plasma. Analytica Chimica Acta 971, 78-87.
Paukstelis, P.J., Seeman, N.C., 2016. 3D DNA Crystals and Nanotechnology. Crystals 6(8), 14.

Pei, Z., Anderson, H., Myrskog, A., Dunér, G., Ingemarsson, B., Aastrup, T., 2010. Optimizing immobilization on two-dimensional carboxyl surface: pH dependence of antibody orientation and antigen binding capacity. Analytical Biochemistry 398(2), 161-168.
Peppas, N.A., Hilt, J.Z., Khademhosseini, A., Langer, R., 2006. Hydrogels in biology and medicine: From molecular principles to bionanotechnology. Adv. Mater. 18(11), 1345-1360.
Pereira, A.d.l.S., Rodriguez-Emmenegger, C., Surman, F., Riedel, T., Alles, A.B., Brynda, E., 2014. Use of pooled blood plasmas in the assessment of fouling resistance. RSC Adv. 4(5), 2318-2321.
Peskir, G., 2003. On the Diffusion Coefficient: The Einstein Relation and Beyond. Stochastic Models 19(3), 383-405.
Peterlinz, K.A., Georgiadis, R., 1996. In situ kinetics of self-assembly by surface plasmon resonance spectroscopy. Langmuir 12(20), 4731-4740.
Pickup, J.C., Hussain, F., Evans, N.D., Rolinski, O.J., Birch, D.J.S., 2005. Fluorescence-based glucose sensors. Biosensors and Bioelectronics 20(12), 2555-2565.
Piehler, J., Brecht, A., Valiokas, R., Liedberg, B., Gauglitz, G., 2000. A high-density poly(ethylene glycol) polymer brush for immobilization on glass-type surfaces. Biosensors and Bioelectronics 15(9), 473-481.
Pignatello, J.J., Xing, B.S., 1996. Mechanisms of slow sorption of organic chemicals to natural particles. Environ. Sci. Technol. 30(1), 1-11.
Piletsky, S.A., Matuschewski, H., Schedler, U., Wilpert, A., Piletska, E.V., Thiele, T.A., Ulbricht, M., 2000. Surface functionalization of porous polypropylene membranes with molecularly imprinted polymers by photograft copolymerization in water. Macromolecules 33(8), 3092-3098.
Piliarik, M., Bocková, M., Homola, J., 2010. Surface Plasmon Resonance Biosensor for Parallelized Detection of Protein Biomarkers in Diluted Blood Plasma. Biosensors and Bioelectronics 26(4), 1656-1661.
Pohanka, M., 2009. Monoclonal and polyclonal antibodies production - preparation of potent biorecognition element. J. Appl. Biomed. 7(3), 115-121.
Polshettiwar, V., Kaushik, M.P., 2004. CsF–Celite catalyzed regio- and chemoselective SN2 type ring opening of epoxides with thiol. Catalysis Communications 5(9), 515-518.
Pop-Georgievski, O., Popelka, S.t.p.n., Houska, M., Chvostová, D., Proks, V.r., Rypáček, F., 2011. Poly(ethylene oxide) Layers Grafted to Dopamine-melanin Anchoring Layer: Stability and Resistance to Protein Adsorption. Biomacromolecules 12(9), 3232-3242.
Pounder, R.J., Stanford, M.J., Brooks, P., Richards, S.P., Dove, A.P., 2008. Metal free thiol-maleimide 'Click' reaction as a mild functionalisation strategy for degradable polymers. Chemical Communications(41), 5158-5160.
Prime, K.L., Whitesides, G.M., 1993. Adsorption of proteins onto surfaces containing end-attached oligo(ethylene oxide): a model system using self-assembled monolayers. Journal of the American Chemical Society 115(23), 10714-10721.
Qin, B., Zhang, S., Song, Q., Huang, Z.H., Xu, J.F., Zhang, X., 2017. Supramolecular Interfacial Polymerization: A Controllable Method of Fabricating Supramolecular Polymeric Materials. Angew. Chem.-Int. Edit. 56(26), 7639-7643.
Qiu, Y., Park, K., 2001. Environment-sensitive hydrogels for drug delivery. Advanced Drug Delivery Reviews 53(3), 321-339.
Quintana, R., Janczewski, D., Vasantha, V.A., Jana, S., Lee, S.S.C., Parra-Velandia, F.J., Guo, S.F., Parthiban, A., Teo, S.L.M., Vancso, G.J., 2014. Sulfobetaine-based polymer brushes in marine environment: Is there an effect of the polymerizable group on the antifouling performance? Colloid Surf. B-Biointerfaces 120, 118-124.
Raus, V., Kostka, L., 2019. Optimizing the Cu-RDRP of N-(2-hydroxypropyl) methacrylamide toward biomedical applications. Polymer Chemistry 10(5), 564-568.
Ray, A., Norden, B., 2000. Peptide nucleic acid (PNA): its medical and biotechnical applications and promise for the future. Faseb J. 14(9), 1041-1060.

Riedel, T., Hageneder, S., Surman, F., Pop-Georgievski, O., Noehammer, C., Hofner, M., Brynda, E., Rodriguez-Emmenegger, C., Dostálek, J., 2017. Plasmonic Hepatitis B Biosensor for the Analysis of Clinical Saliva. Analytical Chemistry 89(5), 2972-2977.
Riedel, T., Riedelová-Reicheltová, Z., Májek, P., Rodriguez-Emmenegger, C., Houska, M., Dyr, J.E., Brynda, E., 2013. Complete Identification of Proteins Responsible for Human Blood Plasma Fouling on Poly(ethylene glycol)-Based Surfaces. Langmuir 29(10), 3388-3397.
Riedel, T., Surman, F., Hageneder, S., Pop-Georgievski, O., Noehammer, C., Hofner, M., Brynda, E., Rodriguez-Emmenegger, C., Dostálek, J., 2016. Hepatitis B plasmonic biosensor for the analysis of clinical serum samples. Biosensors and Bioelectronics 85, 272-279.
Richter, A., Paschew, G., Klatt, S., Lienig, J., Arndt, K.F., Adler, H.J.P., 2008. Review on hydrogel-based pH sensors and microsensors. Sensors 8(1), 561-581.
Richter, A.W., Åkerblom, E., 1984. Polyethylene glycol reactive antibodies in man: titer distribution in allergic patients treated with monomethoxy polyethylene glycol modified allergens or placebo, and in healthy blood donors. International Archives of Allergy and Immunology 74(1), 36-39.
Robinson, K., Khan, M., de Paz Banez, M., Wang, X., Armes, S., 2001. Controlled polymerization of 2-hydroxyethyl methacrylate by ATRP at ambient temperature. Macromolecules 34(10), 3155-3158.
Rodahl, M., Höök, F., Fredriksson, C., A. Keller, C., Krozer, A., Brzezinski, P., Voinova, M., Kasemo, B., 1997. Simultaneous frequency and dissipation factor QCM measurements of biomolecular adsorption and cell adhesion. Faraday Discussions 107(0), 229-246.
Rodrigues, R.C., Ortiz, C., Berenguer-Murcia, Á., Torres, R., Fernández-Lafuente, R., 2013. Modifying enzyme activity and selectivity by immobilization. Chemical Society reviews 42(15), 6290-6307.
Rodriguez-Emmenegger, C., Avramenko, O.A., Brynda, E., Skvor, J., Bologna Alles, A., 2011a. Poly(HEMA) brushes emerging as a new platform for direct detection of food pathogen in milk samples. Biosensors and Bioelectronics 26, 4545-4551.
Rodriguez-Emmenegger, C., Brynda, E., Riedel, T., Houska, M., Šubr, V., Bologna Alles, A., Hasan, E., Gautrot, J.E., Huck, W.T.S., 2011b. Polymer Brushes Showing Non-Fouling in Blood Plasma Challenge the Currently Accepted Design of Protein Resistant Surfaces. Macromolecular Rapid Communications 32(12), 952–957.
Rodriguez-Emmenegger, C., Brynda, E., Riedel, T., Sedlakova, Z., Houska, M., Alles, A.B., 2009. Interaction of Blood Plasma with Antifouling Surfaces. Langmuir 25(11), 6328-6333.
Rodriguez-Emmenegger, C., Hasan, E., Pop-Georgievski, O., Houska, M., Brynda, E., Alles, A.B., 2012a. Controlled/Living Surface-Initiated ATRP of Antifouling Polymer Brushes from Gold in PBS and Blood Sera as a Model Study for Polymer Modifications in Complex Biological Media. Macromolecular Bioscience 12(4), 525-532.
Rodriguez-Emmenegger, C., Houska, M., Brynda, E., Bologna Alles, A., 2012b. Surfaces resistant to fouling from biological fluids: toward biosensors for real applications. Macromolecular Bioscience. DOI: 10.1002/mabi.201200171.
Rodriguez-Emmenegger, C., Kylian, O., Houska, M., Brynda, E., Artemenko, A., Kousal, J., Bologna Alles, A., Biederman, H., 2011c. Substrate-Independent Approach for the Generation of Functional Protein Resistant Surfaces. Biomacromolecules 12(4), 1058-1066.
Rodriguez-Emmenegger, C., Schmidt, B.V.K.J., Sedlakova, Z., Subr, V., Alles, A.B., Brynda, E., Barner-Kowollik, C., 2011d. Low Temperature Aqueous Living/Controlled (RAFT) Polymerization of Carboxybetaine Methacrylamide up to High Molecular Weights. Macromolecular Rapid Communications 32(13), 958-965.
Rodriguez-Emmenegger, C., Surman, F., Brynda, E., Riedel, T., Houska, M., Lisalova, H., Homola, J., 2016. COPOLYMER OF N-(2-HYDROXYPROPYL) METHACRYLAMIDE AND CARBOXYBETAINE METHACRYLAMIDE, POLYMER BRUSHES. In: Ustav Makromolekularni Chemie AV CR, v.v.i., Ustav Fotoniky A Elektroniky Av Cr, V.v.i. (Eds.).

Rostovtsev, V.V., Green, L.G., Fokin, V.V., Sharpless, K.B., 2002. A stepwise huisgen cycloaddition process: copper (I)-catalyzed regioselective “ligation” of azides and terminal alkynes. Angewandte Chemie 114(14), 2708-2711.
Roth, C.M., Lenhoff, A.M., 1993. Electrostatic and van der Waals contributions to protein adsorption: computation of equilibrium constants. Langmuir 9(4), 962-972.
Ruckenstein, E., Li, Z.F., 2005. Surface modification and functionalization through the self-assembled monolayer and graft polymerization. Adv Colloid Interface Sci 113(1), 43-63.
Rusmini, F., Zhong, Z., Feijen, J., 2007. Protein Immobilization Strategies for Protein Biochips. Biomacromolecules 8(6), 1775-1789.
Sauerbrey, G., 1959. Verwendung von Schwingquarzen zur Wägung dünner Schichten und zur Mikrowägung. Zeitschrift für Physik 155(2), 206-222.
Sauter, A., Richter, G., Micoulet, A., Martinez, A., Spatz, J.P., Appel, S., 2013. Effective polyethylene glycol passivation for the inhibition of surface interactions of peripheral blood mononuclear cells and platelets. Biointerphases 8(1), 14.
Scarano, S., Mascini, M., Turner, A.P.F., Minunni, M., 2010. Surface plasmon resonance imaging for affinity-based biosensors. Biosensors & bioelectronics 25(5), 957-966.
Seeman, N.C., Sleiman, H.F., 2017. DNA nanotechnology. Nature Reviews Materials 3(1), 17068.
Seo, J.-s., Lee, S., Poulter, C.D., 2013. Regioselective Covalent Immobilization of Recombinant Antibody-Binding Proteins A, G, and L for Construction of Antibody Arrays. Journal of the American Chemical Society 135(24), 8973-8980.
Seyedi, S., Martin, D.R., Matyushov, D.V., 2019. Screening of Coulomb interactions in liquid dielectrics. Journal of Physics: Condensed Matter 31(32), 325101.
Sharma, S., Byrne, H., O'Kennedy, R.J., 2016. Antibodies and antibody-derived analytical biosensors. Essays Biochem 60(1), 9-18.
Shen, C.-H., Lin, J.-C., 2013. Solvent and concentration effects on the surface characteristics and platelet compatibility of zwitterionic sulfobetaine-terminated self-assembled monolayers. Colloids and Surfaces B: Biointerfaces 101, 376-383.
Shirtliff;, M.E., Leid;, J.G., 2009. The Role of Biofilms in Device-Related Infections, 1 ed. Springer-Verlag Berlin Heidelberg.
Schlenoff, J.B., 2014. Zwitteration: coating surfaces with zwitterionic functionality to reduce nonspecific adsorption. Langmuir : the ACS journal of surfaces and colloids 30(32), 9625-9636.
Schönherr, H., Feng, C., Shovsky, A., 2003. Interfacial Reactions in Confinement: Kinetics and Temperature Dependence of Reactions in Self-Assembled Monolayers Compared to Ultrathin Polymer Films. Langmuir 19(26), 10843-10851.
Schrader, B., 2008. Infrared and Raman spectroscopy: methods and applications. John Wiley & Sons.
Schuck, P., 1997. Use of surface plasmon resonance to probe the equilibrium and dynamic aspects of interactions between biological macromolecules. Annu. Rev. Biophys. Biomolec. Struct. 26, 541-566.
Schweikl, H., Müller, R., Englert, C., Hiller, K.-A., Kujat, R., Nerlich, M., Schmalz, G., 2007. Proliferation of osteoblasts and fibroblasts on model surfaces of varying roughness and surface chemistry. Journal of Materials Science: Materials in Medicine 18(10), 1895-1905.
Sikorski, Z.E., 2006. Chemical and functional properties of food components. CRC press.
Simpson, J.T., Hunter, S.R., Aytug, T., 2015. Superhydrophobic materials and coatings: a review. Reports on Progress in Physics 78(8), 086501.
Socrates, G., 2004. Infrared and Raman characteristic group frequencies : tables and charts, 3rd ed. Chichester : Wiley.
Stenzel, M.H., 2013. Bioconjugation Using Thiols: Old Chemistry Rediscovered to Connect Polymers with Nature's Building Blocks. ACS Macro Lett. 2(1), 14-18.

Stephanopoulos, N., Liu, M.H., Tong, G.J., Li, Z., Liu, Y., Yan, H., Francis, M.B., 2010. Immobilization and One-Dimensional Arrangement of Virus Capsids with Nanoscale Precision Using DNA Origami. Nano Letters 10(7), 2714-2720.
Stevens, M.M., George, J.H., 2005. Exploring and engineering the cell surface interface. Science 310(5751), 1135-1138.
Subrahmanyam, S., Piletsky, S.A., Turner, A.P.F., 2002. Application of Natural Receptors in Sensors and Assays. Analytical Chemistry 74(16), 3942-3951.
Sulakvelidze, A., Alavidze, Z., Morris, J.G., 2001. Bacteriophage Therapy. Antimicrobial Agents and Chemotherapy 45(3), 649-659.
Sultan, I., Rahman, S., Jan, A.T., Siddiqui, M.T., Mondal, A.H., Haq, Q.M.R., 2018. Antibiotics, Resistome and Resistance Mechanisms: A Bacterial Perspective. Frontiers in Microbiology 9, 16.
Sun, X., Wang, H., Wang, Y., Gui, T., Wang, K., Gao, C., 2018. Creation of antifouling microarrays by photopolymerization of zwitterionic compounds for protein assay and cell patterning. Biosensors & bioelectronics 102, 63-69.
Sundaram, H.S., Han, X., Nowinski, A.K., Ella-Menye, J.-R., Wimbish, C., Marek, P., Senecal, K., Jiang, S., 2014. One-Step Dip Coating of Zwitterionic Sulfobetaine Polymers on Hydrophobic and Hydrophilic Surfaces. ACS applied materials & interfaces 6(9), 6664-6671.
Szleifer, I., 1997. Protein adsorption on surfaces with grafted polymers: A theoretical approach. Biophysical Journal 72(2), 595-612.
Špringer, T., Hemmerová, E., Finocchiaro, G., Krištofiková, Z., Vyhnálek, M., Homola, J., 2020. Surface plasmon resonance biosensor for the detection of tau-amyloid β complex. Sensors and Actuators B: Chemical 316, 128146.
Švitel, J., Dzgoev, A., Ramanathan, K., Danielsson, B., 2000. Surface plasmon resonance based pesticide assay on a renewable biosensing surface using the reversible concanavalin A monosaccharide interaction. Biosensors and Bioelectronics 15(7), 411-415.
Takada, Y., Ye, X.J., Simon, S., 2007. The integrins. Genome Biol. 8(5), 9.
Tang, Y., Lu, J.R., Lewis, A.L., Vick, T.A., Stratford, P.W., 2001. Swelling of Zwitterionic Polymer Films Characterized by Spectroscopic Ellipsometry. Macromolecules 34(25), 8768-8776.
Tao, C., Yang, S., Zhang, J., Wang, J., 2009. Surface modification of diamond-like carbon films with protein via polydopamine inspired coatings. Applied Surface Science 256(1), 294-297.
Tegoulia, V.A., Rao, W.S., Kalambur, A.T., Rabolt, J.R., Cooper, S.L., 2001. Surface properties, fibrinogen adsorption, and cellular interactions of a novel phosphorylcholine-containing self-assembled monolayer on gold. Langmuir 17(14), 4396-4404.
Thomas, H.R., Marsden, A.J., Walker, M., Wilson, N.R., Rourke, J.P., 2014. Sulfur-Functionalized Graphene Oxide by Epoxide Ring-Opening. Angewandte Chemie International Edition 53(29), 7613-7618.
Thubagere, A.J., Li, W., Johnson, R.F., Chen, Z., Doroudi, S., Lee, Y.L., Izatt, G., Wittman, S., Srinivas, N., Woods, D., Winfree, E., Qian, L., 2017. A cargo-sorting DNA robot. Science 357(6356), eaan6558.
Tokarev, I., Minko, S., 2009. Stimuli-responsive hydrogel thin films. Soft Matter 5(3), 511-524.
Trmcic-Cvitas, J., Hasan, E., Ramstedt, M., Li, X., Cooper, M.A., Abell, C., Huck, W.T.S., Gautrot, J.E., 2009. Biofunctionalized Protein Resistant Oligo(ethylene glycol)-Derived Polymer Brushes as Selective Immobilization and Sensing Platforms. Biomacromolecules 10(10), 2885-2894.
Tsarevsky, N.V., Matyjaszewski, K., 2005. Combining Atom Transfer Radical Polymerization and Disulfide/Thiol Redox Chemistry: A Route to Well-Defined (Bio)degradable Polymeric Materials. Macromolecules 38(8), 3087-3092.
Ulijn, R.V., Bibi, N., Jayawarna, V., Thornton, P.D., Todd, S.J., Mart, R.J., Smith, A.M., Gough, J.E., 2007. Bioresponsive hydrogels. Mater. Today 10(4), 40-48.
Ulman, A., 1996. Formation and structure of self-assembled monolayers. Chemical Reviews 96(4), 1533-1554.

Um, H.J., Kim, M., Lee, S.H., Min, J., Kim, H., Choi, Y.W., Kim, Y.H., 2011. Electrochemically oriented immobilization of antibody on poly-(2-cyano-ethylpyrrole)-coated gold electrode using a cyclic voltammetry. Talanta 84(2), 330-334.
Unsworth, L.D., Sheardown, H., Brash, J.L., 2005a. Polyethylene oxide surfaces of variable chain density by chemisorption of PEO-thiol on gold: Adsorption of proteins from plasma studied by radiolabelling and immunoblotting. Biomaterials 26(30), 5927-5933.
Unsworth, L.D., Sheardown, H., Brash, J.L., 2005b. Protein Resistance of Surfaces Prepared by Sorption of End-Thiolated Poly(ethylene glycol) to Gold: Effect of Surface Chain Density. Langmuir 21(3), 1036-1041.
Urbic, T., 2014. Ions increase strength of hydrogen bond in water. Chemical Physics Letters 610-611, 159-162.
Uygun, M., Tasdelen, M.A., Yagci, Y., 2010. Influence of Type of Initiation on Thiol-Ene "Click" Chemistry. Macromolecular Chemistry and Physics 211(1), 103-110.
Vaisocherová-Lísalová, H., Surman, F., Víšová, I., Vala, M., Špringer, T., Ermini, M.L., Šípová, H., Šedivák, P., Houska, M., Riedel, T., Pop-Georgievski, O., Brynda, E., Homola, J., 2016a. Copolymer Brush-Based Ultralow-Fouling Biorecognition Surface Platform for Food Safety. Analytical Chemistry 88(21), 10533-10539.
Vaisocherová-Lísalová, H., Víšová, I., Ermini, M.L., Špringer, T., Song, X.C., Mrázek, J., Lamačová, J., Scott Lynn, N., Šedivák, P., Homola, J., 2016b. Low-fouling surface plasmon resonance biosensor for multi-step detection of foodborne bacterial pathogens in complex food samples. Biosensors and Bioelectronics 80, 84-90.
Vaisocherova, H., Brynda, E., Homola, J., 2015a. Functionalizable low-fouling coatings for label-free biosensing in complex biological media: advances and applications. Anal. Bioanal. Chem. 407(14), 3927-3953.
Vaisocherova, H., Sevcu, V., Adam, P., Spackova, B., Hegnerova, K., Pereira, A.D., Rodriguez-Emmenegger, C., Riedel, T., Houska, M., Brynda, E., Homola, J., 2014. Functionalized ultra-low fouling carboxy- and hydroxy-functional surface platforms: functionalization capacity, biorecognition capability and resistance to fouling from undiluted biological media. Biosensors & bioelectronics 51, 150-157.
Vaisocherova, H., Sipova, H., Visova, I., Bockova, M., Springer, T., Laura Ermini, M., Song, X., Krejcik, Z., Chrastinova, L., Pastva, O., Pimkova, K., Dostalova Merkerova, M., Dyr, J.E., Homola, J., 2015b. Rapid and sensitive detection of multiple microRNAs in cell lysate by low-fouling surface plasmon resonance biosensor. Biosensors & bioelectronics 70, 226-231.
Vaisocherova, H., Yang, W., Zhang, Z., Cao, Z., Cheng, G., Piliarik, M., Homola, J., Jiang, S., 2008. Ultralow fouling and functionalizable surface chemistry based on a zwitterionic polymer enabling sensitive and specific protein detection in undiluted blood plasma. Analytical Chemistry 80(20), 7894-7901.
Vakurov, A., Simpson, C., Daly, C., Gibson, T., Millner, P., 2005. Acetylecholinesterase-based biosensor electrodes for organophosphate pesticide detection: II. Immobilization and stabilization of acetylecholinesterase. Biosensors and Bioelectronics 20(11), 2324-2329.
Van Kooten, T., Schakenraad, J., Van der Mei, H., Busscher, H., 1992. Influence of substratum wettability on the strength of adhesion of human fibroblasts. Biomaterials 13(13), 897-904.
Van Wachem, P., Hogt, A., Beugeling, T., Feijen, J., Bantjes, A., Detmers, J., Van Aken, W., 1987. Adhesion of cultured human endothelial cells onto methacrylate polymers with varying surface wettability and charge. Biomaterials 8(5), 323-328.
van Wachem, P.B., Beugeling, T., Feijen, J., Bantjes, A., Detmers, J.P., van Aken, W.G., 1985. Interaction of cultured human endothelial cells with polymeric surfaces of different wettabilities. Biomaterials 6(6), 403-408.
Vancoillie, G., Frank, D., Hoogenboom, R., 2014. Thermoresponsive poly(oligo ethylene glycol acrylates). Progress in Polymer Science 39(6), 1074-1095.

Vaughan, R.D., O'Sullivan, C.K., Guilbault, G.G., 1999. Sulfur based self-assembled monolayers (SAM's) on piezoelectric crystals for immunosensor development. Fresenius J. Anal. Chem. 364(1-2), 54-57.
Víšová, I., Smolková, B., Uzhytchak, M., Vrabcová, M., Chafai, D.E., Houska, M., Pastucha, M., Skládal, P., Farka, Z., Dejneka, A., Vaisocherová-Lísalová, H., 2020a. Functionalizable Antifouling Coatings as Tunable Platforms for the Stress-Driven Manipulation of Living Cell Machinery. Biomolecules 10(8), 1146.
Víšová, I., Smolková, B., Uzhytchak, M., Vrabcová, M., Zhigunova, Y., Houska, M., Surman, F., de los Santos Pereira, A., Lunov, O., Dejneka, A., Vaisocherová-Lísalová, H., 2020b. Modulation of Living Cell Behavior with Ultra-Low Fouling Polymer Brush Interfaces. Macromolecular Bioscience 20(3), 1900351.
Víšová, I., Vrabcová, M., Forinová, M., Zhigunová, Y., Mironov, V., Houska, M., Bittrich, E., Eichhorn, K.-J., Hashim, H., Schovánek, P., Dejneka, A., Vaisocherová-Lísalová, H., 2020c. Surface Preconditioning Influences the Antifouling Capabilities of Zwitterionic and Nonionic Polymer Brushes. Langmuir 36(29), 8485-8493.
Vogler, E.A., 1998. Structure and reactivity of water at biomaterial surfaces. Advances in Colloid and Interface Science 74(1), 69-117.
Voinova, M.V., Rodahl, M., Jonson, M., Kasemo, B., 1999. Viscoelastic Acoustic Response of Layered Polymer Films at Fluid-Solid Interfaces: Continuum Mechanics Approach. Physica Scripta 59(5), 391-396.
Vroman, L., Adams, A.L., 1969. Findings With Recording Ellipsometer Suggesting Rapid Exchange Of Specific Plasma Proteins At Liquid/Solid Interfaces. Surf. Sci. 16, 438-&.
Vroman, L., Adams, A.L., Fischer, G.C., Munoz, P.C., 1980. Interaction of high molecular weight kininogen, factor XII, and fibrinogen in plasma at interfaces. BLOOD 55(1), 156-159.
Wahlgren, M., Arnebrant, T., 1991. Protein adsorption to solid surfaces. Trends in biotechnology 9(1), 201-208.
Walter, J.-G., Kökpinar, Ö., Friehs, K., Stahl, F., Scheper, T., 2008. Systematic Investigation of Optimal Aptamer Immobilization for Protein−Microarray Applications. Analytical Chemistry 80(19), 7372-7378.
Wang, G., Su, X., Xu, Q., Xu, G., Lin, J., Luo, X., 2018. Antifouling aptasensor for the detection of adenosine triphosphate in biological media based on mixed self-assembled aptamer and zwitterionic peptide. Biosensors and Bioelectronics 101, 129-134.
Wang, H., Liu, Y., Yang, Y., Deng, T., Shen, G., Yu, R., 2004. A protein A-based orientation-controlled immobilization strategy for antibodies using nanometer-sized gold particles and plasma-polymerized film. Analytical Biochemistry 324(2), 219-226.
Wang, P., Tan, K.L., Kang, E.T., Neoh, K.G., 2001. Surface functionalization of low density polyethylene films with grafted poly(ethylene glycol) derivatives. Journal of Materials Chemistry 11(12), 2951-2957.
Wang, T., Wang, Y.Q., Su, Y.L., Jiang, Z.Y., 2006a. Antifouling ultrafiltration membrane composed of polyethersulfone and sulfobetaine copolymer. Journal of Membrane Science 280(1-2), 343-350.
Wang, W.J., Yu, S., Huang, S., Bi, S., Han, H.Y., Zhang, J.R., Lu, Y., Zhu, J.J., 2019. Bioapplications of DNA nanotechnology at the solid-liquid interface. Chemical Society reviews 48(18), 4892-4920.
Wang, Y., Huang, C.-J., Jonas, U., Wei, T., Dostalek, J., Knoll, W., 2010. Biosensor based on hydrogel optical waveguide spectroscopy. Biosensors and Bioelectronics 25(7), 1663-1668.
Wang, Y., Joshi, P.P., Hobbs, K.L., Johnson, M.B., Schmidtke, D.W., 2006b. Nanostructured biosensors built by layer-by-layer electrostatic assembly of enzyme-coated single-walled carbon nanotubes and redox polymers. Langmuir 22(23), 9776-9783.
Wang, Y., Sims, C.E., Marc, P., Bachman, M., Li, G.P., Allbritton, N.L., 2006c. Micropatterning of Living Cells on a Heterogeneously Wetted Surface. Langmuir 22(19), 8257-8262.
Weber, P., Ohlendorf, D., Wendoloski, J., Salemme, F., 1989. Structural origins of high-affinity biotin binding to streptavidin. Science 243(4887), 85-88.

Wheatley, J.B., Schmidt Jr, D.E., 1999. Salt-induced immobilization of affinity ligands onto epoxide-activated supports. Journal of Chromatography A 849(1), 1-12.
Whitesides, G., Mathias, J., Seto, C., 1991. Molecular self-assembly and nanochemistry: a chemical strategy for the synthesis of nanostructures. Science 254(5036), 1312-1319.
Wiarachai, O., Vilaivan, T., Iwasaki, Y., Hoven, V.P., 2016. Clickable and Antifouling Platform of Poly[(propargyl methacrylate)-ran-(2-methacryloyloxyethyl phosphorylcholine)] for Biosensing Applications. Langmuir 32(4), 1184-1194.
Wink, T., J. van Zuilen, S., Bult, A., P. van Bennekom, W., 1997. Self-assembled Monolayers for Biosensors. Analyst 122(4), 43R-50R.
Wittebole, X., De Roock, S., Opal, S.M., 2014. A historical overview of bacteriophage therapy as an alternative to antibiotics for the treatment of bacterial pathogens. Virulence 5(1), 226-235.
Wölfel, R., Corman, V.M., Guggemos, W., Seilmaier, M., Zange, S., Müller, M.A., Niemeyer, D., Jones, T.C., Vollmar, P., Rothe, C., Hoelscher, M., Bleicker, T., Brünink, S., Schneider, J., Ehmann, R., Zwirglmaier, K., Drosten, C., Wendtner, C., 2020. Virological assessment of hospitalized patients with COVID-2019. Nature 581(7809), 465-469.
Wu, Y., Ma, H., Gu, D., He, J.a., 2015. A quartz crystal microbalance as a tool for biomolecular interaction studies. RSC Adv. 5(79), 64520-64525.
Wyszogrodzka, M., Haag, R., 2009. Synthesis and Characterization of Glycerol Dendrons, Self-Assembled Monolayers on Gold: A Detailed Study of Their Protein Resistance. Biomacromolecules 10(5), 1043-1054.
Xing, Y., Liu, B., Chao, J., Wang, L., 2017. DNA-based nanoscale walking devices and their applications. RSC Adv. 7(75), 47425-47434.
Xu, F., Geiger, J.H., Baker, G.L., Bruening, M.L., 2011. Polymer brush-modified magnetic nanoparticles for His-tagged protein purification. Langmuir 27(6), 3106-3112.
Xu, J.-J., Zhao, W., Luo, X.-L., Chen, H.-Y., 2005. A sensitive biosensor for lactate based on layer-by-layer assembling MnO 2 nanoparticles and lactate oxidase on ion-sensitive field-effect transistors. Chemical Communications(6), 792-794.
Yamazoe, H., 2019. Antibody immobilization technique using protein film for high stability and orientation control of the immobilized antibody. Materials Science and Engineering: C 100, 209-214.
Yan, J., Pan, X., Schmitt, M., Wang, Z., Bockstaller, M.R., Matyjaszewski, K., 2016. Enhancing Initiation Efficiency in Metal-Free Surface-Initiated Atom Transfer Radical Polymerization (SI-ATRP). ACS Macro Lett. 5(6), 661-665.
Yan, Q., Zheng, H.-N., Jiang, C., Li, K., Xiao, S.-J., 2015. EDC/NHS activation mechanism of polymethacrylic acid: anhydride versus NHS-ester. RSC Adv. 5(86), 69939-69947.
Yang, L., Heatley, F., Blease, T.G., Thompson, R.I., 1996. A study of the mechanism of the oxidative thermal degradation of poly (ethylene oxide) and poly (propylene oxide) using 1H-and 13C-NMR. European polymer journal 32(5), 535-547.
Yang, Q., Jacobs, T.M., McCallen, J.D., Moore, D.T., Huckaby, J.T., Edelstein, J.N., Lai, S.K., 2016. Analysis of Pre-existing IgG and IgM Antibodies against Polyethylene Glycol (PEG) in the General Population. Analytical Chemistry 88(23), 11804-11812.
Yang, Q., Lai, S.K., 2015. Anti-PEG immunity: emergence, characteristics, and unaddressed questions. WIREs Nanomedicine and Nanobiotechnology 7(5), 655-677.
Yang, W., Ella-Menye, J.-R., Liu, S., Bai, T., Wang, D., Yu, Q., Li, Y., Jiang, S., 2014. Cross-Linked Carboxybetaine SAMs Enable Nanoparticles with Remarkable Stability in Complex Media. Langmuir 30(9), 2522-2529.
Yang, W., Chen, S., Cheng, G., Vaisocherová, H., Xue, H., Li, W., Zhang, J., Jiang, S., 2008. Film Thickness Dependence of Protein Adsorption from Blood Serum and Plasma onto Poly(sulfobetaine)-Grafted Surfaces. Langmuir 24(17), 9211-9214.
Yang, W., Xue, H., Carr, L.R., Wang, J., Jiang, S., 2011a. Zwitterionic poly(carboxybetaine) hydrogels for glucose biosensors in complex media. Biosensors and Bioelectronics 26(5), 2454-2459.

Yang, W., Xue, H., Li, W., Zhang, J., Jiang, S., 2009. Pursuing “Zero” Protein Adsorption of Poly(carboxybetaine) from Undiluted Blood Serum and Plasma. Langmuir 25(19), 11911-11916.
Yang, W.J., Cai, T., Neoh, K.-G., Kang, E.-T., Dickinson, G.H., Teo, S.L.-M., Rittschof, D., 2011b. Biomimetic anchors for antifouling and antibacterial polymer brushes on stainless steel. Langmuir 27(11), 7065-7076.
Yao, G., Zhang, F., Wang, F., Peng, T., Liu, H., Poppleton, E., Šulc, P., Jiang, S., Liu, L., Gong, C., Jing, X., Liu, X., Wang, L., Liu, Y., Fan, C., Yan, H., 2020. Meta-DNA structures. Nature Chemistry 12(11), 1067-1075.
Yasir, M., Dutta, D., Hossain, K.R., Chen, R., Ho, K.K.K., Kuppusamy, R., Clarke, R.J., Kumar, N., Willcox, M.D.P., 2020. Mechanism of Action of Surface Immobilized Antimicrobial Peptides Against Pseudomonas aeruginosa. Frontiers in Microbiology 10(3053).
Ye, L., Zhang, Y., Wang, Q., Zhou, X., Yang, B., Ji, F., Dong, D., Gao, L., Cui, Y., Yao, F., 2016. Physical Cross-Linking Starch-Based Zwitterionic Hydrogel Exhibiting Excellent Biocompatibility, Protein Resistance, and Biodegradability. ACS applied materials & interfaces 8(24), 15710-15723.
Yin, Y., Nosworthy, N.J., McKenzie, D.R., Bilek, M.M.M., 2011. Ellipsometry analysis of conformational change of immobilized protein monolayer on plasma polymer surfaces. Thin Solid Films 519(9), 2968-2971.
Yoshikawa, C., Hattori, S., Honda, T., Huang, C.-F., Kobayashi, H., 2012. Non-biofouling property of well-defined concentrated poly(2-hydroxyethyl methacrylate) brush. Materials Letters 83, 140-143.
Young, B.R., Pitt, W.G., Cooper, S.L., 1988. Protein adsorption on polymeric biomaterials: II. Adsorption kinetics. Journal of Colloid and Interface Science 125(1), 246-260.
Yu, B.-Y., Zheng, J., Chang, Y., Sin, M.-C., Chang, C.-H., Higuchi, A., Sun, Y.-M., 2014. Surface Zwitterionization of Titanium for a General Bio-Inert Control of Plasma Proteins, Blood Cells, Tissue Cells, and Bacteria. Langmuir 30(25), 7502-7512.
Yu, I., Mori, T., Ando, T., Harada, R., Jung, J., Sugita, Y., Feig, M., 2016. Biomolecular interactions modulate macromolecular structure and dynamics in atomistic model of a bacterial cytoplasm. Elife 5, e19274.
Yu, Y.B., 2002. Coiled-coils: stability, specificity, and drug delivery potential. Advanced Drug Delivery Reviews 54(8), 1113-1129.
Yu, Z., Kastenmüller, G., He, Y., Belcredi, P., Möller, G., Prehn, C., Mendes, J., Wahl, S., Roemisch-Margl, W., Ceglarek, U., Polonikov, A., Dahmen, N., Prokisch, H., Xie, L., Li, Y., Wichmann, H.E., Peters, A., Kronenberg, F., Suhre, K., Adamski, J., Illig, T., Wang-Sattler, R., 2011. Differences between human plasma and serum metabolite profiles. PloS one 6(7), e21230.
Yuan, X., Fabregat, D., Yoshimoto, K., Nagasaki, Y., 2012. Development of a high-performance immunolatex based on “soft landing” antibody immobilization mechanism. Colloids and Surfaces B: Biointerfaces 99, 45-52.
Zeng, H.B., Shi, C., Huang, J., Li, L., Liu, G.Y., Zhong, H., 2016. Recent experimental advances on hydrophobic interactions at solid/water and fluid/water interfaces. Biointerphases 11(1), 10.
Zhang, B., Li, M., Lin, M., Yang, X., Sun, J., 2020. A convenient approach for antibacterial polypeptoids featuring sulfonium and oligo(ethylene glycol) subunits. Biomater. Sci. 8(24), 6969-6977.
Zhang, H., Chiao, M., 2015. Anti-fouling coatings of poly (dimethylsiloxane) devices for biological and biomedical applications. Journal of medical and biological engineering 35(2), 143-155.
Zhang, X., Shi, F., Niu, J., Jiang, Y., Wang, Z., 2008. Superhydrophobic surfaces: from structural control to functional application. Journal of Materials Chemistry 18(6), 621-633.
Zhang, X.B., Kong, R.M., Lu, Y., 2011. Metal Ion Sensors Based on DNAzymes and Related DNA Molecules. In: Cooks, R.G., Yeung, E.S. (Eds.), Annual Review of Analytical Chemistry, Vol 4, pp. 105-128. Annual Reviews, Palo Alto.

Zhao, C., Li, L., Wang, Q., Yu, Q., Zheng, J., 2011. Effect of Film Thickness on the Antifouling Performance of Poly(hydroxy-functional methacrylates) Grafted Surfaces. Langmuir 27(8), 4906 - 4913.
Zhao, C., Li, L., Zheng, J., 2010. Achieving Highly Effective Nonfouling Performance for Surface-Grafted Poly(HPMA) via Atom-Transfer Radical Polymerization. Langmuir 26(22), 17375-17382.
Zhdanov, V.P., Kasemo, B., 2010. Diffusion-limited kinetics of adsorption of biomolecules on supported nanoparticles. Colloids and Surfaces B: Biointerfaces 76(1), 28-31.
Zheng, J., Li, L., Chen, S., Jiang, S., 2004. Molecular Simulation Study of Water Interactions with Oligo (Ethylene Glycol)-Terminated Alkanethiol Self-Assembled Monolayers. Langmuir 20(20), 8931-8938.
Zheng, J., Li, L., Tsao, H.K., Sheng, Y.J., Chen, S., Jiang, S., 2005. Strong repulsive forces between protein and oligo (ethylene glycol) self-assembled monolayers: A molecular simulation study. Biophysical Journal 89(1), 158-166.
Zhu, L.P., Jiang, J.H., Zhu, B.K., Xu, Y.Y., 2011. Immobilization of bovine serum albumin onto porous polyethylene membranes using strongly attached polydopamine as a spacer. Colloids and Surfaces B: Biointerfaces 86(1), 111-118.
Zhu, L.P., Yu, J.Z., Xu, Y.Y., Xi, Z.Y., Zhu, B.K., 2009. Surface modification of PVDF porous membranes via poly(DOPA) coating and heparin immobilization. Colloids and Surfaces B: Biointerfaces 69(1), 152-155.
Zisman, W.A., 1964. Relation of the Equilibrium Contact Angle to Liquid and Solid Constitution. Contact Angle, Wettability, and Adhesion, pp. 1-51. AMERICAN CHEMICAL SOCIETY.
Zolk, M., Eisert, F., Pipper, J., Herrwerth, S., Eck, W., Buck, M., Grunze, M., 2000. Solvation of Oligo(ethylene glycol)-Terminated Self-Assembled Monolayers Studied by Vibrational Sum Frequency Spectroscopy. Langmuir 16(14), 5849-5852.
Zoungrana, T., Findenegg, G.H., Norde, W., 1997. Structure, stability, and activity of adsorbed enzymes. Journal of Colloid and Interface Science 190(2), 437-448.

List of Abbreviations

3-MPA	3-mercaptopropionic acid
AEAA	(2-aminoethoxy) acetic acid
AFM	Atomic force microscopy
ATP	Adenosine-triphosphate
ATRP	atom transfer radical polymerization
BE	bioactive element
BSA	Bovine serum albumin
CFU	Colony-forming unit
ConA	Concanavalin A
CTA	Chain transfer agent (Raft agent)
CuAAC	Copper-catalyzed azide-alkyne cycloaddition
D1	2-aminoethyl hydrogen sulfate
D2	aminomethanesulfonic acid
DCC	dicyclohexylcarbodiimide
DIC	diisopropylcarbodiimide
DNA	Deoxyribonucleic Acid
DOPA	3,4-dihydroxy-L-phenylalanine
E. coli	*Escherichia coli*
EDC	1-ethyl-3-(3-dimethyl aminopropyl)carbodiimide
Fab	Antigen-binding fragment
Fc	Constant fragment
Huh7 cells	Human hepatocellular carcinoma cell line
Ig	Imunoglobulin
LOD	Limit of detection
MIPs	Molecularly imprinted polymers
miRNA	MicroRNA
NHS	*N*-hydroxysuccinimide
OEG	oligo(ethylen glycol)
p(CB)	poly(carboxybetaine)
p(SB)	poly(sulfobetaine)
P68	Phage vB_SauP_P68
pCBAA	poly(carboxybetaine acrylamide)
pCBMAA	poly(carboxybetaine methacrylamide)
PEG	poly(ethylen glycol)
PEM	photoelastic modulator
PFU	Plaque-forming unit
pHEMA	poly(2-hydroxyethyl methacrylate)
pHOEGMA	poly[oligo(ethylene glycol)methacrylate]
pHPMA	poly(3-hydroxypropyl methacrylate)
pHPMAA	poly(N-(2-hydroxypropy) methacrylamide)
PI	Isoelectirc point

pMeOEGMA	poly[oligo(ethylene glycol) methyl ether methacrylate]
PM-IRRAS	Polarization modulation-infrared reflection-adsorption spectroscopy
PNA	Peptide nucleic acid
pSBMAA	poly(sulfobetaine methacrylamide)
QCM	Quartz crystal microbalance
RAFT	Reversible addition-fragmentation chain transfer
RNA	Ribonucleic Acid
RT-qPCR	Reverse transcription real-time polymerase chain reaction
S. aureus	*Staphylococcus aureus*
SAM	Self-assembled monolayer
SARS-Cov-2	Severe acute respiratory syndrome coronavirus 2
SB	sulfobetaine
SEM	Scanning electron microscopy
SI-ATRP	Surface-initiated atom transfer radical polymerization
SPAAC	Strain-promoted 1,3-dipolar cycloaddition
SPP	Surface plasmon polariton
SPR	Surface plasmon resonance
YAP	Yes-associated protein

List of Publications

To date: 2/18/2021

A total of 19 publications has been attached to this doctoral dissertation thesis. This list consists of several categories of scientific achievements, including 8 publications in high-impact journals, 4 journal publications in preparation or recently submitted, 5 local and international patent applications, as well as 2 additional results of applied research.

JOURNAL PUBLICATIONS

A total of 9 records has been reported via Web of Science™; A sum of citations without self-citations is 186, H-index is 4 (according to WOS, 02/2021).

1. Vaisocherová, H., H. Šípová, I. Víšová, M. Bocková, T. Špringer, M. Laura Ermini, X. Song, Z. Krejcik, L. Chrastinová, O. Pastva, K. Pimková, M. Dostálová Merkerová, J. E. Dyr, and J. Homola (2015). "Rapid and sensitive detection of multiple microRNAs in cell lysate by low-fouling surface plasmon resonance biosensor." *Biosensors and Bioelectronics* **70**: 226-231. Impact factor: 10.3. Times Cited: 59

2. Vaisocherová-Lísalová, H., I. Víšová, M. L. Ermini, T. Špringer, X. C. Song, J. Mrázek, J. Lamačová, N. Scott Lynn, P. Šedivák and J. Homola (2016). "Low-fouling surface plasmon resonance biosensor for multi-step detection of foodborne bacterial pathogens in complex food samples." *Biosensors and Bioelectronics* **80**: 84-90. Impact factor: 10.3. Times Cited: 92

3. Vaisocherová-Lísalová, H., F. Surman, I. Víšová, M. Vala, T. Špringer, M. L. Ermini, H. Šípová, P. Šedivák, M. Houska, T. Riedel, O. Pop-Georgievski, E. Brynda and J. Homola (2016). "Copolymer Brush-Based Ultralow-Fouling Biorecognition Surface Platform for Food Safety." *Analytical Chemistry* **88**(21): 10533-10539. Impact factor: 6.8. Times Cited: 17

4. Lísalová, H., E. Brynda, M. Houska, I. Víšová, K. Mrkvová, X. C. Song, E. Gedeonová, F. Surman, T. Riedel, O. Pop-Georgievski and J. Homola (2017). "Ultralow-Fouling Behavior of Biorecognition Coatings Based on Carboxy-Functional Brushes of Zwitterionic Homo- and Copolymers in Blood Plasma: Functionalization Matters." *Analytical Chemistry* **89**(6): 3524-3531. Impact factor: 6.8. Times Cited: 25

5. Víšová, I., B. Smolková, M. Uzhytchak, M. Vrabcová, D. E. Chafai, M. Houska, M. Pastucha, P. Skládal, Z. Farka, A. Dejneka and H. Vaisocherová-Lísalová (2020). "Functionalizable Antifouling Coatings as Tunable Platforms for the Stress-Driven Manipulation of Living Cell Machinery." *Biomolecules* **10**(8): 1146. Impact factor: 4.1. Times Cited: 0

6. Víšová, I., B. Smolková, M. Uzhytchak, M. Vrabcová, Y. Zhigunova, M. Houska, F. Surman, A. de los Santos Pereira, O. Lunov, A. Dejneka and H. Vaisocherová-Lísalová (2020). "Modulation of Living Cell Behavior with Ultra-Low Fouling Polymer Brush Interfaces." *Macromolecular Bioscience* **20**(3): 1900351. Impact factor: 3.4. Times Cited: 4

7. Víšová, I., M. Vrabcová, M. Forinová, Y. Zhigunová, V. Mironov, M. Houska, E. Bittrich, K.-J. Eichhorn, H. Hashim, P. Schovánek, A. Dejneka and H. Vaisocherová-Lísalová (2020). "Surface Preconditioning Influences the Antifouling Capabilities of Zwitterionic and Nonionic Polymer Brushes." *Langmuir* **36**(29): 8485-8493. Impact factor: 3.6. Times Cited: 3

8. Hashim, H., M. Kozhaev, P. Kapralov, L. Panina, V. Belotelov, I. Víšová, D. Chvostova, A. Dejneka, I. Shpetnyi, V. Latyshev, S. Vorobiov and V. Komanicky (2020). "Controlling the Transverse Magneto-Optical Kerr Effect in Cr/NiFe Bilayer Thin Films by Changing the Thicknesses of the Cr Layer." *Nanomaterials* **10**(2): 10. Impact factor: 4.3. Times Cited: 1

SUBMITTED JOURNAL PUBLICATIONS:

9. Víšová, I., M. Forinová, A. Pilipenco, K. Mezuláníková, M. Tomandlová, M. Vrabcová, M. Houska, A. Dejneka, J. Dostálek, H. Vaisocherová-Lísalová (2021): "Recovery of Antifouling Properties of Zwitterionic Brushes after Postmodification with Bioactive Molecules Significantly Improves Label-Free Biosensing in Complex Media." Submitted in *ACS Applied Materials & Interfaces*. Impact factor: 8.8.

PUBLICATIONS IN PREPARATION:

10. Víšová, I., M. Houska, H. Vaisocherová-Lísalová (2021): "Coatings Exhibiting Anti-Fouling Behavior and Biorecognition Activity in Complex Biological Media: A Review of Functionalization Aspects", review. To be submitted in *Analyst*. Impact factor: 4.0.

11. Obořilová, R., H. Šimečková, M. Pastucha, Š. Klimovič, I. Víšová, J. Přibyl, H. Vaisocherová-Lísalová, R. Pantůček, P. Skládal, I. Mašlaňová, Z. Farka (2021): "Atomic Force Microscopy for Real-time Single-cell Study of the Bacteriophage-mediated Lysis". To be submitted in *Nanoscale.* Impact factor: 6.9.

12. Forinová, M., A. Pilipenco, I. Víšová, N. S. Lynn, J. Dostálek, V. Honig, M. Palus, J. Stěrba, M. Houska, M. Vrabcová, P. Horák, C-P. Tung, C-M. Yu, C-Y. Chen, Y-C. Huang, P-H. Tsai, S-Y. Lin, H-J. Hsu, A-S. Yang, A. Dejneka, H. Vaisocherová-Lísalová (2021): "Rapid one-step quantitative detection of SARS-CoV-2 virus in crude clinical samples using antifouling quartz crystal microbalance biosensor". To be sumbmitted in *Science Advances*. Impact factor: 13.1.

PATENTS:

13. H. Lísalová, E. Brynda, I. Víšová, X. Song Chadtová, K. Mrkvová, F. Surman, M. Riedel, M. Houska, E. Brynda, J. Homola: "Způsob přípravy povrchu substrátu obsahujícího

karboxybetainové funkční skupiny." Patent application PV 2016-361 filed in 6/2016, approved 10/2017.

14. H. Lísalová, E. Brynda, I. Víšová, X. Song Chadtová, K. Mrkvová, F. Surman, T. Riedel, M. Houska, E. Brynda, J. Homola, "Method of preparation of a substrate containing carboxybetaine groups and bound bioactive substances which is resistant against undesirable deposition from biological media". Patent application PCT/CZ2017/050025, filed in 6/2017.

15. H. Lísalová, M. Vrabcová, I. Víšová, M. Houska, A. Dejneka, "Terpolymer pro použití proti nespecifické adsorpci látek z biologických médií." Patent application PV 2020-270, filed in 5/2020.

16. Víšová I., H. Lísalová, M. Vrabcová, M. Houska, M. Forinová, A. Pilipenco. "Vylepšení resistentnosti substrátu obsahujícího karboxybetainové funkční skupiny po aktivaci či aktivaci a funkcionalizaci". To be filed in March 2021

17. H. Lísalová, M. Vrabcová, I. Víšová, M. Houska, A. Dejneka: "Terpolymer and polymer brushes for use against non-specific adsorption of substances from biological media". To be filed in March 2021.

RESULTS OF APPLIED RESEARCH:

18. Lísalová H., I. Víšová, P. Horák, M. Forinová, M. Vrabcová, A. Dejneka: "Biodetekční systém na bázi ultra-rezistnentních funkčních polymerů pro rychlou detekci patogenních bakterií v potravninách", HL1/FZU/2019 (Functional sample).

19. Forinová M., A. Pilipenco, I. Víšová, P. Horák, M. Vrabcová, V. Hönig, M. Palus, J. Štěrba, A. Dejneka, H. Lísalová: "Funkční biočip s ultra-rezistentní polymerní vrstvou pro rychlou detekci viru SARS-CoV-2 pomocí metody QCM", HL1/FZU/2020 (Functional sample).

List of Appendices

Appendix I

Vaisocherová et al. 2015: Rapid and sensitive detection of multiple microRNAs in cell lysate by low-fouling surface plasmon resonance biosensor. *Biosensors and Bioelectronics* **70**: 226-231.

Appendix II

Vaisocherová-Lísalová et al. 2016: Low-fouling surface plasmon resonance biosensor for multi-step detection of foodborne bacterial pathogens in complex food samples. *Biosensors and Bioelectronics* **80**: 84-90.

Appendix III

Vaisocherová-Lísalová et al. 2016: Copolymer Brush-Based Ultralow-Fouling Biorecognition Surface Platform for Food Safety. *Analytical Chemistry* **88**(21): 10533-10539.

Appendix IV

Lísalová et al. 2017: Ultralow-Fouling Behavior of Biorecognition Coatings Based on Carboxy-Functional Brushes of Zwitterionic Homo- and Copolymers in Blood Plasma: Functionalization Matters. *Analytical Chemistry* **89**(6): 3524-3531.

Appendix V

Víšová et al. 2020: Modulation of Living Cell Behavior with Ultra-Low Fouling Polymer Brush Interfaces. *Macromolecular Bioscience* **20**(3): 1900351.

Appendix VI

Víšová et al. 2020: Surface Preconditioning Influences the Antifouling Capabilities of Zwitterionic and Nonionic Polymer Brushes. *Langmuir* **36**(29): 8485-8493.

Appendix VII

Víšová et al. 2020: Functionalizable Antifouling Coatings as Tunable Platforms for the Stress-Driven Manipulation of Living Cell Machinery. *Biomolecules* **10**(8): 1146.

Appendix VIII

Hashim et al. 2020: Controlling the Transverse Magneto-Optical Kerr Effect in Cr/NiFe Bilayer Thin Films by Changing the Thicknesses of the Cr Layer. *Nanomaterials* **10**(2): 10.

Appendix IX

Víšová et al. 2021: Recovery of Antifouling Properties of Zwitterionic Brushes after Postmodification with Bioactive Molecules Significantly Improves Label-Free Biosensing in Complex Media. Manuscript submitted in *ACS Applied Materials & Interfaces.*

Appendix X

Víšová et al.: Coatings Exhibiting Anti-Fouling Behavior and Biorecognition Activity in Complex Biological Media: A Review of Functionalization Aspects. Manuscript in preparation to be submitted in *Analyst.*

Appendix XI

Obořilová et al.: Atomic Force Microscopy for Real-time Single-cell Study of the Bacteriophage-mediated Lysis. Manuscript in preparation to be submitted in *Nanoscale.*

Appendix XII

Forinová et al.: Rapid one-step quantitative detection of SARS-CoV-2 virus in crude clinical samples using antifouling quartz crystal microbalance biosensor. Manuscript in preparation to be submitted in *Science Advances.*

Appendix XIII

Lísalová et al.: Způsob přípravy povrchu substrátu obsahujícího karboxybetainové funkční skupiny. Patent application PV 2016-361 approved 10/2017.

Appendix XIV

Lísalová et al.: Method of preparation of a substrate containing carboxybetaine groups and bound bioactive substances which is resistant against undesirable deposition from biological media. Patent application PCT/CZ2017/050025, filed in 6/2017.

Appendix XV

Lísalová et al.: Terpolymer pro použití proti nespecifické adsorpci látek z biologických médií. Patent application PV 2020-270, filed in 5/2020.

Appendix XVI

Víšová et al.: Vylepšení resistentnosti substrátu obsahujícího karboxybetainové funkční skupiny po aktivaci či aktivaci a funkcionalizaci. Patent application to be filed in 3/2021.

Appendix XVII

Lísalová et al.: Terpolymer and polymer brushes for use against non-specific adsorption of substances from biological media. Patent application to be filed in 3/2021.

Appendix XVIII

Lísalová et al.: Biodetekční systém na bázi ultra-rezistnentních funkčních polymerů pro rychlou detekci patogenních bakterií v potravninách. Functional sample HL1/FZU/2019.

Appendix XIX

Forinová et al.: Funkční biočip s ultra-rezistentní polymerní vrstvou pro rychlou detekci viru SARS-CoV-2 pomocí metody QCM. Functional sample HL1/FZU/2020.